2 mlp

PALEOMAGNETISM OF THE MESOZOIC IN ALASKA

A

DISSERTATION

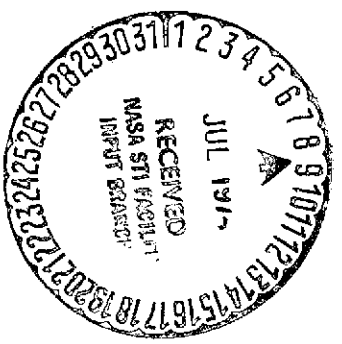

Presented to the Faculty of the

University of Alaska in Partial Fulfillment

of the Requirements

for the Degree of

DOCTOR OF PHILOSOPHY

by

Duane R. Packer

College, Alaska

May 1972

PALEOMAGNETISM OF THE MESOZOIC

IN ALASKA

APPROVED:

_____

_____

_____

_____

_____
Chairman

APPROVED: _____ DATE: _____
Dean of the College of
Earth Sciences and
Mineral Industry

_____
Vice President for Research
and Advanced Study

ABSTRACT

Over 400 oriented cores of Permian, Triassic, Jurassic, and Cretaceous sedimentary and igneous rocks were collected from 34 sites at 10 areas throughout southern Alaska. After magnetic 'cleaning' in successively higher alternating fields 179 samples were considered to be stable and to give statistically consistent results within each site and age group. Due to the lack of a sufficient number of stable samples, the results from Permian, Triassic, and Cretaceous rocks were inconclusive. The nine remaining Jurassic sites represent 100 samples from three general areas in southern Alaska.

The mean paleomagnetic declinations calculated with respect to the present, Carey's model, and Grantz's model are not significantly different from one another and do not show a systematic change along the strike of the orocline. The paleomagnetic poles for the Jurassic from southern Alaska and North America are separated in the opposite direction to be explained by the Alaskan orocline. The Alaskan orocline as Carey defined it, therefore, does not appear to be a valid concept.

The southern Alaskan Jurassic paleomagnetic pole is significantly different from the North American Jurassic pole. This suggests that since the Jurassic, southern Alaska must have moved approximately 18 degrees north and rotated 52 degrees clockwise to reach its present position. Tectonic interpretation of these results give a possible explanation for many of the geologic features observed in southern Alaska.

ACKNOWLEDGEMENTS

I would like to acknowledge with sincere gratitude and indebtedness the continual guidance, support, and encouragement offered by Dr. David B. Stone, who suggested this research topic originally and who was always more than willing to discuss its many aspects at length. I would also like to thank Dr. Douglas K. Bingham for "initiation" into the practical intricacies of paleomagnetic collection and data refinement.

For invaluable support in many ways while in the field and for other assistance I offer sincere thanks to Dr. R. B. Forbes of the Geophysical Institute and to J. W. Deininger of the Geology Department, University of Alaska; D. H. Richter, N. A. Matson, and F. R. Weber of the Alaska Branch, United States Geological Survey; and B. Bender of the Columbia-Ward Cannery at Chignik, Alaska. I also thank G. W. Newman of Humble Oil and Refining Co., for field support and joint collection and analysis of results.

A special tribute is due to Genevieve Edsall for the myriad of top-quality paleomagnetic measurements she conducted and for her close attention in completing the numerous other details of the work. Thanks are due to Pat Kirton for typing the preliminary draft. I would like also to thank LuAnne, my wife, for her typing and editing of the first drafts, and for her patience with long hours.

This work was supported by a National Defense Education Act, Title IV, fellowship through the Geology Department, University of Alaska; and by grants GA 1216 and GA 12014 from the National Science

Foundation, Geophysics and Earth Science Section, grant NGL-02-001-063 from the National Aeronautics and Space Administration, and State of Alaska funds through the Geophysical Institute, University of Alaska.

TABLE OF CONTENTS

LIST OF ILLUSTRATIONS

LIST OF TABLES

I. ARCUATE TECTONIC FORM OF ALASKA

The arcuate form of Alaskan topography and tectonics has been a topic of speculation for many years, especially since the acceptance of continental drift ideas spurred real interest in global geology.

TOPOGRAPHIC EXPRESSION

Besides the southern shoreline, the most obvious topographic feature in Alaska with an arcuate form is the Alaska Range, which is a part of the Cordillera that bounds the western edge of the Americas. The trend traced by the Coast Mountains of Canada, the Alaska Range and the Aleutian Range curves approximately 75 degrees in mid-Alaska. The Tanana River and the Kuskokwim and Nushagak Rivers create a lowland to the north that parallels the Alaska Range. Still farther north the Kuskokwim Mountains and the Tanana-Yukon Uplands follow the general trend of the Alaska Range, as does the Yukon River, which has its headwaters in Canada. The Brooks Range in northern Alaska forms an angle of about 30 degrees to the trend of the Rocky Mountains. To the south of the Alaska Range, the Saint Elias Mountains, the Chugach Mountains, and the Kenai Mountains also form an arcuate belt along the Gulf of Alaska. There are less obvious topographic features that parallel the trends of the Alaska Range and the Brooks Range, but few other features are continuous across Alaska.

GEOLOGIC EXPRESSION

Payne (1955) mapped the Mesozoic and Cenozoic tectonic elements of Alaska and explained the tectonic history of central and southern Alaska with a series of arcuate geosynclines and geanticlines of different ages. The Paleozoic Seldovia, Talkeetna, and Tanana geanticlines, the lower Cretaceous Yakataga geosyncline, and the upper Cretaceous Chugach Mountains, Matanuska, Alaska Range, and Kuskokwim geosynclines are all examples of this.

Most of the following discussion of faults in Alaska is from Grantz (1966). The right-lateral strike-slip Denali fault system, which is well expressed topographically and defines the curvature of the Alaska Range, consists of relatively straight fault segments that extend from Chatham Strait to Bristol Bay. The Denali fault shows a curve of about 30 degrees (Fig. 1-1).

From east to west, the Chatham Strait, Chilkat River, Shakwak, Denali, Holitna, and Togiak-Tikchik faults compose the Denali fault system. The Denali fault consists of the Farewell segment, the Hines Creek strand and the McKinley strand. Most of the faults of the Denali fault system are thought to be older faults of an unknown type, with imposed Cenozoic or latest Mesozoic to Recent right-lateral displacement along a length of over 2150 km. The Chatham Strait and Chilkat River faults became active in the early Cretaceous; the Togiak-Tikchik and Holitna faults became active in the late Cretaceous; and the various Denali fault segments became active in late Cretaceous or Paleocene. All but the Chatham Strait and Chilkat River faults have

Figure 1-1. Major fault trends in Alaska and northwestern Canada. (After King, 1969; Grantz, 1966; Richter and Matson, 1971; and Churkin, 1970a)

Denali Fault System

1. Chatham Strait fault
2. Chilkat River fault zone
3. Shakwak fault
4. Denali fault
    - 4a. McKinley strand
    - 4b. Hines Creek strand
    - 4c. Farewell segment
5. Holitna fault
6. Togiak-Tikchik fault

Southeastern Alaska

7. Fairweather fault
8. Totschunda fault system
9. Queen Charlotte Islands fault

Central and Southwestern Alaska

10. Rocky Mountain trench
11. Tintina trench and fault
12. Stevens Creek fault zone
13. Kaltag fault
14. Yukon Delta conjugate fault zone
15. Aniak-Thompson Creek fault
16. Iditarod-Nixon Fork fault
17. Porcupine lineament
18. Kobuk trench
19. Castle Mountain fault
20. Bruin Bay fault

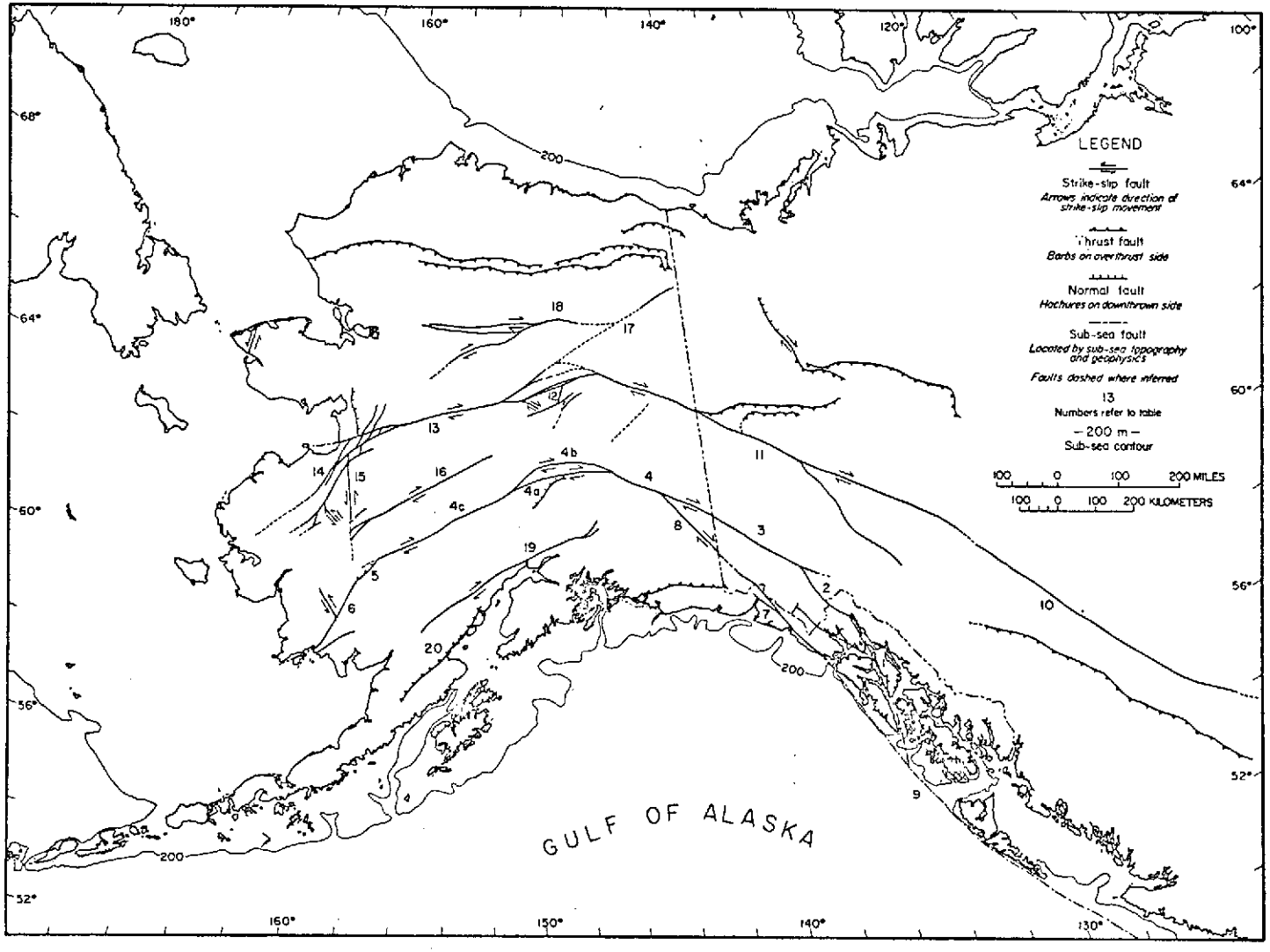
LEGEND
Strike-slip fault
Arrows indicate direction of strike-slip movement
Thrust fault
Barbs on overthrust side
Normal fault
Hachures on downthrown side
Sub-sea fault
Located by sub-sea topography and geophysics
Faults dashed where inferred
13
Numbers refer to table
– 200 m –
Sub-sea contour
100 0 100 200 MILES
100 0 100 200 KILOMETERS
GULF OF ALASKA
180°
160°
140°
120°
100°
68°
64°
60°
56°
52°
150°
130°

Figure 1-1.

experienced motion in Recent times. Estimates of the total right-lateral offset of the Denali fault system range from 240 km (St. Amand, 1957), to 80 km (Brew and others, 1966). The Totschunda fault system, which is an extension of the Fairweather fault, intersects the Denali fault system in the Mentasta Mountains at 144 degrees west longitude (Richter and Matson, 1971). The Fairweather fault and Totschunda fault systems are apparently no older than early Pleistocene and are active today. The motion of these faults is predominantly right-lateral, with up to 10 km displacement. All of these faults are relatively straight but intersect to form a complex and definitely arcuate fault trace.

The Tintina and the Kaltag faults may also form an arcuate fault system (Fig. 1-1), approximately 150 miles north of the Denali fault system (Churkin, 1970a). From Canada, the Rocky Mountain trench, extrapolated across the Liard Plain, trends into the Tintina trench and Tintina fault which extend into Alaska (Roddick, 1967). It is unclear whether the Tintina fault bends westward into the Stevens Creek fault zone and still further west into the Kaltag fault or trends into the Kobuk trough. The right-lateral Tintina fault was active in lower Paleozoic (Roddick, 1967), from Jurassic through late Cretaceous, and from Oligocene through Pliocene (Grantz, 1966). The Tintina fault and Tintina trench have a combined length of approximately 1300 km with postulated offsets ranging from 80 km, estimated in Alaska (Grantz, 1966), to 400 km, estimated in Canada by Roddick (1967). It should be noted that the existence of faulting along the Kobuk trough as suggested by Grantz (1966) and King (1969) is now being questioned (Fritts, personal communication, 1972).

The Kaltag fault may bend into the Tintina fault or trend northeast into the Porcupine lineament as mentioned above (Fig. 1-1). The right-lateral Kaltag fault can be traced westward onto the Bering shelf (Scholl et al., 1970). The Kaltag, which is 400 km long on land, has been active from the late Cretaceous to the Recent and has a displacement of approximately 140 km.

In western Alaska, approximately half-way between the Farewell segment of the Denali fault and the Kaltag fault, lies the right-lateral Iditarod-Nixon Fork fault. The Iditarod-Nixon Fork fault became active in late Cretaceous and has displacement until Recent time with a maximum total offset of 110 km. This 500 km long fault, although predominantly strike-slip, has a reverse dip-slip component which is upthrown on the north. Even though the Iditarod-Nixon Fork fault cannot be traced east beyond 152 degrees west longitude, and thus cannot be traced around the bend, its sense of motion, age, and trend are identical to the western portions of the Denali fault system and the Kaltag-Tintina faults. Trending north from the Togiak-Tikchik fault, terminating the Iditarod-Nixon Fork fault, and ending in the Kaltag fault, is the left-lateral Aniak-Thompson Creek fault, which has about 40 km of late Cretaceous or Tertiary displacement.

Approximately 110 miles south of the Farewell segment of the Denali fault, the Castle Mountain fault follows a parallel trend. The Castle Mountain fault has had possibly up to tens of kilometers of right-lateral displacement along a length of approximately 450 km since late Cretaceous. Apparently the Castle Mountain fault does not

make a bend and trend into the Chitina Valley to connect with the Fairweather fault as postulated by St. Amand (1957), but splays out in the southern Talkeetna Mountains just north of the upper Matanuska Valley (Grantz, 1966).

On the west coast of Cook Inlet, to the southwest of the Castle Mountain fault, is the Bruin Bay fault, which is nearly parallel to the Holitna fault of the Denali fault system. Both the Bruin Bay fault, and a parallel fault along the northwest shore of Kodiak Island, are high-angle reverse faults upthrown on the north. On the southeast shore of Kodiak Island are at least two major normal faults upthrown on the northwest, which are nearly parallel to the Holitna fault. The Bruin Bay fault became active in the mid to late Jurassic, while the faults on Kodiak Island became active in the early to mid Tertiary. Other areas in southern Alaska also have thrust faulting that parallels the general trend of the Denali fault system, as shown in Figure 1-1.

DISCUSSION OF ORIGIN

Alaska appears arcuate in both topographic and geologic form. In view of the increasing evidence for plate tectonics, an understanding of the contact between Eurasian and North American plates would answer many questions about the geologic history of the North Pacific and Arctic Oceans. The arcuate form of Alaska either developed as such from the beginning, is tectonically controlled, or is the result of some combination of the two. Carey (1958) explained the arcuate tectonic form of Alaska by the Alaskan orocline (Fig. 1-2), which is

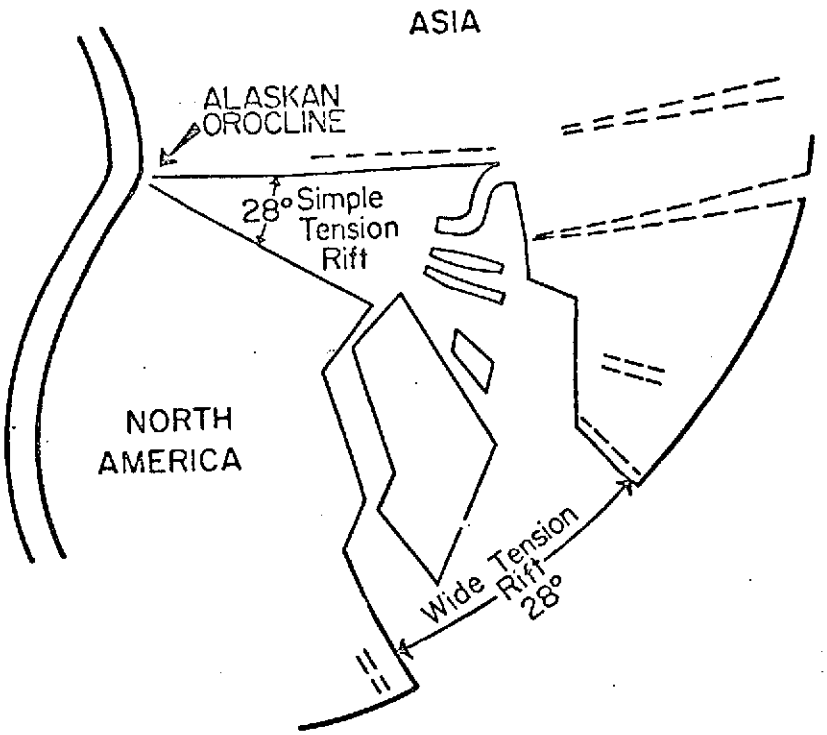

Figure 1-2. Alaskan orocline and Arctic sphenochasm. (From Carey, 1958.)

the compressional side of a rift that he called the Arctic sphenochasm. The Arctic sphenochasm has an opening of about 30 degrees which is distributed into two en echelon tension rifts, forming the Arctic Ocean and the Greenland, Barents, and Kara Seas and the Khatanga, Davis Strait, and Baffin Bay troughs. Carey also developed explanations for many other features around the Arctic Ocean that followed from the Alaskan orocline hypothesis.

Carey's pivot point for the Alaskan orocline is approximately 148 degrees west longitude and 64 degrees north latitude, which is a point just north of the bend in the Alaska Range. He divides the hinge region of the orocline into a complex array of orotaths, sphenochasms, rhombochasms, and megashears in an attempt to match similar topographic and geologic features of Alaska and eastern Siberia. Further evidence Carey uses in support of the Alaskan orocline are the Precambrian through present virtual geomagnetic poles for Britain and North America, whose curves intersect at 30 degrees and fit the Alaskan orocline better than other explanations of that time for opening of the Atlantic. However, due to the few data that these poles represent, and to the large statistical error limits involved, all that is proven is that North America and Britain did drift apart; the data may not be used to demonstrate with any certainty about what axis this occurred. Another supporting factor for the Alaskan orocline is the coherent pattern of paleogeography it presents.

Grantz (1966) argues that insofar as the mountains are a late Miocene and Pliocene feature, younger than the postulated formation

of the arcuate tectonics, they cannot be a direct result of oroclinal bending. In fact, the trend of the Cenozoic mountains show greater curvature than that of the Mesozoic tectonic elements and late Mesozoic faults. The curves of the present mountains, though, are probably the result of earlier orogenic trends which may reflect oroclinal bending. Curved late Mesozoic features, such as strike-slip fault zones, might lead to evidence of oroclinal origin.

Grantz (1966), in his study of strike-slip faults in Alaska, presents two possibilities for the internal rotation of Alaska along the arcuate fault patterns. The first possibility is that the faults were once straight but have been bent up to 50 degrees along a northerly striking axial plane; the second is that the right-lateral--the most recent--motion has adopted favorably situated members of an old and extensive fault system.

Grantz pursues several lines of reasoning regarding these possibilities. One is based on a hypothesis of St. Amand (1957), which suggests the right-lateral faults are in response to counterclockwise rotation of the Pacific Basin; however, in light of recent plate tectonic evidence (Atwater, 1970; McKenzie and Parker, 1967; and others) this hypothesis seems an unlikely explanation. Work by Richter and Matson (1971) on the Totschunda fault system also indicates a different sense of stress for southern Alaska. This line of reasoning, in any case, would not apply to interior Alaska and the Tintina-Kaltag faults. Another way of creating the arcuate form is by regional compression, which would result in conjugate strike-slip faulting. Most of the strike-slip faults in Alaska are straight;

however there appear to be no conjugate faults except in the Yukon Delta area (Grantz, 1966).

Restoring the movement along the faults on the western side of the bend by a simple mechanical model, Grantz (1966) was able to demonstrate how the bend could be straightened by rotations of up to 50 degrees. Rotation in this mechanical model is around individual pivots along a north trending axis at about 148 degrees west longitude. Fifty degrees is also approximately the amount by which the Mesozoic tectonic elements (Payne, 1955) are bent. Despite similarities, it seems that such a simple model of bending does not adequately explain several factors, such as only 7 degrees of rotation required to restore the Castle Mountain fault and the apparent lack of maximum stress concentration in the axial region of the bending (Grantz, 1966). Of course interpretation is complicated by lack of data on the type and extent of Paleozoic and earlier displacements along the faults. Grantz (1966) also suggested that the arcuate tectonic form of Alaska might represent one limb of a buckle created by longitudinal drift of North America toward Siberia and not by a simple rotation about a pivot in Alaska, as was Carey's (1958) hypothesis.

Churkin (1969, 1970a, 1970b) has correlated Pre-Cambrian, Paleozoic, and early Mesozoic rocks of Alaska and Siberia. Work reported on by Churkin (1970a) indicates that Wrangell Island, north of Siberia, is connected across the Chukchi Sea to the Lisburne Peninsula by bathymetric and gravity anomalies, and that these represent a structural extension of the Brooks Range. Fossiliferous

Mississippian rocks, which are a part of a sequence of marine sediments and non-marine conglomerates with outcrops of comparable sections on Wrangell Island, in the Brooks Range, and in the Arctic Islands, thus probably represent a clastic wedge deposited around the Canada Basin (Fig. 1-3). Paleozoic plutonic history also appears to be similar.

At Cape Dezhneva, the easternmost tip of the Chukotsk Peninsula, there is a gneiss and amphibolite dome surrounded by marble and schist. A similar structure is present in the Kigluiak Mountains on the Seward Peninsula across the Bering Strait, about 60 miles east of Cape Dezhneva. Fossils of Ordovician and Silurian age have been found in limestones overlying both structures. Rubidium-strontium ages on both metamorphic domes indicate Precambrian and Cretaceous metamorphic-plutonic events. Thrust faulting and plutonic activity also appear to have a good correlation on both sides of the Bering Strait (Churkin, 1970a).

Churkin (1970a) also reports that St. Lawrence Island has an almost complete Devonian through Triassic section that resembles rocks of both the Chukotsk Peninsula and the western Brooks Range. Farther inland, the Yukon-Porcupine Rivers area in Alaska and the Kolmski massif in Siberia have similar sections of carbonate and terrigenous rocks.

Churkin (1970b) attempts to correlate the Paleozoic submarine volcanic rocks and volcanoclastic sedimentary rocks--eugeosynclinal deposits--that occur in southeastern Alaska, western Canada, and the Alaska Range with Chukotka (Fig. 1-3). The best section, where Ordovician through Permian rocks (including plutonic rocks and

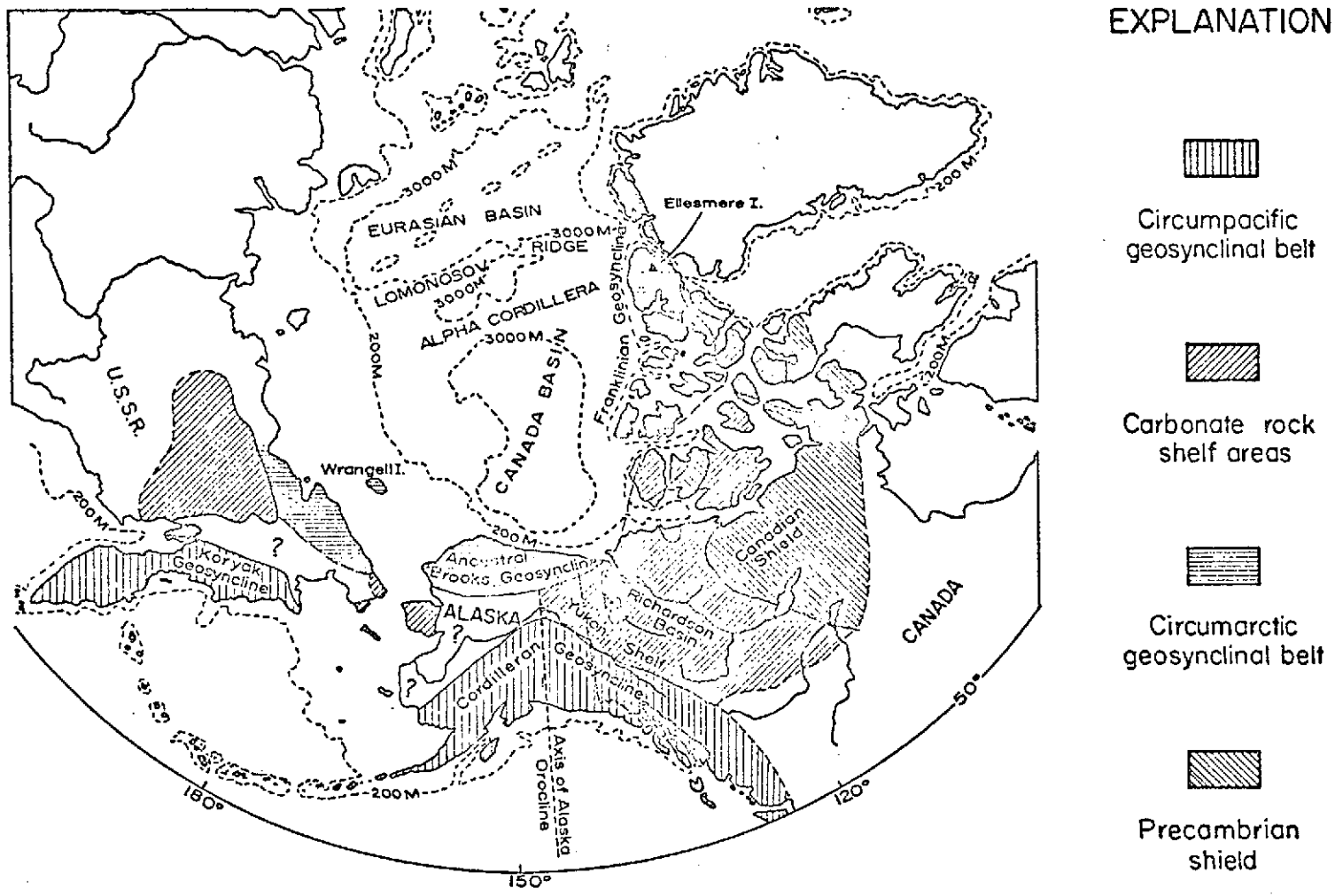

Figure 1-3. Correlation of tectonic elements between Alaska and Siberia in mid Paleozoic time. (From Churkin, 1970b.)

associated conglomerates) are exposed, is in southeastern Alaska. This same rock sequence is found in incomplete sections in some areas of the Alaska Range and farther south. Churkin (1970b) cites Russian work that reports similar volcanic-terrigeneous rock units around the northwestern rim of the Pacific Basin in the Koryak Mountains of Chukotka. Churkin (1970b) proposes that, based on the correlation of these Paleozoic sections, the Cordilleran geosyncline of southern Alaska continues west to become the Koryak geosyncline.

The conclusion Churkin (1970a) draws is that Alaska and Chukotka have been connected since Paleozoic time and probably since the Precambrian. This, of course, precludes any large-scale continental drift between Alaska and Siberia. Recent geologic and geophysical evidence from the Arctic Ocean indicates that Carey's (1958) idea of a single rifting creating the Arctic Ocean is probably incorrect. The geometry of the Canada Basin opposed to the Eurasian Basin, the active Nansen Cordillera, the inactive Alpha Cordillera, and the non-volcanic Lomonosov Ridge all indicate a complex origin for the Arctic Ocean Basin. Rather than Carey's simple rifting, Churkin has proposed spreading along the Nansen Cordillera in the Eurasian Basin, as the extension of the opening of the Atlantic Ocean, and compression in the Verkhoyansk and Cherski Mountains in Western Siberia. This implies that the Canada Basin formed earlier. Hamilton (1970) believes that the Nansen Ridge ends in a right-lateral fault that trends east along the northern coast of Siberia, through the Chukotsk Peninsula and into the Bering Sea. The pole of rotation for the drifting of North America with respect to Eurasia, based on azimuths of fractures across the

northern part of the mid-Atlantic ridge, is 78 degrees north, 102 degrees east (LePichon, 1968). The pole based on best fit for Greenland against Europe is 73 degrees north, 96.5 degrees east (Bullard et al., 1965). More recent work by Pitman and Talwani (1972), show the pole of rotation for the Atlantic north of the Azores to be around 149 degrees east longitude and 65 degrees north latitude. These poles are near the apex of Churkin's proposed hinge zone.

Compression of this magnitude, Churkin (1970b) feels, was taken up by closing a break in the Verkhoyansk Mountain region rather than creating a buckle between Alaska and Siberia. The Verkhoyansk Mountain area is a fold belt that forms the boundary between the Precambrian and Paleozoic Siberian platform and the more intensely deformed Mesozoic Chukotka fold belt (Churkin, 1970b). Churkin (1969) proposed that the bend in Alaska is largely the result of a long period of regional stress created by spreading of the Pacific sea floor, oriented against the continental margin of the Gulf of Alaska. This is supported by faults and folds in the Koryak Mountains and around the Gulf of Alaska (Stoneley, 1967), and by magnetic anomalies in the Gulf of Alaska (Pitman and Hayes, 1968). Land movements associated with the 1964 Alaska earthquake also support this concept (Plafker, 1965).

The arcuate Alaskan form thus may be the result of a combination of tectonic bending and formation under regional stress; however, the complexities involved are obvious from the above discussion. The question is far from being resolved, and Alaska is in a unique posi-

tion for interpretation of the tectonic history of the Arctic and North Pacific regions. St. Amand (1957) suggested that remanent magnetization of appropriate rocks in Alaska be measured to see if any rotation was indicated. Chantry-Price (1967) attempted a preliminary study of the Alaskan orocline by collecting rocks of different ages at six sites. Due to questionable stability of the samples collected or an intensity too small to measure successfully, his results were inconclusive. The results of a more detailed study are presented here.

II. PALEOMAGNETIC APPROACH

REMANENT MAGNETIZATION

Rocks containing magnetic minerals may acquire a remanent magnetization known as natural remanent magnetization or NRM. Minerals having ferrimagnetic properties at normal temperatures lie predominantly within the $FeO-TiO_2-Fe_2O_3$ ternary system but also include minerals such as the pyrrhotites and various oxyhydroxides of iron. Irving (1964), Nagata (1961), Strangway (1970), and others discuss the magnetic properties of rocks in great detail.

Rocks may obtain an NRM through thermal, chemical, or mechanical processes or through some combination of these. Rocks become magnetized in the direction of the ambient magnetic field as the rock's constituent magnetic minerals cool through their respective blocking temperature or T_b. This process is called thermo-remanent magnetization or TRM, and is generally very stable. Thus, for igneous rocks, the geomagnetic field present at the time of formation is 'frozen' in by TRM. A metamorphic event with temperatures above T_b also records the geomagnetic field. T_b is determined mainly by particle size, crystal structure, and composition (Nagata, 1961).

Chemical remanent magnetization or CRM is also important in recording field directions. This type of NRM is the result of either the formation of new magnetic minerals or recrystallization of existing minerals at temperatures below their blocking temperatures. As the mineral grains grow through their blocking diameter (Irving, 1964) they obtain an NRM parallel to the ambient field.

Another low-temperature NRM is viscous remanent magnetization, or VRM. At the expense of previously acquired TRM or CRM, the magnetic vector in minerals with a low coercivity and/or a short relaxation time may change direction to become aligned with a changing geomagnetic field. For most rock types VRM only affects 2 or 3% of TRM during periods up to 10^9 years, except at elevated temperatures (Nagata, 1961). Both CRM and VRM are often regarded as secondary magnetization or 'noise' on top of the primary TRM, and various techniques can be used to separate, eliminate or reduce their effects.

A mechanical process by which sedimentary rocks may acquire an NRM is called detrital remanent magnetization, or DRM. Small magnetic particles become oriented by the geomagnetic field as they settle and are eventually consolidated into the sediment. Even though mechanical interactions--such as shape, relative size, water velocity, and compaction--have an effect, experiments with different types of sediments in still, running, and turbulent water, and tests on natural sediments, have shown that the accuracy with which sediments record the ambient magnetic field is good. Nagata (1961) and Irving (1964) explore DRM in detail and have shown the existence of two types of error--an inclination error, and an error due to the slope of the original bedding. These errors may result in an inclination that is generally 20 degrees less than that of the geomagnetic field (Nagata, 1961). However, consistency tests on slumped beds in sediments, such as fine-grained sandstone or coarse-grained siltstone, in which the magnetic particle size was relatively smaller (at least by a factor of 2) than the sediment particle size, have shown inclination errors to be extremely

small. This is believed to be a result of the magnetic minerals aligning themselves within the interstitial spaces until compaction and cementation locks them in place. The error caused by compaction in most cases has been found to be small. Errors in declination are easily averaged out.

Since secondary effects such as weathering, metamorphism, heating or VRM can alter the primary NRM, a stability check is generally made before using magnetic data. Successively higher alternating field (AF) demagnetization and successively higher temperature (thermal) demagnetization techniques are widely used. Both methods determine the magnetic stability by measuring the resistance of NRM to heat and magnetically induced changes. Collinson et al. (1967), Nagata (1961), and Irving (1964) describe both methods.

PALEOMAGNETISM

Paleomagnetism is based on the use of NRM in various rock types throughout the geologic past. Oriented samples are collected from in situ outcrops, and the direction of the NRM vector is measured. A number of samples from the same outcrop should be averaged to mean out random errors in both the collection and measurement processes, and the way in which the rock has recorded the geomagnetic field. This NRM direction serves as a "spot" reading of the geomagnetic field.

A basic assumption of paleomagnetism is that the average geomagnetic field is that of a geocentric axial dipole (Briden, 1968; Creer, 1967; Runcorn, 1959a, b; Opdyke and Henry, 1969; and others). The

position of a geocentric dipole axis is easily calculated from a magnetic vector at a given site, using the basic equation

$$\tan I = 2 \tan \lambda$$

where I is the vector inclination and λ is the paleolatitude. This pole, calculated from a spot paleomagnetic reading, is called a virtual geomagnetic pole, or VGP (after Cox and Doell, 1960), because it probably does not represent a true pole. If the secular variation component of the earth's field (which can be averaged in about 10^4 years) is taken into account, by averaging poles from rock units that span at least 10^4 years, the pole positions are called paleomagnetic poles (Irving, 1964) and probably represent true poles. Statistical treatment is required because of the dispersion of paleomagnetic directions which can be the result of a variety of factors--such as secular variation, wandering of the rotational axis of the earth, magnetic reversals, and errors both experimental in nature and related to the acquisition of NRM. Excellent summaries of paleomagnetic dispersions and their relative importance are given by Doell and Cox (1963), Bingham (1971), Irving (1964), and others.

Paleomagnetic data which are assumed to have a Fisherian, or 'spherical normal' distribution (Fisher, 1953), can be treated by statistics that deal with the directions of unit vectors, i.e. points on a unit sphere. A set of statistical parameters, which have become nearly standard within the literature, make possible the treatment of paleomagnetic data (Irving, 1964; Bingham, 1971; and others). The best estimate of precision is $k = \frac{(N-1)}{(N-R)}$ where R is the length of the sum of N unit vectors whose directions correspond to the data points

on the sphere. The radius of the circle of confidence at the 95% level around the mean is

$$\alpha_{95} = \cos^{-1}\left[1 - \frac{N-R}{R}\left(\left(\frac{1}{1-.95}\right)^{\frac{1}{N-1}} - 1\right)\right] \approx \frac{140}{\sqrt{kN}} \quad .$$

TECHNIQUES

The methods and equipment used to collect and measure the samples for this study are similar to those used by others and are described in the literature (Collinson et al., 1967). The particular methods and equipment used in this study are described by Cameron (1970), Cameron and Stone (1970), and Bingham (1971).

Cores, 2.54 cm in diameter, were drilled by a gas powered backpack drill which drives a stainless steel shaft tipped by diamonds set in a phosphor-bronze matrix. Doell and Cox (1967) describe a similar drill. While still attached to bedrock, the core is fitted with a slotted copper tube through which a fiducial line is inscribed with a brass wire. The fiducial line is oriented with respect to magnetic north, topographic features, the sun, and the horizontal from a moveable platform at the top of the tube which has an inclinometer and mounts for both a Brunton compass and a sun compass.

The cores, cut into 2.1 cm discs and marked, were measured in either a 5 Hz spinner magnetometer (Foster, 1966) or a 5 Hz Schonstedt Model SSM-1A spinner magnetometer, which has a sensitivity of 10^{-9} emu. Errors due to orientation in the field and positioning in the spinner magnetometer are thought to average less than 2 degrees (Doell and Cox, 1963). Measurement error is less than 5 degrees.

Cores were collected in groups, referred to here as sites, with an attempt to collect three cores or more from a stratigraphic level, and to sample as many levels as time and conditions permitted. The spacing laterally within a site was usually at least 100 feet, and geographic spacing was achieved where possible by collecting at more than one site, separated by more than one quarter mile, within the same rock unit. The number of cores collected per site, depending largely on logistic circumstances, numbered usually ten or more but never less than six, as per Doell and Cox (1963). Generally samples from a single rock unit at a given area were treated together, statistically unweighted, if the individual sites were one mile or less from each other. When the sites within the same rock unit from the same sampling area have a separation of greater than one mile, the samples were treated statistically unweighted within the site, and the site means were then used in comparison with other areas (Irving, 1964). Treatment to the contrary is noted within the description of individual areas. Cores were taken only from in situ outcrops and at least one quarter mile from faulting, in an attempt to avoid local rotation, although in many areas in Alaska geologic mapping or exposure is insufficient to assess this properly.

The samples, tumbled about two mutually perpendicular axes in field free space, were subjected to sucessively higher levels of alternating (60 Hz) field (AF) demagnetization for magnetic 'cleaning' and as a stability test. Low-field bulk susceptibility measurements for the samples were also made with a total and anisotropic susceptibility meter (Collinson, et al., 1963; Cameron, 1970; Cameron and Stone, 1970).

Magnetic vector measurements, bedding orientations, and orientation calculations were used to calculate final magnetic direction and VGP on an IBM 360/40 electronic digital computer. Statistical parameters were calculated on the same computer, and the results were hand plotted on a Wulff stereographic projection.

APPLICATION TO STRUCTURAL PROBLEMS

Irving (1964) describes many applications of paleomagnetism to structural problems, including detection of relative rotation about a vertical axis. This rotation may be on the local fault block or regional oroclinal scale, and is detected from the divergence of declinations between two different areas of the same age. Of course, the method is dependent upon the accuracy with which the declination is measured. Irving (1964) points out that $\delta D = \alpha_{95} \sec I$. Thus, when the inclination is steep, the declination is poorly defined.

In several areas where oroclinal bending has been postulated on geological grounds, paleomagnetism has shown rotation of a similar magnitude. Geologic and paleomagnetic evidence together suggest that Japan underwent an early Tertiary bending of 58 degrees (Irving, 1964). Divergent declinations on the Eocene Siletz River volcanics of Oregon compared to the Eocene Green River Formation of Colorado, indicate a 63 degree clockwise rotation between the two areas (Irving, 1964). This rotation corresponds to the rotation required in the formation of the Mendocino orocline postulated by Carey (1958). A 35 degree counterclockwise rotation of Spain, the result of the formation of the Biscay sphenochasm, was postulated

by Carey (1958) to have taken place since the Mesozoic. Carey based his idea largely on fit; however rotation of this amount brings declinations of Permian formations from Spain into agreement with those from Northern Europe (Irving, 1964).

The technique used in this study will consist of both a comparison of the declinations from sites throughout Alaska and an analysis of the VGP's of North America, Asia, and Europe, with respect to Alaska. A systematic change in declination would be the only acceptable proof of oroclinal bending. On the other hand, a lack of significant change would mean no bending or one too small to be detectable with these data. Scattered declinations could be the result of local fault block rotation or one or more of the undetected factors that affect NRM as discussed above, and would be inconclusive.

The VGP for Alaska will give its latitude with respect to the north pole assuming the geocentric axial dipole. By comparison with the equivalent North American pole position, Alaska's relative latitude with respect to North America can also be determined, as can the relationships between Asia, Europe, and North America.

III. MESOZOIC PALEOMAGNETIC RESULTS FROM ALASKA

ALASKA PENINSULA

Over 260 samples were collected at 21 different sites from the Chignik Lake, Chignik Lagoon, Puale Bay, Cape Kekurnoi, Katmai, and Tuxedni Bay areas on the Alaska Peninsula (Fig. 3-1). Rocks of Permian, Triassic, Jurassic, and Cretaceous ages were represented. The majority of the samples were sedimentary rocks with fossil age control, but some K-Ar dated intrusive rocks were also collected.

Geologic setting of the Alaska Peninsula

The largest part of this geologic summary was taken from C. A. Burk's G.S.A. Memoir 99, Geology of the Alaska Peninsula-Island Arc and Continental Margin (1965), which includes an excellent bibliography of previous geologic work on the Alaska Peninsula.

Permo-Triassic detrital volcanic rocks, extrusive flows, and limestones are exposed at various localities along the Alaska Peninsula, and smaller amounts of sandstones, argillites, slates, and graywackes occur locally. These rocks, part of which are metamorphosed, constitute the oldest rocks on the Alaska Peninsula, and appear to be at least 10,000 feet thick in the Puale Bay region. Their age is determined, due to lack of fossil control, from their relationship to the 1500 feet of overlying late Triassic limestone and chert.

The volcanic-rich rock units of early Jurassic age conformably overlie the late Triassic strata. Along the southern coast of the

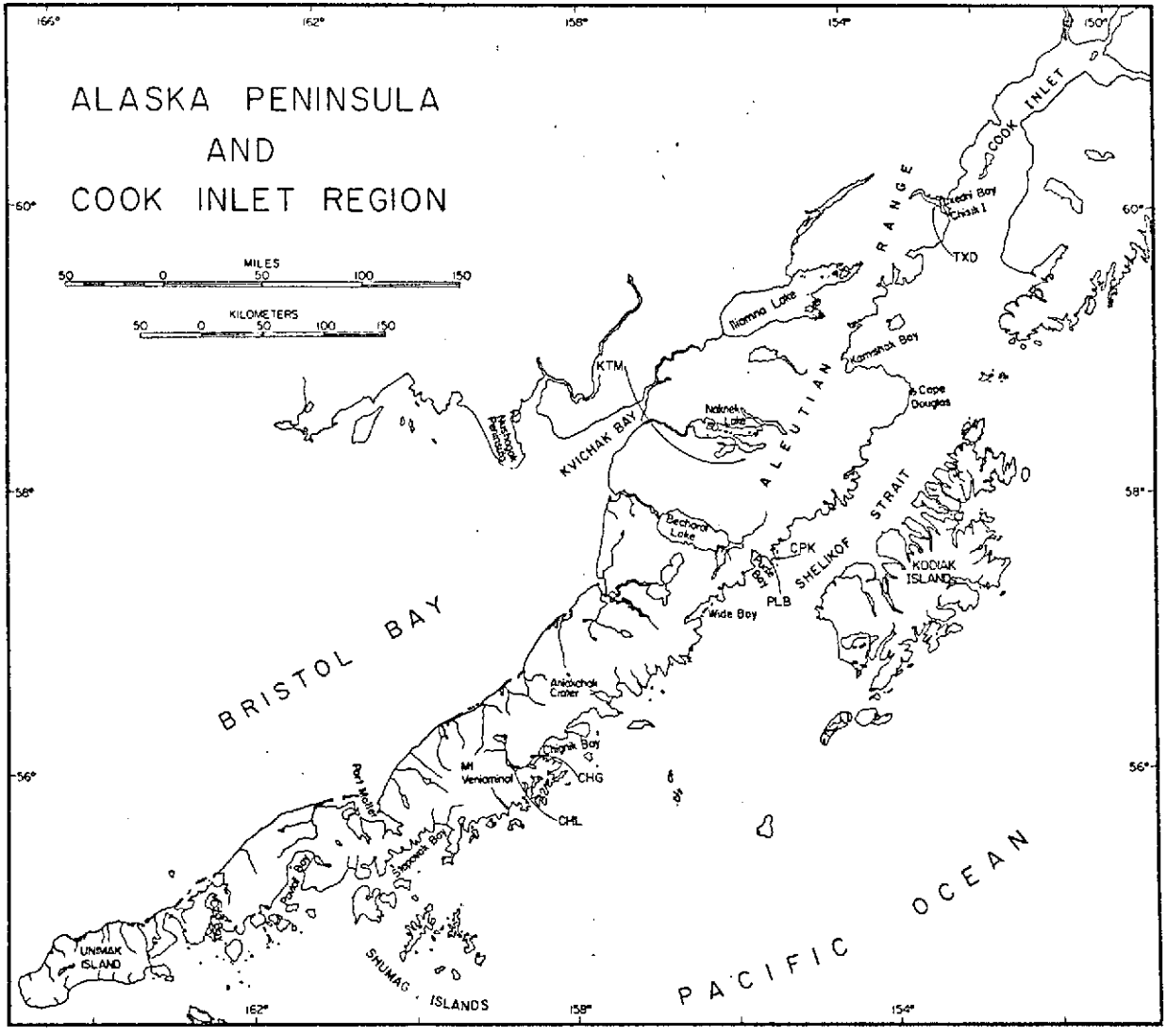

Figure 3-1. Location map for place names and sampling localities on the Alaska Peninsula and in the Cook Inlet Region.

Alaska Peninsula the fossiliferous early Jurassic consists of tuffaceous sandstone, calcareous sandstone and shale, limestone, and volcanic conglomerate grading upward to fine-grained shales and sandstones. Inland, porphyritic flows (latite to basalt), breccias, and tuffs form up to 8000 feet of section, and from their stratigraphic position are presumed to be of early Jurassic age.

A very complete section of middle and late Jurassic sedimentary rocks is well-exposed in the Tuxedni Bay region, and conformably overlies the early Jurassic. Part of this section, the Tuxedni group, is composed of siltstones, arkoses, graywacke sandstones, conglomerates, massive sandstones, and shales, and has been divided into six formations (Detterman and Hartsock, 1966). Conformably overlying the Tuxedni group, the Chinitna Formation--massive to thinly bedded siltstone, ellipsoidal limestone concretions and sandstone--is divided into two members (Detterman and Hartsock, 1966). A total of at least 10,000 feet of the combined Tuxedni group and the Chinitna formation are exposed at Tuxedni Bay. Further southwest along the Peninsula, early Jurassic formations occur only locally, leaving only the late Jurassic.

The upper Jurassic Naknek Formation conformably overlies the Chinitna Formation, and is composed of a basal conglomerate, arkosic sandstone, and siltstone. Exposed the entire length of the Alaska Peninsula, the Naknek Formation forms a distinctive marine rock type that reaches its maximum thickness of 10,000 feet in the Wide Bay area. Southwest of Wide Bay the late Jurassic-early Cretaceous Staniukovich Formation conformably overlies the Naknek. The Stan-

iukovich Formation, composed of fine-grained feldspathic sandstones and arkoses, reaches a maximum thickness of 2000 feet in the Wide Bay area and thickens and thins irregularly to the southwest. In the Cape Douglas area the Staniukovich is conformably overlain by the lower Cretaceous Herendeen limestone.

The sedimentary section on the southeastern shore of the Alaska Peninsula, from the middle Jurassic through the early Cretaceous, represents sediments deposited in a rapidly subsiding area close to an eroding granitic source. The Aleutian Range batholiths of Jurassic age (Reed and Lanphere, 1969) separated from the sedimentary sequence by the Bruin Bay fault appear to have served as the source area. The Bruin Bay fault, a high-angle reverse fault upthrown on the northwest side, uplifted the granitic body relative to the Jurassic sediments. On the basis of the sedimentary record, the fault must have become active in the mid to late Jurassic time. The Jurassic batholiths, although not exposed southwest of Wide Bay, must now be covered by Tertiary and Quaternary age rocks, because the sedimentary sequence contains a record of granitic erosion similar to that northeast of Wide Bay. Similarly, the Bruin Bay fault is not exposed southwest of Becharof Lake.

Uplift and minor deformation must have occurred on the Alaska Peninsula in the mid Cretaceous, because all late Cretaceous rocks rest unconformably on early Cretaceous rocks. The late Cretaceous Chignik Formation, exposed irregularly southwest of Wide Bay, is composed of 1250 feet of a thick basal coal member and 2000 feet of argillaceous sandstone and siltstone. The Hoodoo Formation confor-

mably overlies the Chignik Formation and consists of 2000 feet or more of siltstone and shale. The Kaguyak Formation exposed at Cape Douglas is equivalent, in age and composition, to the Hoodoo Formation.

The Tertiary is characterized by an almost complete rock record, consisting largely of basaltic and andesitic flows, sills and their sedimentary debris. Paleocene rocks lie with a slight unconformity on the upper Cretaceous or older rocks, indicating that the Alaska Peninsula underwent minor uplift and erosion. From Wide Bay southwest to Pavlof Bay, 5000 feet of non-marine volcanic siltstones and interbedded flows and sills, called the Tolstoi Formation, were deposited during the Paleocene and early Eocene. The Oligocene Stepovak Formation, 15,000 to 20,000 feet of volcanic sandstone and conglomerate, conformably overlies the Tolstoi and is exposed southwest of Port Moller. Its age equivalent, the Meshik Formation, consists of 5000 feet of coarse volcanic debris, and extends from Port Moller to Wide Bay. In many areas it is impossible to separate the Stepovak and Tolstoi Formations; the combined Paleocene through Oligocene section has been called the Beaver Bay Group. The Miocene Bear Lake Formation, composed of 5,000 feet of marine and non-marine volcano-clastic material with chert and a basal conglomerate member locally, unconformably overlies the Stepovak Formation. The Bear Lake Formation is exposed from Aniakchak Crater southwest to the tip of the Peninsula.

During earliest Tertiary time a quartz diorite body was intruded into upper Cretaceous slate and graywacke on Kodiak Island. This perhaps corresponds to the slight uplift in the early Paleocene. The

slight deformation and uplift in late Oligocene-early Miocene time is thought to correspond to the intrusion of a mid Tertiary granodiorite body along the Pacific coast of the Alaska Peninsula.

The deformation responsible for most of the anticlinal and synclinal folding, and the local faulting associated with the anticlinal complexes, culminated in the Pliocene. From Kamishak Bay northeast along the west coast of Cook Inlet, a narrow strip of land southeast of the Bruin Bay fault has undergone tight anticlinal folding and three types of minor faulting (Detterman and Hartsock, 1966). Detterman and Hartsock (1966) describe cross faults, both normal and reverse, oblique to the trend of the Bruin Bay fault. These are thought to be due to differential uplift and stresses involved in the movement along the Bruin Bay fault. Hinge faults that have minor rotational movement, and normal faults that generally parallel the Bruin Bay fault, are present but do not create any major offsets.

From Kamishak Bay southwest to Becharof Lake folding is reduced to a broad anticline, the Kamishak anticline, and minor gentle folds that have a general homoclinal dip toward Shelikof Strait. Northwest of the Bruin Bay fault folding is local and generally restricted to early Mesozoic age rocks, and is thought to be due to the intrusion of the Jurassic Aleutian Range batholiths.

Southwest of Becharof Lake the style of folding changes. Three long anticlinal arches can be seen: one from Puale Bay to Aniakchak Crater area; one from Chignik Bay to Stepovak Bay; and one from Port Moller to Cold Bay. All are broad features with two anticlines and minor high-angle reverse faults on the southern margin.

Volcanism has continued from the Pliocene to the present, and is continuing along the length of the Alaska Peninsula. Quaternary and recent flows and associated pyroclastic material, glacial material, and stream deposits, make up the recent rock record on the Alaska Peninsula.

Sites on the Alaska Peninsula

Chignik Lake (CHL)

Fifty-two cores from the Upper Jurassic Naknek Formation were collected at five sites along the northeast shore of Chignik Lake. These sites are separated geographically by approximately four miles. It is difficult to estimate the total number of stratigraphic feet represented by all five sites; however, each site represents at least 10 stratigraphic feet. The samples collected consist of fine- to coarse-grained sandstone, composed of sub-angular quartz, plagioclase, biotite, opaques, and rock fragments of granitic, volcanic, and metamorphic rocks. The beds for the three sites at the northwest end of the lake have a 5 to 15 degree dip to the northeast, and the two sites at the southeast end of the lake have dips of 10 degrees to the southwest and southeast, respectively.

The vector directions and pole positions for CHL-1 to 5 at NRM and demagnetization levels are given in Table 3-1, and are shown in Figures 3-2 to 3-6. The mean NRM P (with respect to the present horizontal) direction does not lie along the present axial dipole field direction. An AF level of 95 oe caused a slight shift in the position of the mean and probably removed any VRM components or

Explanation to Tables 3-1 to 3-10

Location gives local name and approximate latitude and longitude of collection locality, number of individual sites, and age and name of unit from which the samples were collected.

Treatment explanation is as follows:

NRM P - mean NRM vector direction with respect to present horizontal (not given if bedding is horizontal).

NRM - with respect to ancient horizontal.

AF - alternating field demagnetization followed by the level in oersteds (peak to peak).

N - number of samples used in the determination of the mean directions.

D - mean declination in degrees east of true north.

I - mean inclination in degrees below (+) or above (-) horizontal.

A95, K - radius in degrees of the 95% circle of confidence about the mean paleomagnetic field direction, and K, the Fisher parameter, k.

LAT, ELONG - coordinates of the mean virtual geomagnetic pole position in degrees north (+) or south (-) latitude, and degrees east longitude.

A95, K - radius in degrees of the 95% circle of confidence about the mean paleomagnetic pole position, and K, the Fisher parameter, k.

TABLE 3-1

PALEOMAGNETIC DIRECTIONS AND POLE POSITIONS

LOCATION	TREATMENT	N	DIRECTION D	DIRECTION I	DIRECTION A95	DIRECTION K	POLE POSITION LAT	POLE POSITION ELONG	POLE POSITION A95	POLE POSITION K
CHL-1 - CHIGNIK LAKE, ALASKA	NRM P	10	26	60	10.6	21.5	67	322		
(56.3N,201.2E)	NRM	10	18	69	10.7	21.5	78	285	16.5	9.5
1 SITE UPPER JURASSIC NAKNEK FM	AF 48 OE	10	5	72	8.0	37.8	86	262	12.9	15.0
	AF 95 OE	10	1	70	6.8	51.2	89	339	10.8	21.0
	AF 190 OE	10	7	63	21.2	6.2	80	352	18.3	8.0
	AF 380 OE	10	5	63	7.2	45.7	79	1	10.6	21.8
CHL-2 (56.3N,201.1E)	NRM P	10	54	60	14.2	12.6	52	292		
	NRM	10	54	55	14.2	12.6	50	296	18.4	7.8
1 SITE	AF 48 OE	10	59	57	13.3	14.2	48	289	18.2	8.0
	AF 95 OE	10	62	61	13.5	13.8	49	282	19.5	7.1
	AF 190 OE	10	75	54	19.8	6.9	39	280	25.1	4.7
	AF 380 OE	10	88	41	26.9	4.2	22	279	30.8	3.4
CHL-3 (56.3N,201.1E)	NRM P	11	32	61	16.4	8.7	65	313		
	NRM	11	49	59	16.4	8.7	56	291	22.6	5.0
1 SITE	AF 48 OE	11	54	49	21.9	5.3	46	300	23.0	4.9

TABLE 3-1 (CONTINUED)

PALEOMAGNETIC DIRECTIONS AND POLE POSITIONS

LOCATION	TREATMENT	N	DIRECTION D	I	A95	K	POLE POSITION LAT	ELONG	A95	K
CHL-3 (CONT'D)	AF 95 OE	11	47	58	29.4	3.4	57	297	33.3	2.8
	AF 190 OE	11	18	46	38.6	2.4	62	340	38.3	2.4
	AF 380 OE	11	27	33	42.5	2.1	51	340	39.0	2.3
CHL-4 (56.3N,201.1E)	NRM P	9	77	53	15.5	12.0	34	281		
	NRM	9	81	38	15.5	12.0	24	285	14.7	13.2
1 SITE	AF 48 OE	9	95	33	20.3	7.4	13	275	17.6	9.5
	AF 95 OE	9	90	32	23.1	5.9	15	280	19.3	8.1
	AF 190 OE	9	87	5	33.4	3.3	4	292	26.6	4.7
	AF 380 OE	9	84	-8	28.5	4.2	-1	298	25.2	5.1
CHL-5 (56.3N,201.1E)	NRM P	12	63	59	15.0	9.3	47	286		
	NRM	12	70	45	15.0	9.4	33	290	17.7	7.0
1 SITE	AF 48 OE	12	83	45	15.3	9.0	26	280	17.8	6.9
	AF 95 OE	12	81	39	16.6	7.8	23	284	18.0	6.8
	AF 190 OE	12	70	36	19.3	6.0	29	294	18.2	6.7
	AF 380 OE	12	66	31	26.9	3.6	30	302	24.9	4.0

Explanation to Figures 3-2 to 3-16, 3-18 to 3-22, and 3-24

Paleomagnetic data for the particular sampling locality are shown according to the following notation:

NRM P - Mean NRM vector direction with respect to present horizontal (not given if bedding is horizontal).

NRM - NRM magnetic vector directions of the samples and their mean, with respect to ancient horizontal.

$M \times 10^{-6}$ emu/cm^3 - Magnetic intensity vs. alternating field demagnetization level (oersteds, peak to peak), and the corresponding change in directions of magnetization for pilot samples during AF demagnetization.

Demagnetization - Mean vector direction after AF demagnetization at the indicated level (oersteds, peak to peak). This vector direction and its corresponding VGP (not shown) are used in the analysis of results presented in Chapter IV.

Plots are shown on Wulff stereonets with solid circles indicating lower (+) hemisphere and open circles indicating upper (-) hemisphere.

A hexagon, solid or open as above, indicates the mean vector directions; a circle of radius α_{95} (except where noted) is drawn about the mean. Mean data are from relevant table.

X gives the position of the present axial dipole field.

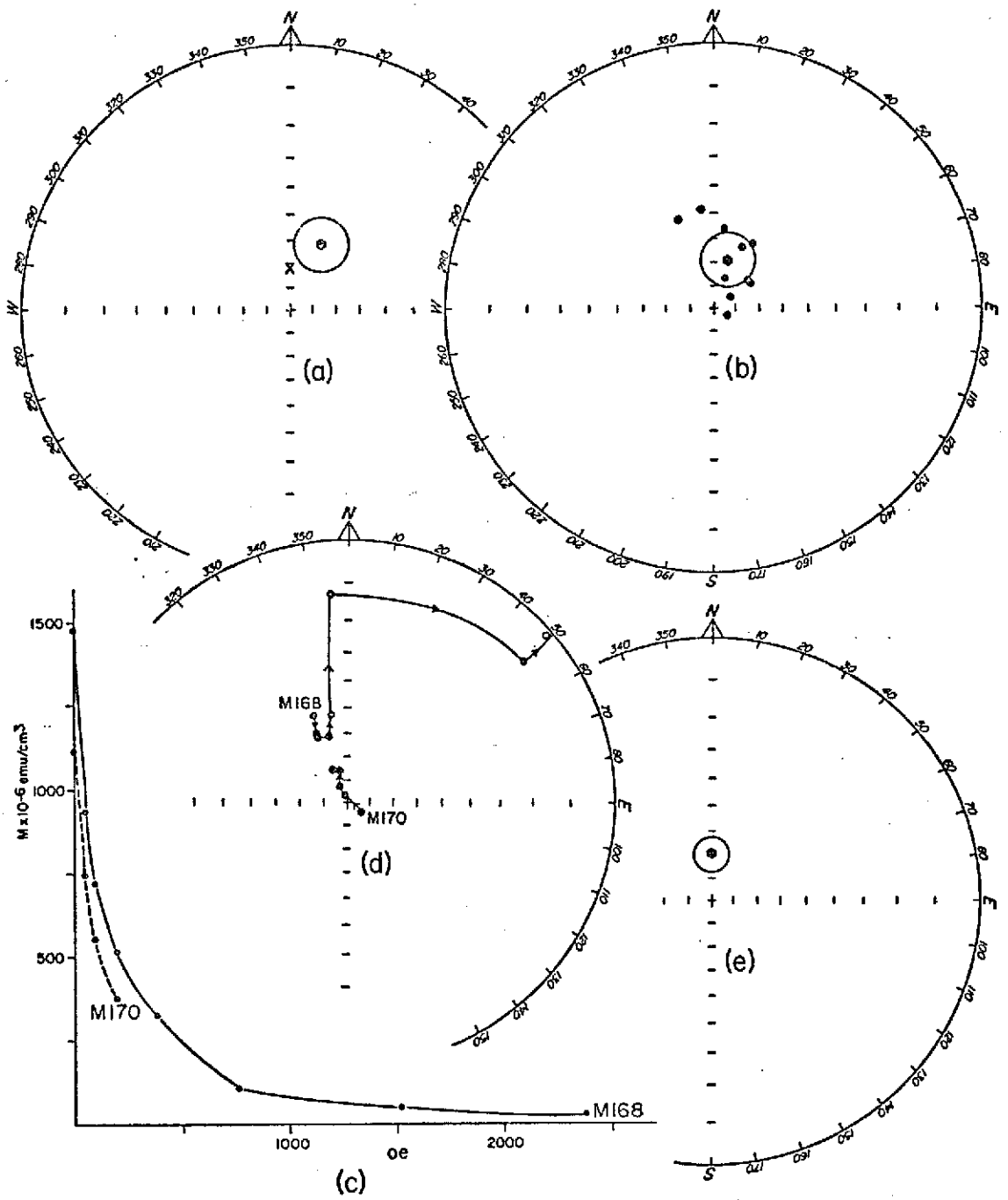

Figure 3-2. Paleomagnetic data for CHL-1, Chignik Lake, Alaska. (a) NRM P. (b) NRM. (c) Magnetic intensity and (d) directions of pilot samples during AF demagnetization. (e) After demagnetization at 95 oe.

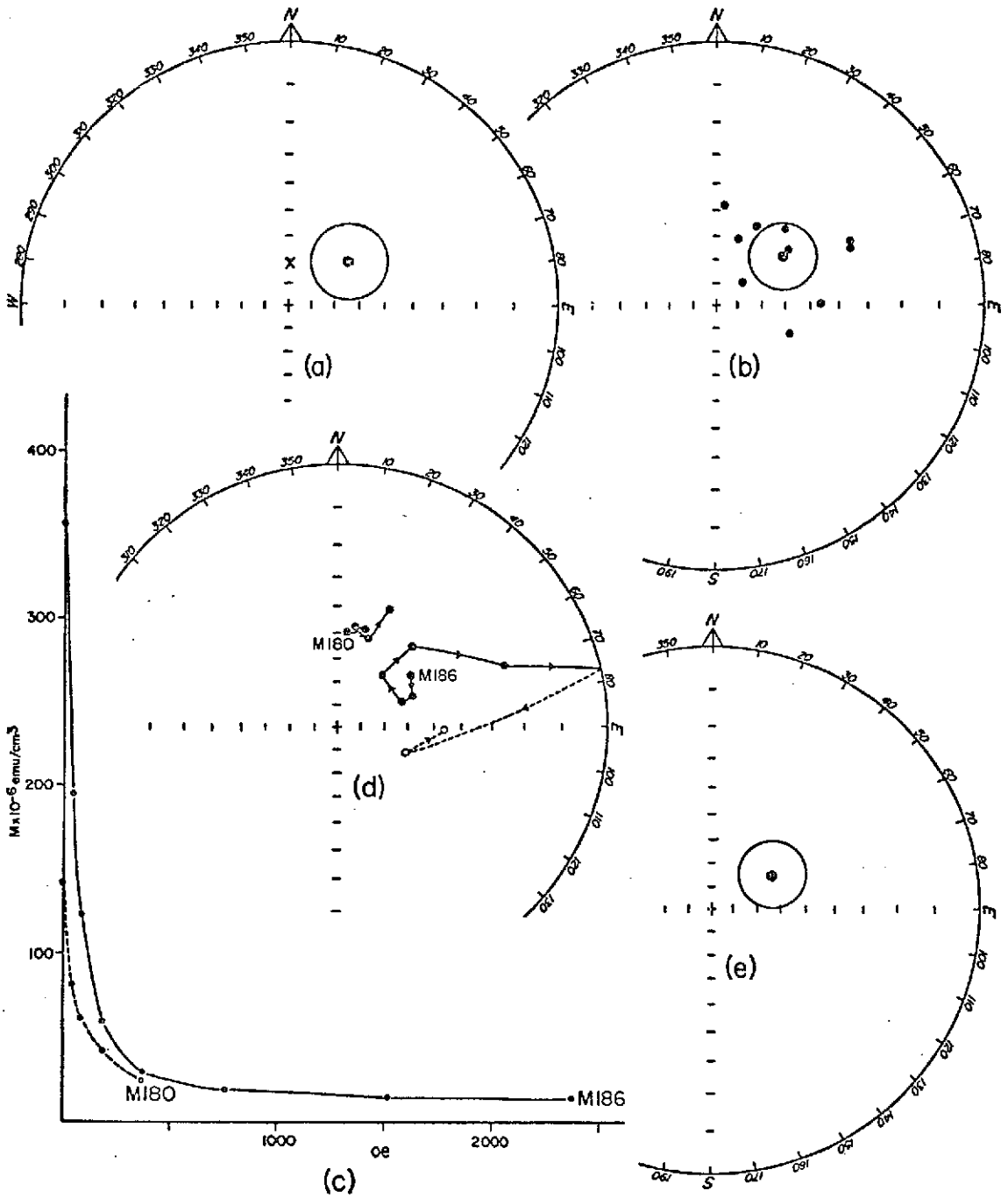

Figure 3-3. Paleomagnetic data for CHL-2, Chignik Lake, Alaska. (a) NRM P. (b) NRM. (c) Magnetic intensity and (d) directions of pilot samples during AF demagnetization. (e) After demagnetization at 95 oe.

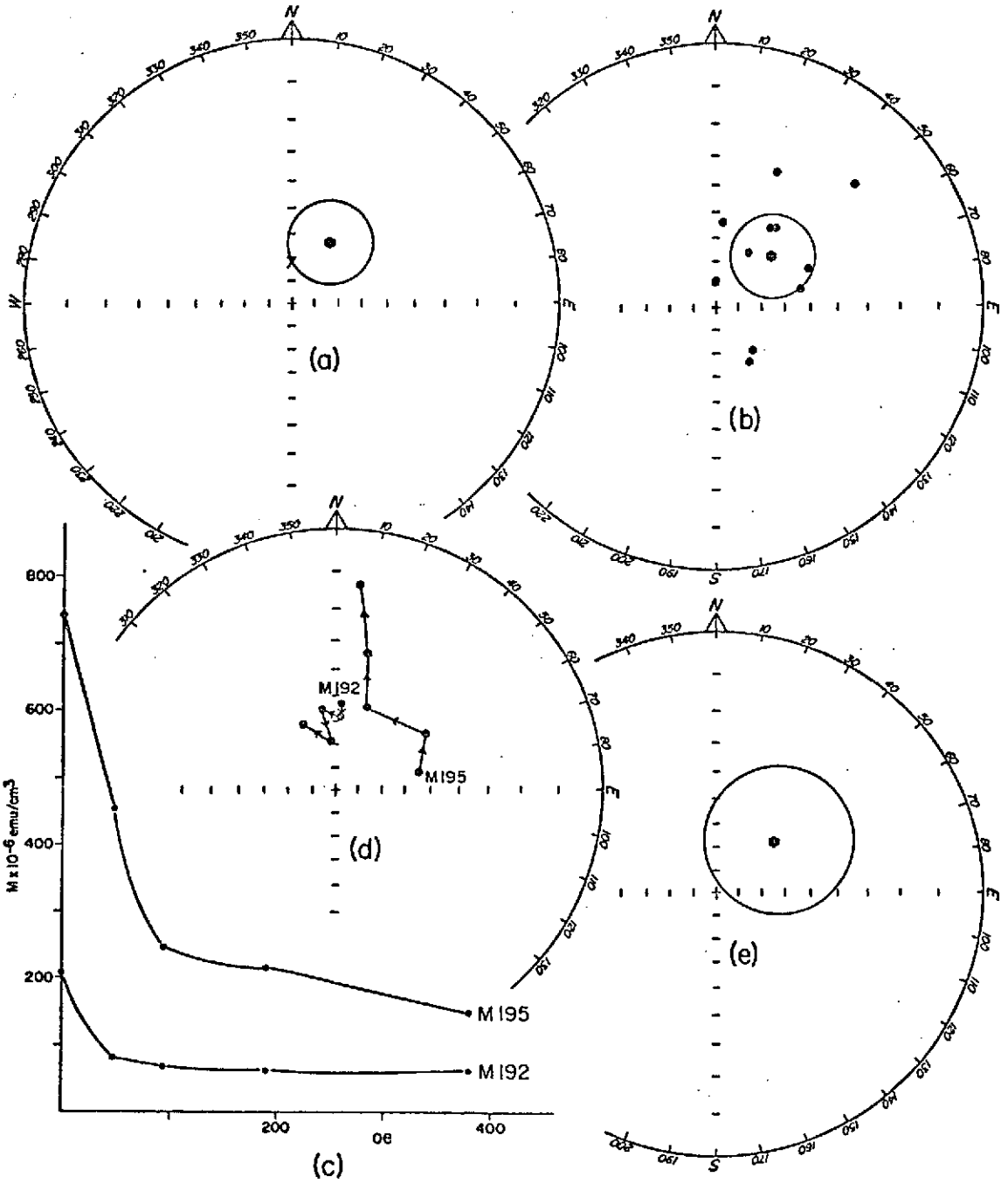

Figure 3-4. Paleomagnetic data for CHL-3, Chignik Lake, Alaska. (a) NRM P. (b) NRM. (c) Magnetic intensity and (d) directions of pilot samples during AF demagnetization. (e) After demagnetization at 95 oe.

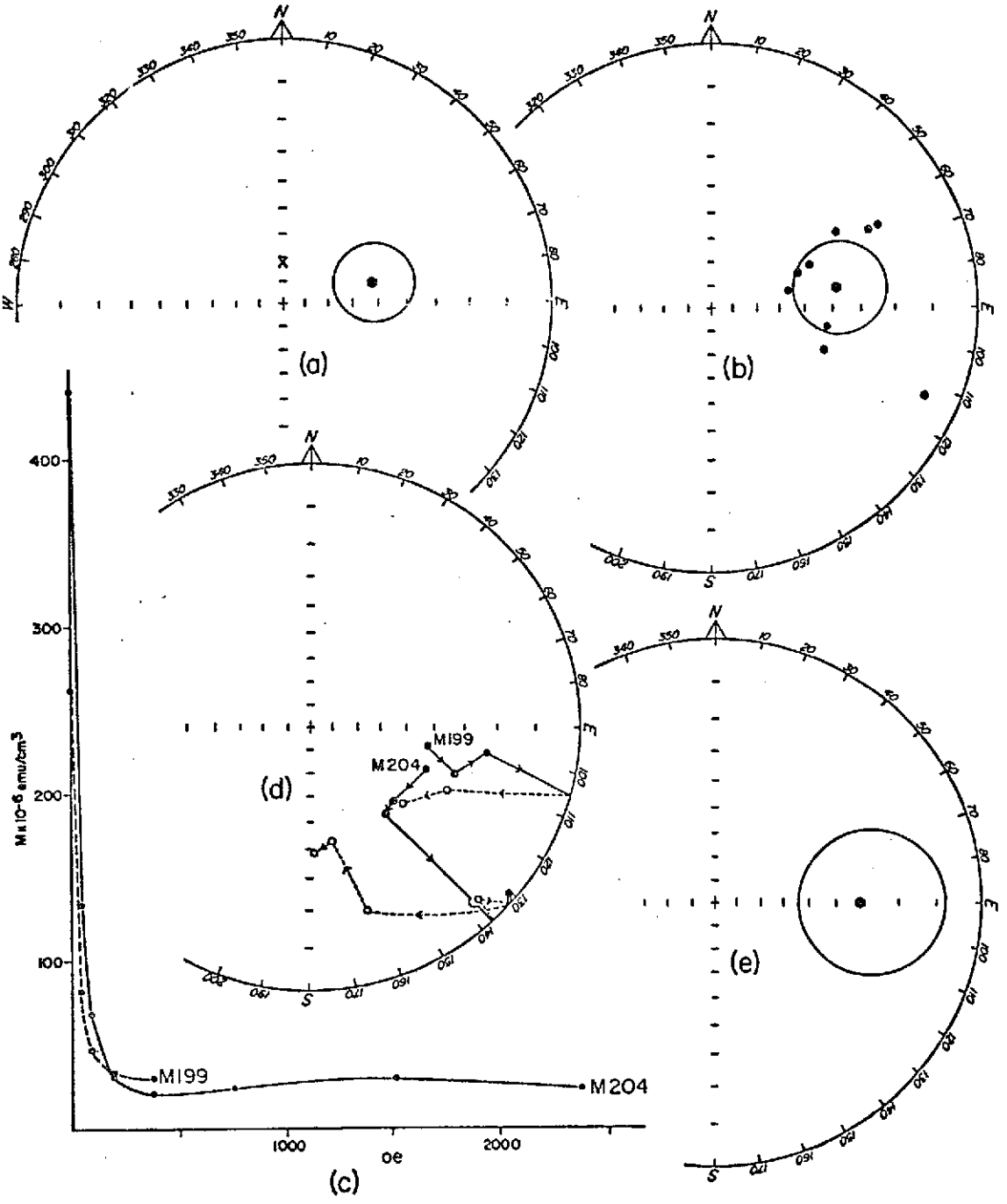

Figure 3-5. Paleomagnetic data for CHL-4, Chignik Lake, Alaska. (a) NRM P. (b) NRM. (c) Magnetic intensity and (d) directions of pilot samples during AF demagnetization. (e) After demagnetization at 95 oe.

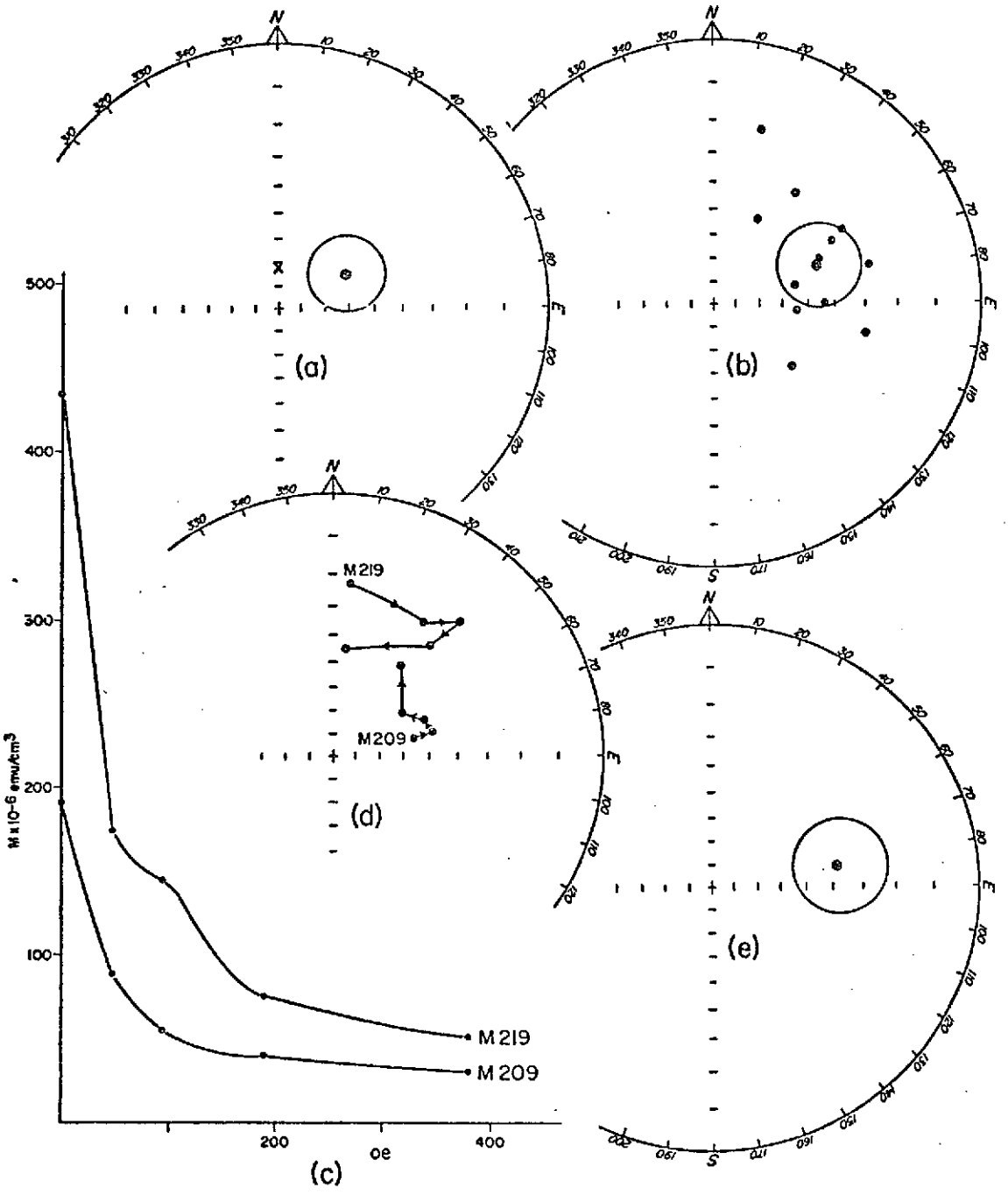

Figure 3-6. Paleomagnetic data for CHL-5, Chignik Lake, Alaska. (a) NRM P. (b) NRM. (c) Magnetic intensity and (d) directions of pilot samples during AF demagnetization. (e) After demagnetization at 95 oe.

secondary magnetizations present. Demagnetization in successively higher alternating fields up to 380 oe only slightly changed the mean directions of magnetization but increased the scatter, due in part to the increasing 'noise' level as the intensity decreases. Above 380 oe up to 2380 oe, the directions became extremely scattered and three samples became reversed. Intensity curves for AF demagnetization levels are shown in Figures 3-2 to 3-6. Mean of the NRM intensity for CHL-1 to 5 is 560 x 10^{-6} emu/cm^3, and the mean susceptibility is 3000 x 10^{-6} emu/cm^3. The scatter of CHL-3 after demagnetization at an AF of 95 oe is large, but the other sites after the same treatment are a good representation of the upper Jurassic VGP.

Chignik Lagoon (CHG)

On the northwest shore of Chignik Lagoon, on both sides of Dago Point, 21 samples were collected from the Chignik Formation of upper Cretaceous age. These samples represent approximately 10 stratigraphic feet per site, and are from two sites about one mile apart. At the northeast site, CHG-1, a very fine-grained sandstone composed of angular quartz, orthoclase, biotite, chlorite, opaques, and plagioclase in an argillaceous matrix was sampled. The southwest site, CHG-2, is a fine-grained carbonaceous sandstone, composed of quartz, plagioclase, biotite, epidote, and opaques in an argillaceous matrix. The beds dip southeast at 15 degrees. A stratigraphic section for this area has been described by Keller and Cass (1956). CHG-1 is one quarter of a mile south of a dip-slip fault which is upthrown on the north.

CHG vector directions and pole positions are given in Table 3-2 and shown in Fig. 3-7. CHG-2 had a mean NRM P that was nearly parallel to the present axial dipole field direction, and a demagnetization at 48 oe removed a present field component from the mean vector direction. Although the mean NRM positions for CHG-1 and 2 were divergent, after demagnetization their mean vector directions converged. Thus CHG-1 and 2 can be treated as a single site. Four of the vector directions were significantly different from the mean (>60°) and were omitted from the final mean. This had negligible effect on the position of the mean, but considerably improved the precision. The NRM intensity of the rocks averaged 6×10^{-6} emu/cm^3, and after demagnetization at 48 oe was too weak to demagnetize further. The mean susceptibility for these samples was 70×10^{-6} emu/cm^3. Thus it would seem that although the samples' intensity was weak, their mean vector direction is a fair approximation of the VGP during the upper Cretaceous.

Puale Bay (PLB)

From the upper Triassic limestone exposed near the entrance on the northeast shore of Puale Bay, 53 cores were collected at two different sites about a half-mile apart. PLB-1 represents over 100 feet of section, including 50 feet of volcanic agglomerate, and PLB-2 about 25 feet of section. The beds at PLB-1 dip nearly west at approximately 13 degrees, and PLB-2 has beds dipping west-southwest at 22 degrees. The limestone consists of round aggregates of calcium carbonate and opaques, probably hematite, in an argillaceous matrix.

TABLE 3-2

PALEOMAGNETIC DIRECTIONS AND POLE POSITIONS

LOCATION	TREATMENT	N	DIRECTION D	I	A95	K	POLE POSITION LAT	ELONG	A95	K
CHG-1 - CHIGNIK LAGOON, ALASKA	NRM P	10	39	53	19.7	7.0	55	318		
(56.3N,201.4E)	NRM	10	53	50	19.5	7.1	46	299	24.5	4.8
1 SITE										
UPPER CRETACEOUS CHIGNIK FM	AF 48 OE	10	54	30	17.5	8.6	33	312	18.4	7.9
CHG-2	NRM P	11	175	15	29.6	3.3	-30	210		
(56.3N,201.4E)	NRM	11	173	7	29.6	3.3	-26	210	24.7	4.4
1 SITE	AF 48 OE	11	24	24	53.7	1.7	42	349	49.7	1.8
CHG-1&2	AF 48 OE	21	43	29	24.1	2.7	38	325	23.6	2.8
(MINUS 4 SAMPLES)	AF 48 OE	17	48	31	13.1	8.4	37	319	13.5	7.9

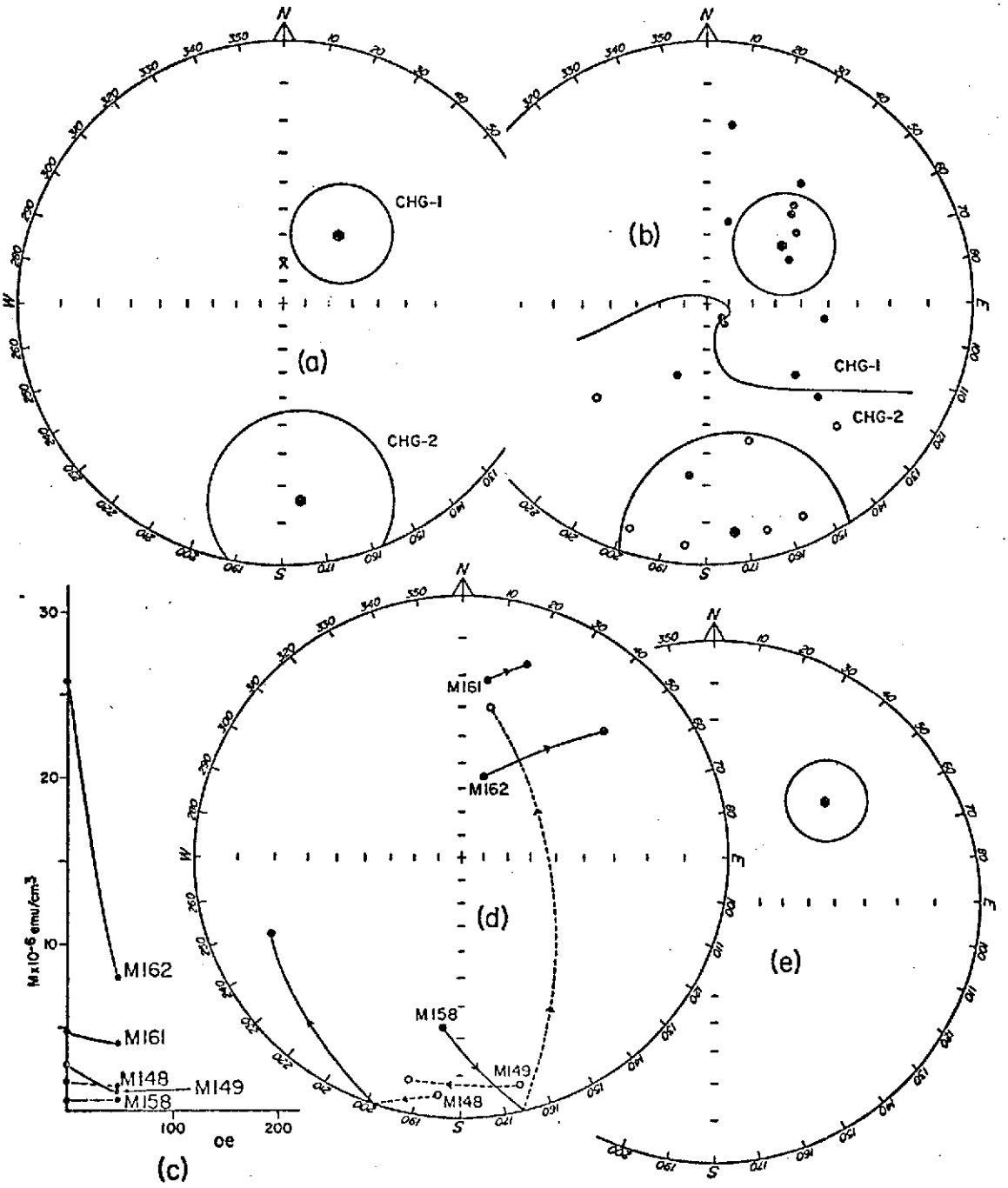

Figure 3-7. Paleomagnetic data for CHG, Chignik Lagoon, Alaska. (a) NRM P. (b) NRM. (c) Magnetic intensity and (d) directions of pilot samples during AF demagnetization. (e) CHG-1 and 2 after demagnetization at 48 oe.

The vector directions and pole positions for PLB are given in Table 3-3, and plotted in Figure 3-8. The mean NRM P direction was nearly parallel to the present axial dipole field direction, and demagnetization at 48 oe did not move this significantly. These rocks had too small an intensity to demagnetize at a higher level. For these limestones the mean NRM intensity was 0.3×10^{-6} emu/cm^3 and their mean susceptibility was 4×10^{-6} emu/cm^3. These results are marginal and should be used only with reservation as an approximation of the upper Triassic VGP for this area.

Cape Kekurnoi (CPK)

A volcanic agglomerate of Permian age containing fragments of volcanic glass, plagioclase, olivine, augite, and opaques, well cemented together by calcium carbonate, was collected about a fourth of a mile north of Cape Kekurnoi (Fig. 3-1). The twelve cores collected represent approximately 10 feet of stratigraphic section. Bedding is horizontal.

The results from paleomagnetic measurements of the samples collected at CPK are presented in Table 3-4 and Figure 3-9. The mean NRM direction was significantly different than the present axial dipole field direction. On demagnetization at an AF of 150 oe the mean shifted; upon further demagnetization at an AF of 190 oe the scatter was reduced and the position of the mean did not change. The samples became unstable when they were demagnetized at an AF of 380 oe. The mean NRM intensity was 150×10^{-6} emu/cm^3 and the mean susceptibility was 1800×10^{-6} emu/cm^3. Both the behavior of the two pilot samples shown and the complete instability of the

TABLE 3-3

PALEOMAGNETIC DIRECTIONS AND POLE POSITIONS

LOCATION	TREATMENT	N	DIRECTION D	I	A95	K	POLE POSITION LAT	ELONG	A95	K
PLB - PUALE BAY, ALASKA	NRM P	53	37	79	8.6	6.2	71	247		
(57.7N,204.6E)	NRM	53	314	78	8.9	5.8	66	169	14.0	2.9
2 SITES UPPER TRIASSIC LIMESTONE	AF 48 OE	53	325	82	12.8	3.3	69	181	18.7	2.1

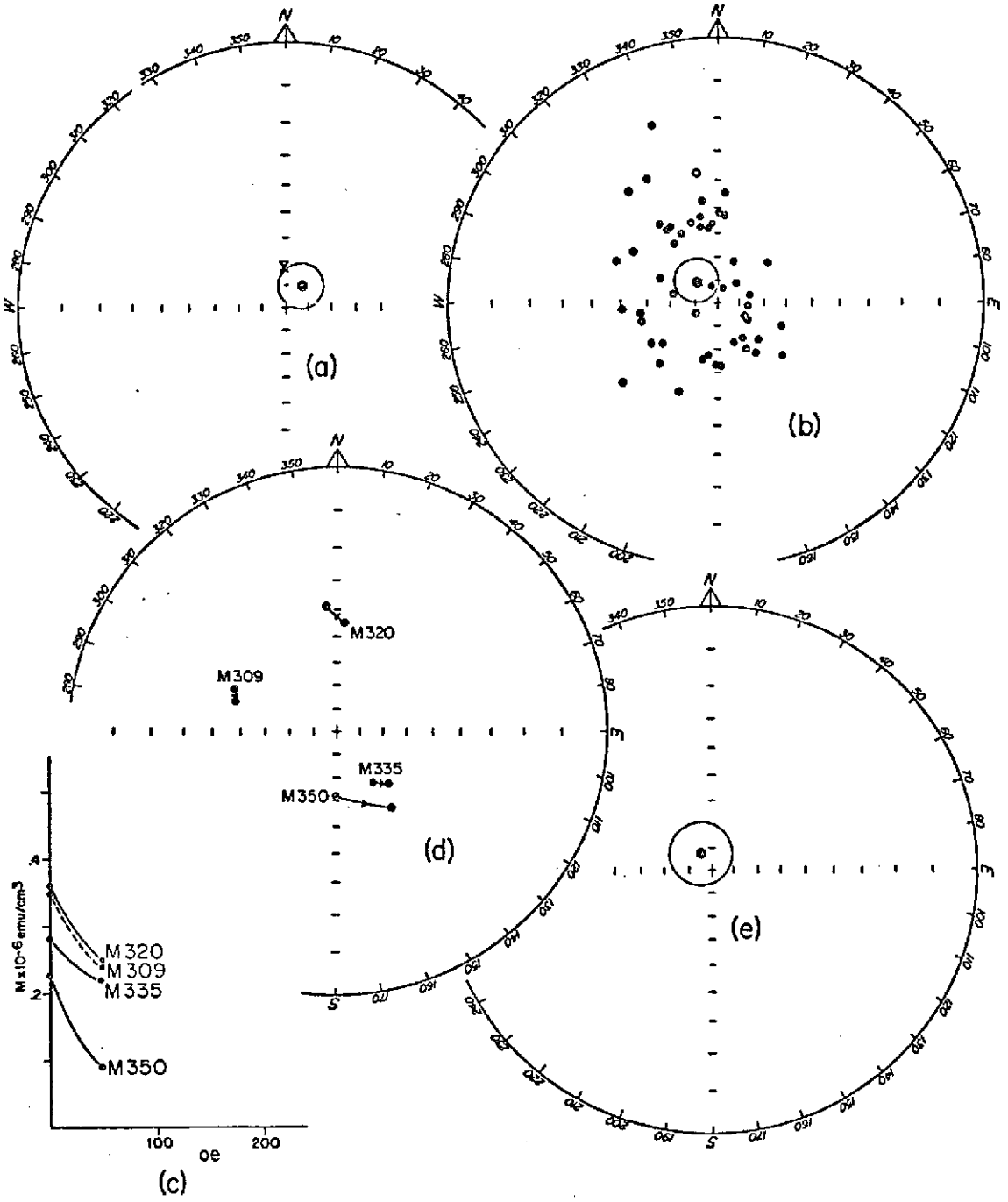

Figure 3-8. Paleomagnetic data for PLB, Puale Bay, Alaska. (a) NRM P. (b) NRM. (c) Magnetic intensity and (d) directions of pilot samples during AF demagnetization. (e) After demagnetization at 48 oe.

TABLE 3-4

PALEOMAGNETIC DIRECTIONS AND POLE POSITIONS

	LOCATION	TREATMENT	N	DIRECTION D	I	A95	K	POLE POSITION LAT	ELONG	A95	K
CPK -	CAPE KEKURNOI, ALASKA	NRM	12	292	68	12.3	13.5	55	138	17.8	6.9
	(57.7N,204.7E)	AF 150 OE	10	219	51	37.0	2.7	9	174	40.5	2.4
1	SITE	AF 190 OE	10	234	57	15.9	10.2	18	162	21.8	5.9
	PERMIAN VOLCANIC SEDS	AF 380 OE	10	207	28	74.9	1.4	-17	177	77.2	1.4

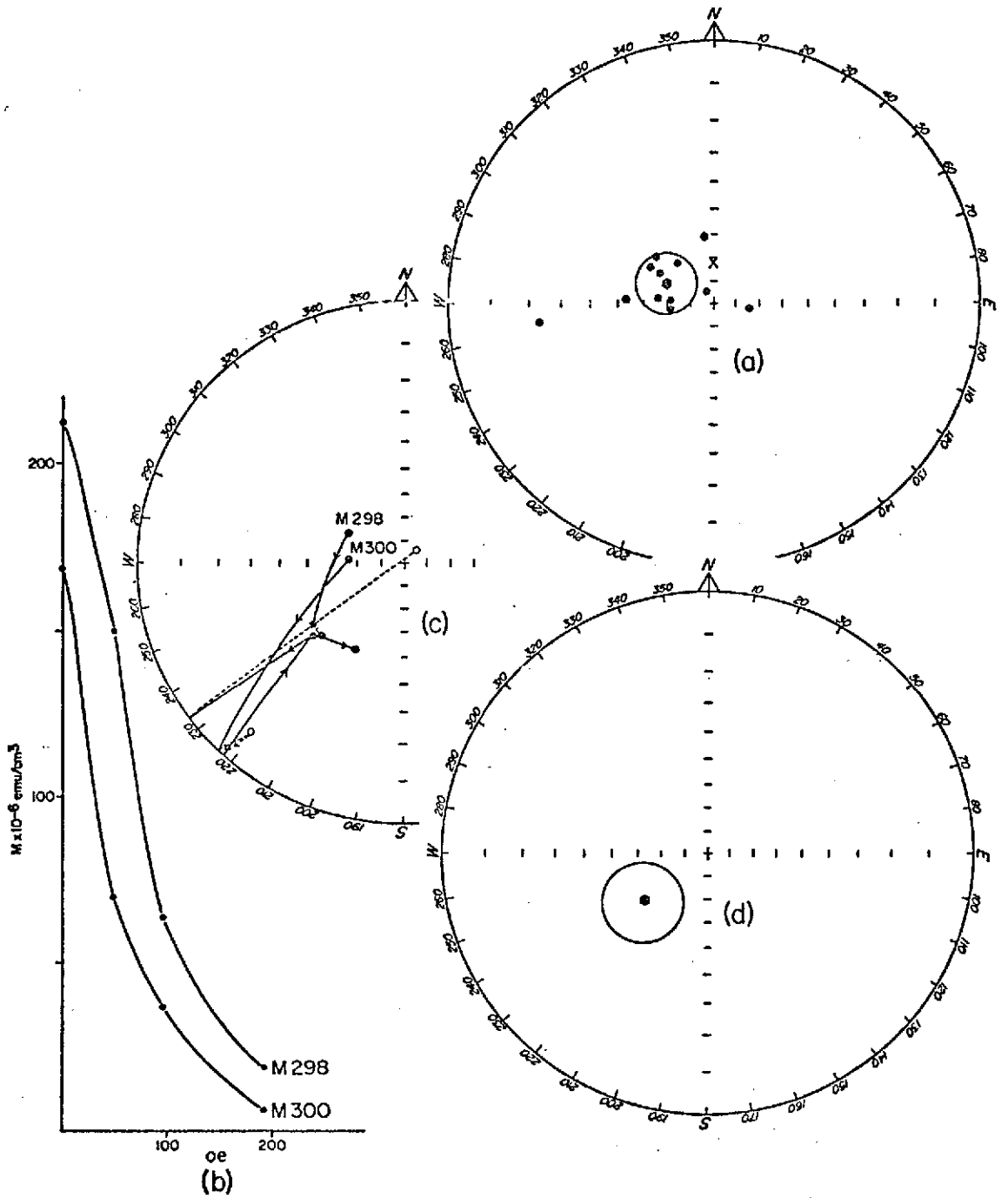

Figure 3-9. Paleomagnetic data for CPK, Cape Kekurnoi, Alaska. (a) NRM. (b) Magnetic intensity and (c) directions of pilot samples during AF demagnetization. (d) After demagnetization at 190 oe.

samples at an AF of 380 oe indicated a general instability of these samples. The results though shown for the NRM and at an AF of 190 oe must be considered to be marginal at best.

Katmai area (KTM)

Cores of the Jurassic Naknek Formation and Jurassic quartz diorite batholith were collected in the Katmai area. Twenty-six cores of gray fine-grained sandstone composed of quartz, plagioclase, and opaques from the Naknek Formation were collected from the lower part of the south flank of Mt. Katolinat. At this location the Naknek is intruded by rhyolite dikes and a hornblende andesite sill, with the sill crosscutting the dikes. The exact age of these intrusives is unknown, and the rocks are too altered to date by the K-Ar method. Samples were taken both of the intrusives (8 samples) and from the Naknek Formation at three different sites, which have a separation of approximately one-half mile and represent approximately 700 stratigraphic feet of section. The Naknek Formation dips at 3 degrees to the east-northeast throughout the section. Six cores of the Naknek Formation were also collected on cliffs above Margot Creek to the south-southeast of Mt. Katolinat. These samples represent approximately 10 feet of stratigraphic section in flat-lying beds of fine-grained sandstone.

Twenty-seven samples of mid Jurassic (Reed and Lanphere, 1969) quartz diorite were collected from the Aleutian Range batholith along the shores of the Iliuk Arm of Naknek Lake. Two sites were on the north shore, mid lake, at the base of Mt. La Gorce, and about 3 1/2 miles apart; and a third site is located on an island on the south

side of the lake, 7 1/2 miles from the entrance to Iliuk Arm. These sites are a mile or more from the trace of a fault (the Bruin Bay fault) that is upthrown on the northwest (Keller and Reiser, 1959). Although no attitude was observed in the reconnaissance study of the area made for this collection, it is assumed that the batholith has not tilted or rotated significantly since its emplacement. This assumption is probably correct considering that a part of the gentle deformation of the sediments in this area is thought to have been caused by emplacement of this batholith (Burk, 1965).

The results of NRM measurements and AF demagnetization are given in Table 3-5 and Fig. 3-10 to Fig. 3-12. The 95% confidence limit about the mean of NRM P for the samples from the three sites on Mt. Katolinat included the present axial dipole field direction. This mean (KTM-1) represents samples of the Naknek Formation only. It appears that the intrusives had little or no effect on the surrounding sediments. Cores from the sediments were at least six feet from the baked zone surrounding the intrusives. Demagnetization at an AF of 48 oe removed most of the present field component but produced a large scatter about the resulting mean. Upon demagnetization at an AF of 95 oe, the scatter was reduced, but further demagnetization at an AF of 142 oe created a nearly random distribution of directions. The mean NRM intensity for these samples was 30×10^{-6} emu/cm^3 and mean susceptibility was 90×10^{-6} emu/cm^3. Although the dispersion is large the moderately stable results obtained after demagnetization at an AF of 95 oe represent a tentative approximation of the upper Jurassic VGP.

TABLE 3-5

PALEOMAGNETIC DIRECTIONS AND POLE POSITIONS

LOCATION	TREATMENT	N	DIRECTION D	I	A95	K	POLE POSITION LAT	ELONG	A95	K
KTM-1 - KATMAI AREA, ALASKA		26	69	87	21.3	2.8	60	215		
(58.4N,204.6E)	NRM	26	64	85	21.3	2.8	66	231	29.6	1.9
3 SITES	AF 48 OE	24	38	12	46.8	1.4	28	332	41.1	1.5
UPPER JURASSIC NAKNEK FM	AF 95 OE	24	72	34	21.8	2.8	29	301	21.8	2.8
KTM-2	NRM	6	354	72	15.3	20.1	89	86	23.5	9.1
(58.4N,204.6E)	AF 48 OE	6	288	50	9.2	54.3	37	118	9.9	47.1
1 SITE	AF 95 OE	6	286	52	10.6	41.0	37	120	12.1	31.5
UPPER JURASSIC NAKNEK FM	AF 190 OE	6	288	47	12.0	31.9	34	115	11.3	36.2
	AF 380 OE	6	278	37	13.8	24.4	22	119	12.2	30.9
	AF 760 OE	6	272	27	15.9	18.7	14	120	13.4	26.1
	AF 1520 OE	6	257	21	20.5	11.6	4	131	17.2	16.1
KTM-3	NRM	27	349	67	11.2	7.1	81	82	15.5	4.2
(58.5N,204.5E)	AF 190 OE	27	333	65	14.1	4.9	72	109	18.4	3.3
3 SITES										
MID JURASSIC GRANODIORITE										

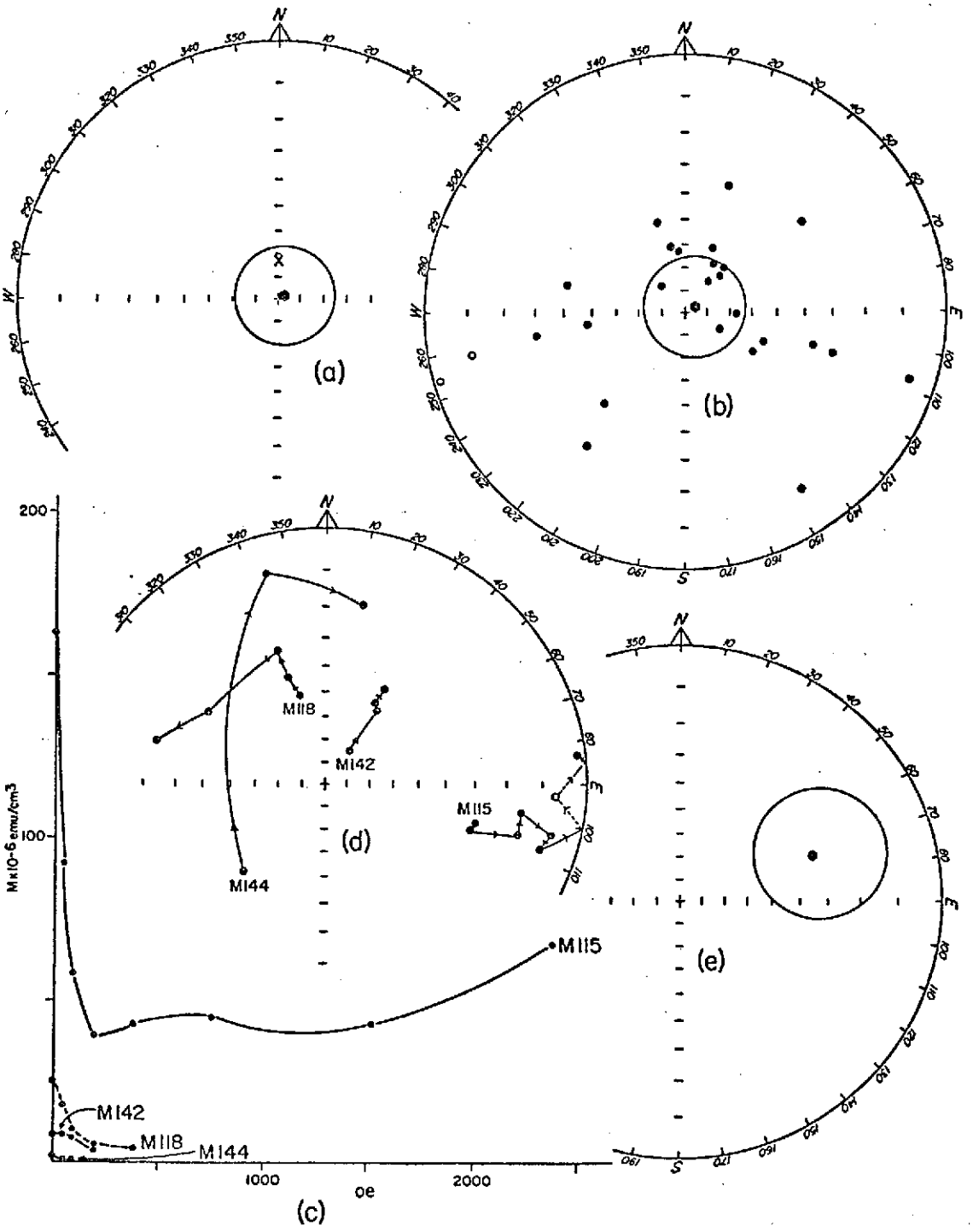

Figure 3-10. Paleomagnetic data for KTM-1, Katmai area, Alaska. (a) NRM P. (b) NRM. (c) Magnetic intensity and (d) directions of pilot samples during AF demagnetization. (e) After demagnetization at 95 oe.

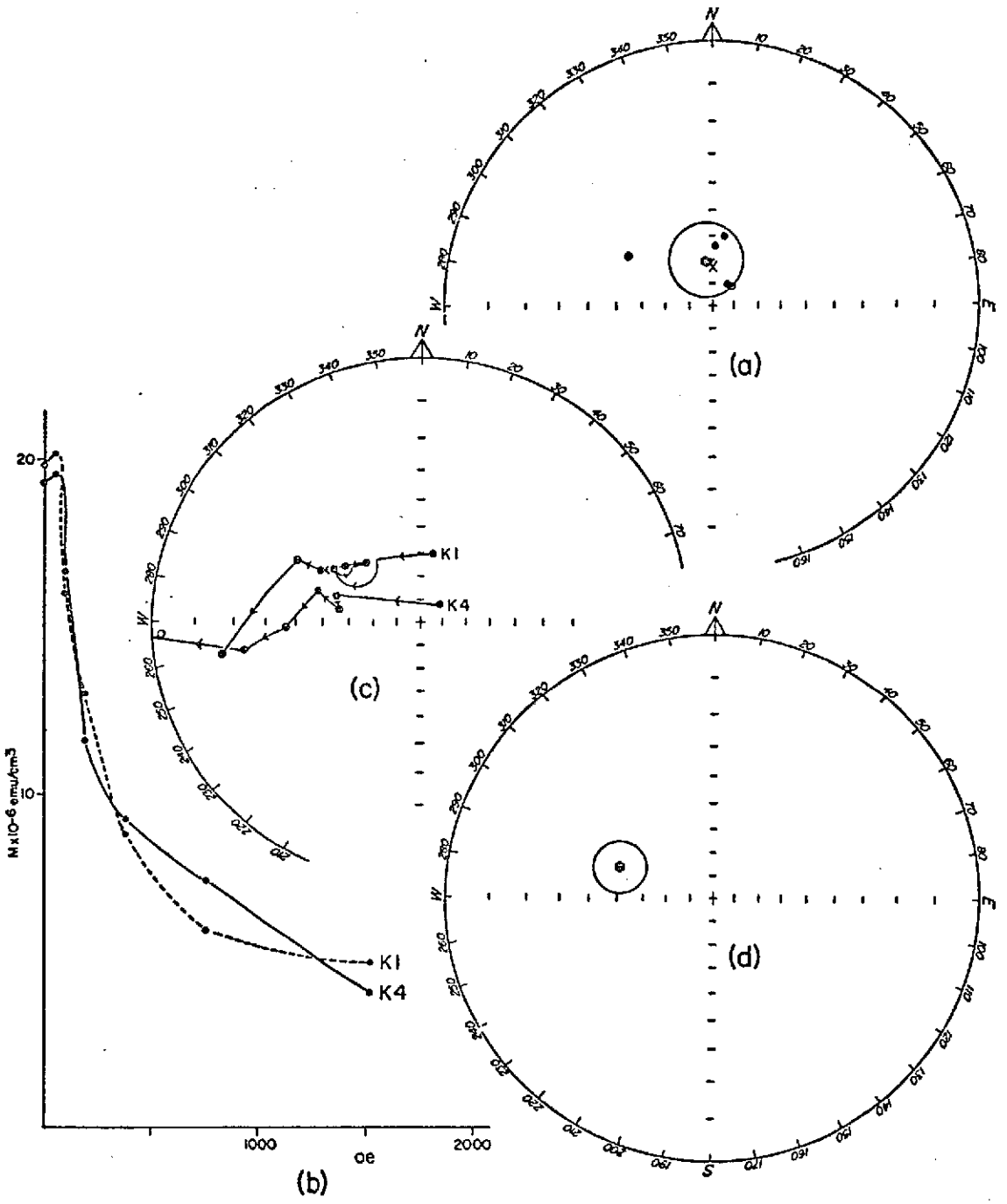

Figure 3-11. Paleomagnetic data for KTM-2, Katmai area, Alaska. (a) NRM. (b) Magnetic intensity and (c) directions of pilot samples during AF demagnetization. (d) After demagnetization at 95 oe.

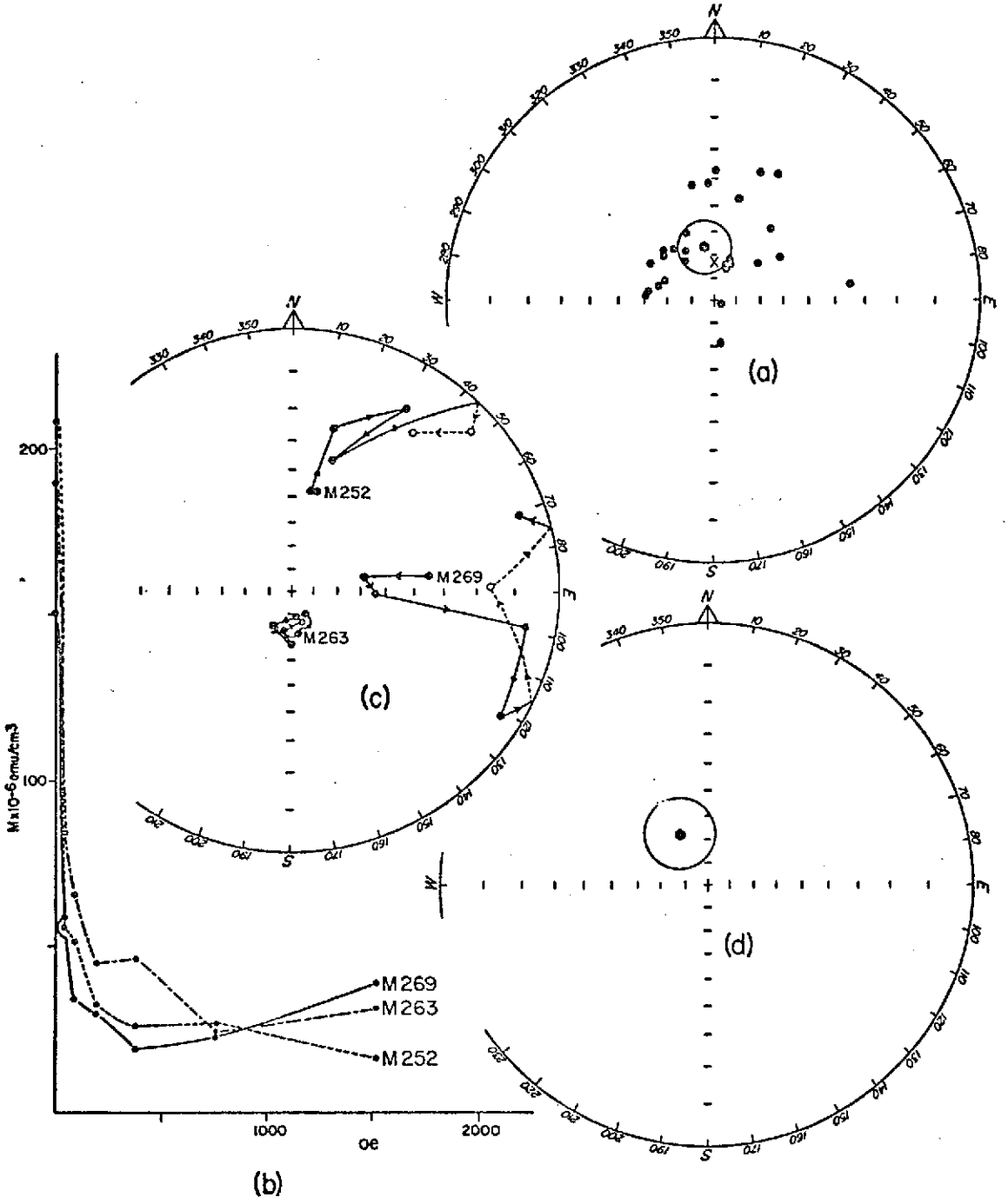

Figure 3-12. Paleomagnetic data for KTM-3, Katmai area, Alaska. (a) NRM. (b) Magnetic intensity and (c) directions of pilot samples during AF demagnetization. (d) After demagnetization at 190 oe.

The mean of NRM measurements on samples from KTM-2 included the present axial dipole field direction within its 95% confidence limits. Demagnetization at an AF of 48 oe removed this present field component and reduced the scatter. Subsequent demagnetization at an AF of 95 oe, 190 oe, and 380 oe did not significantly change the position of the mean. Demagnetization at an AF of 760 oe and 1520 oe however displaced the mean significantly and increased the scatter about it. Although the rocks did not have a particularly high intensity--mean intensity 20 x 10^{-6} emu/cm^3, and mean susceptibility 275 x 10^{-6} emu/cm^3--the intensity decreased slowly on demagnetization. Because the mean of the samples' magnetic direction during demagnetization was apparently still moving the stability of the samples are in question and the results must be considered marginal.

Cores from the granodiorite had a mean NRM vector direction coincident with the present axial dipole field direction. Demagnetization at an AF of 190 oe failed to shift it significantly away from the present field direction. At an AF of 380 oe the samples became unstable, probably due to a large viscous component indicated by a lack of repeatibility of measurements. Although the α_{95} circle of confidence was fairly small after demagnetization at 190 oe, these results were unusable. (Their plots are shown, however, for the sake of completeness.) These samples had a mean NRM intensity of 310 x 10^{-6} emu/cm^3, and the mean susceptibility was 3000 x 10^{-6} emu/cm^3.

Tuxedni Bay (TXD)

At four sites, separated by approximately 16 miles, a total of 48 cores from the Naknek Formation, Tuxedni Group, Chinitna Formation and quartz diorite, all of Jurassic age, were collected along the shores of Tuxedni Bay. The first site (TXD-1), located across Tuxedni Channel from Chisik Island, covers 80 stratigraphic feet of section and ranges from fine to coarse-grained arkosic sandstone composed of quartz, plagioclase, hornblende, biotite, opaques, and fragments of granitic, volcanic and sedimentary rock, in a slightly carbonaceous argillitic matrix. These 15 samples from TXD-1 are from the upper Jurassic Naknek Formation which dips toward the east-southeast at 15 degrees.

Samples from the Red Glacier Formation of the middle Jurassic Tuxedni Group were collected from the southwestern shore of Tuxedni Bay, approximately 1 1/4 miles northwest of Fossil Point. The 14 samples from TXD-2 consist of calcareous fine-grained sandstone composed of quartz, plagioclase, opaques, and shell fragments in a carbonaceous argillitic matrix. Approximately 10 stratigraphic feet were sampled in beds that dip at 15 degrees to the east-southeast.

At the third site, on the northeast shore of Tuxedni Bay less than a quarter mile from the mouth of the Tuxedni River, 10 cores of early Jurassic, 170 to 168 my (Reed and Lanphere, 1969), granodiorite were collected. Although no attitude was observed in the reconnaissance study of the area made for this collection, it is assumed that the batholith has not tilted or rotated significantly since its emplacement. This assumption is probably correct, consider-

ing that a part of the gentle deformation of the sediments in this area is thought to have been caused by emplacement of this batholith (Burk, 1965).

Samples of the upper Jurassic Tonnie Siltstone Member of the Chinitna Formation were collected on the westernmost tip of Chisik Island. These 9 samples at TXD-4 are dense, calcareous fine-grained siltstones containing shell fragments and occurring as lenticular bodies in a coarser grained arenaceous siltstone. The samples came from nearly 10 feet of section in beds that dip east-northeast at 12 degrees. Minor dip-slip faulting has been mapped throughout the Tuxedni Bay area (Detterman and Hartsock, 1966); however, the samples were collected at least one-fourth of a mile from any fault.

Results of measurements on cores from the Tuxedni Bay collection locality are given in Table 3-6 and plotted in Figures 3-13 to 3-16. The mean NRM P field direction for TXD-1 included the present axial dipole field direction within its α_{95} circle of confidence; however upon demagnetization at an AF of 95 oe the present field component was removed. Demagnetization at still higher levels resulted in no significant shift in the position of the mean but increased the scatter. The mean NRM intensity of the samples from TXD-1 was 280 x 10^{-6} emu/cm^3, and the mean susceptibility was 3,800 x 10^{-6} emu/cm^3. Thus, despite a low-coercivity secondary component aligned along the present field these samples are a good approximation of the upper Jurassic VGP.

Results from TXD-2 showed the mean NRM P direction to be displaced from the present axial dipole field direction. Although a

TABLE 3-6

PALEOMAGNETIC DIRECTIONS AND POLE POSITIONS

LOCATION	TREATMENT	N	DIRECTION D	I	A95	K	POLE POSITION LAT	ELONG	A95	K
TXD-1 - TUXEDNI BAY, ALASKA	NRM P	15	15	67	11.1	12.9	77	341		
(60.1N,207.4E)	NRM	15	48	64	11.1	12.9	60	296	14.3	8.1
1 SITE	AF 95 OE	15	14	53	15.2	7.3	65	0	15.2	7.3
UPPER JURASSIC	AF 190 OE	15	358	52	19.1	5.0	67	34	22.1	4.0
NAKNEK FM	AF 380 OE	15	357	56	25.4	3.2	71	42	27.4	2.9
TXD-2	NRM P	14	239	38	14.4	8.6	5	154		
(60.2N,207.3E)	NRM	14	227	42	14.4	8.6	4	165	16.2	7.0
1 SITE	AF 95 OE	14	238	49	12.7	10.8	12	159	15.4	7.6
MID JURASSIC TUXEDNI GROUP	AF 190 OE	14	242	45	16.3	6.9	12	155	17.9	5.9
RED GLACIER FM	AF 380 OE	14	244	43	16.3	6.9	10	153	18.8	5.4
TXD-3	NRM	10	51	52	12.1	17.0	48	314	15.2	11.1
(60.3N,207.1E)	AF 95 OE	10	51	43	19.7	7.0	41	318	21.6	6.0
1 SITE	AF 190 OE	10	36	45	18.4	7.8	50	336	20.5	6.5
LOWER JURASSIC QUARTZ DIORITE	AF 380 OE	10	35	28	23.3	5.3	39	343	22.9	5.4

TABLE 3-6 (CONTINUED)

PALEOMAGNETIC DIRECTIONS AND POLE POSITIONS

	LOCATION	TREATMENT	N	DIRECTION D	I	A95	K	POLE POSITION LAT	ELONG	A95	K
TXD-4	(60.2N,207.4E)	NRM P	9	68	57	20.6	7.2	43	294		
		NRM	9	70	45	20.6	7.2	36	298	19.5	7.9
	1 SITE										
	UPPER JURASSIC CHINITNA FM	AF 48 OE	9	68	58	17.1	10.0	48	290	20.2	7.4
	TONNIE SILTSTONE MEMBER	AF 95 OE	9	71	66	15.8	11.5	52	276	20.4	7.3

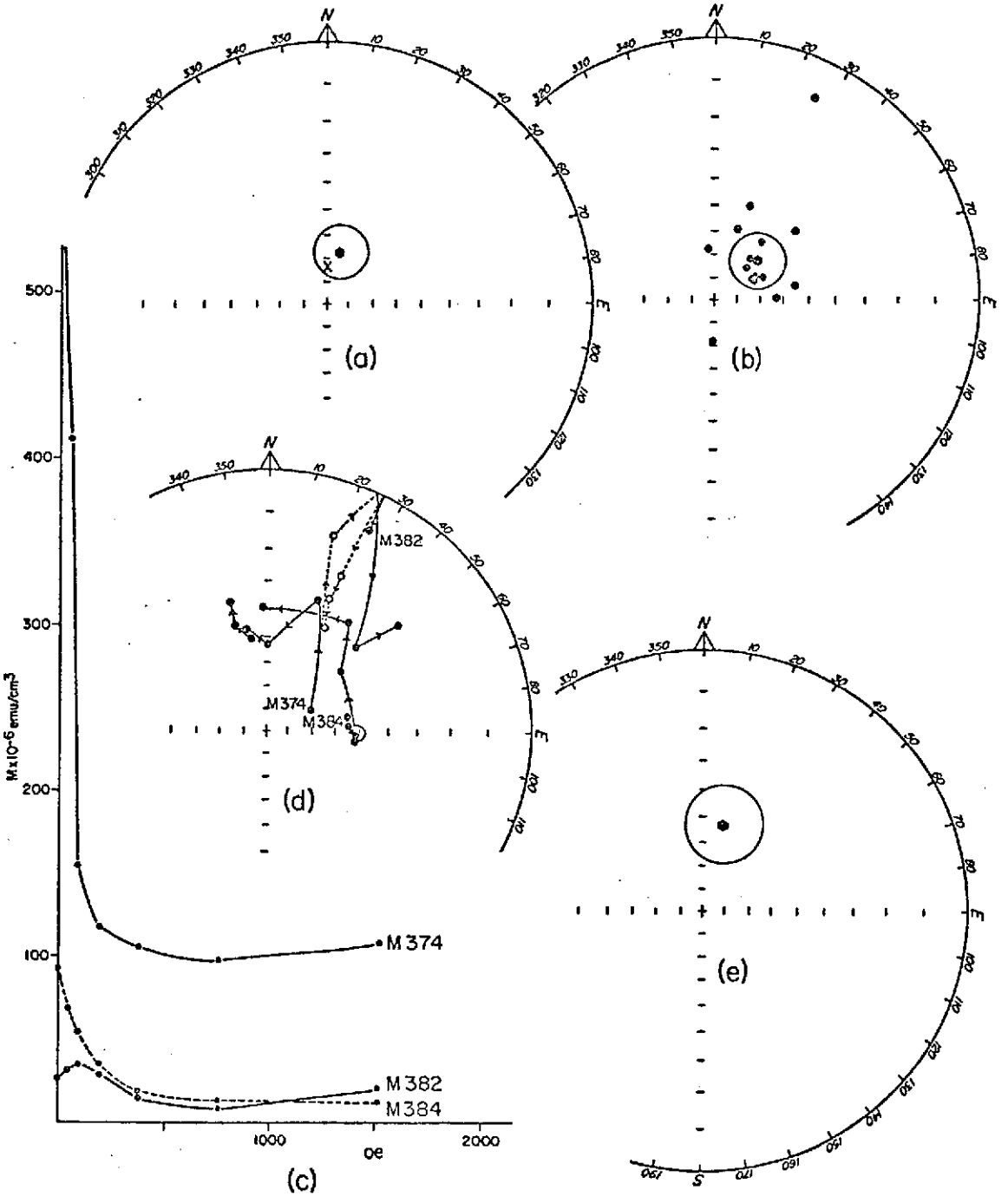

Figure 3-13. Paleomagnetic data for TXD-1, Tuxedni Bay, Alaska. (a) NRM P. (b) NRM. (c) Magnetic intensity and (d) directions of pilot samples during AF demagnetization. (e) After demagnetization at 95 oe.

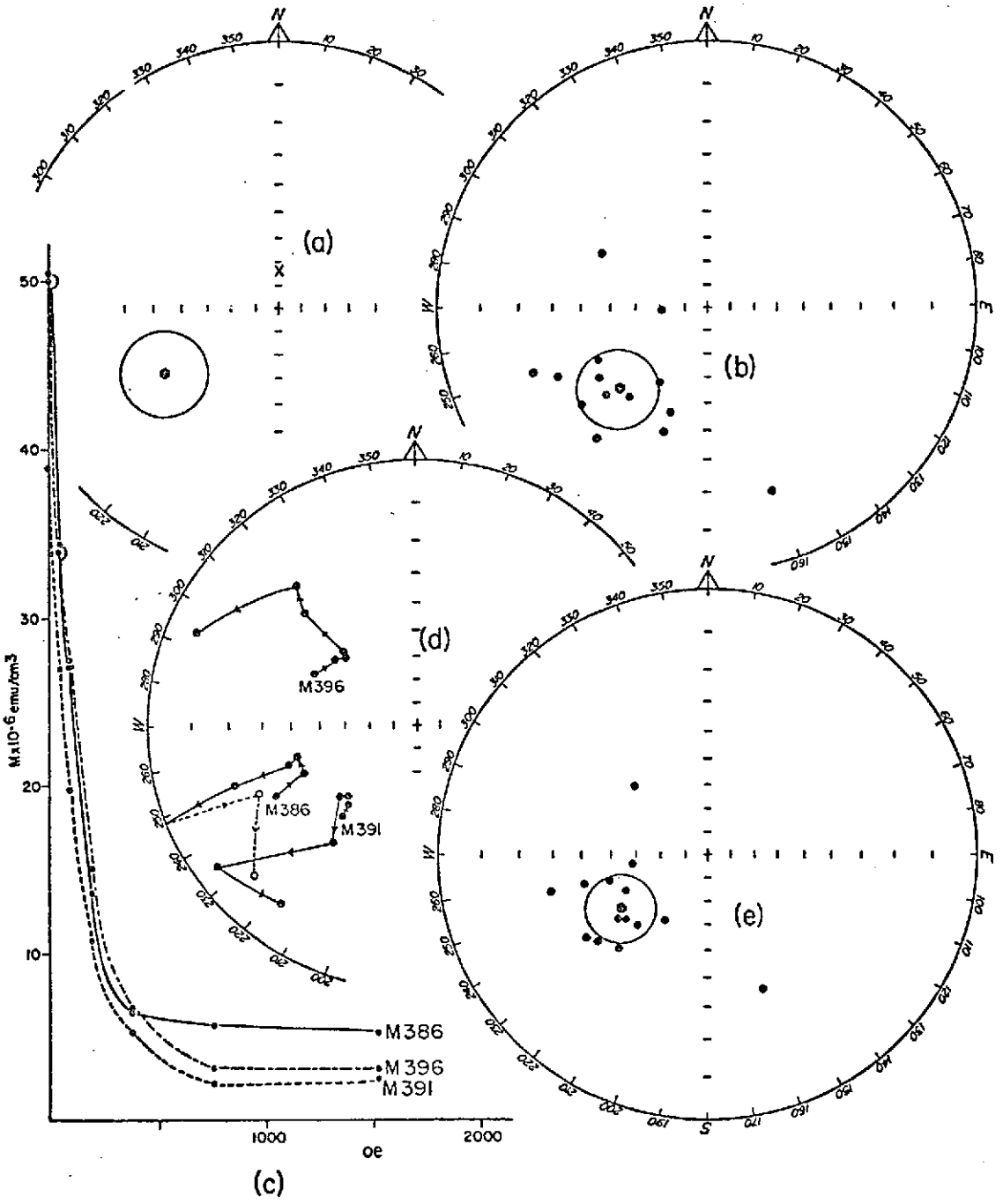

Figure 3-14. Paleomagnetic data for TXD-2, Tuxedni Bay, Alaska. (a) NRM P. (b) NRM. (c) Magnetic intensity and (d) directions of pilot samples during AF demagnetization. (e) After demagnetization at 95 oe.

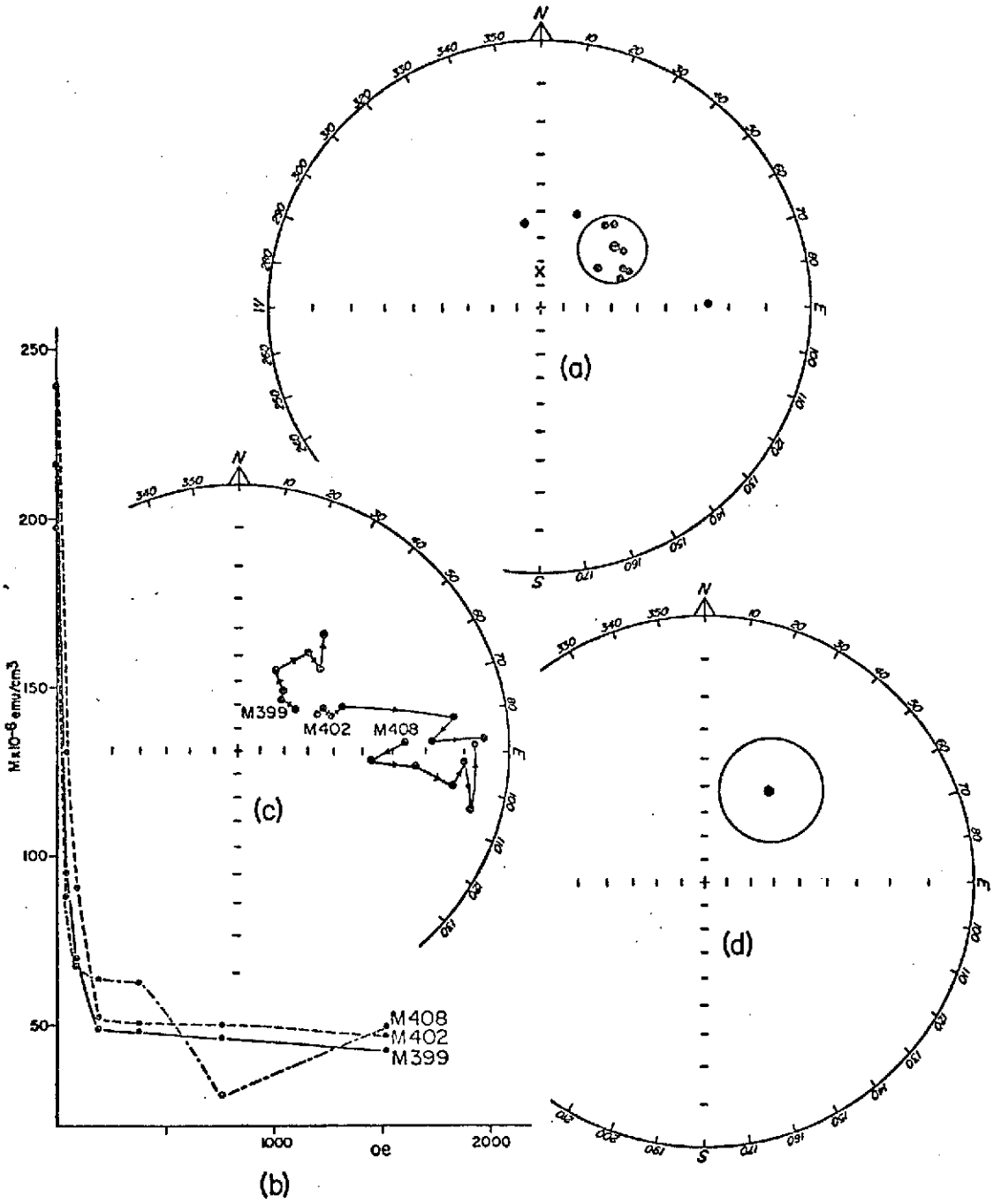

Figure 3-15. Paleomagnetic data for TXD-3, Tuxedni Bay, Alaska. (a) NRM. (b) Magnetic intensity and (c) directions of pilot samples during AF demagnetization. (d) After demagnetization at 190 oe.

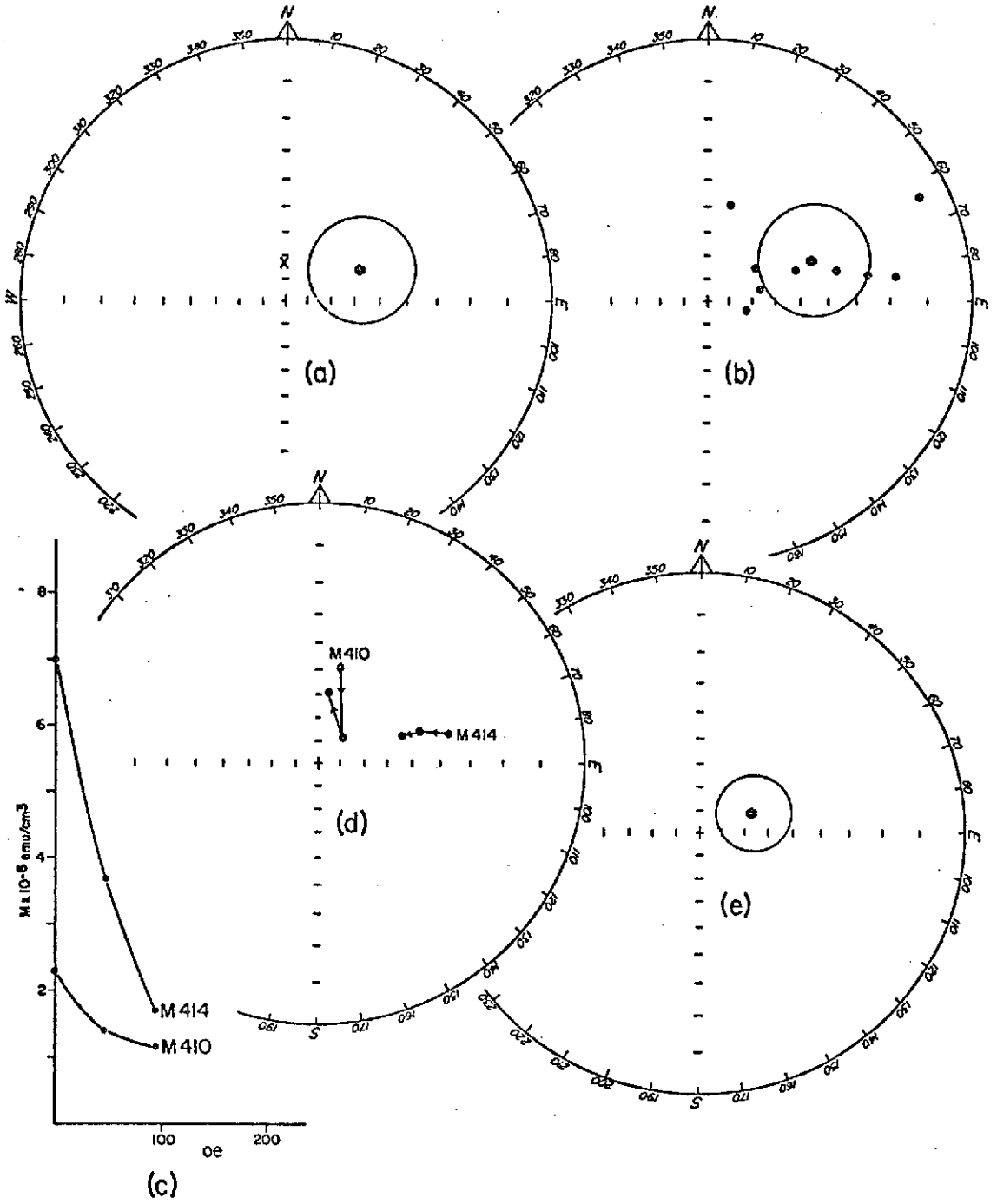

Figure 3-16. Paleomagnetic data for TXD-4, Tuxedni Bay, Alaska. (a) NRM P. (b) NRM. (c) Magnetic intensity and (d) directions of pilot samples during AF demagnetization. (e) After demagnetization at 95 oe.

slight shift of the mean occurred upon demagnetization at 95 oe, demagnetization at higher levels only increased the scatter. The mean NRM intensity and susceptibility for these samples were 45 x 10^{-6} emu/cm^3 and 280 x 10^{-6} emu/cm^3, respectively. Results from the samples collected at TXD-2 thus appear to be a good record of the mid Jurassic VGP.

Samples from the Jurassic granodiorite at Tuxedni Bay, TXD-3, had a mean NRM direction that was not aligned along the present axial dipole field direction. Demagnetization at an AF of 95 and 190 oe caused slight shifts in the position of the mean of the paleomagnetic field direction, but demagnetization at 380 oe only increased the scatter. The mean NRM intensity for these samples was 200 x 10^{-6} emu/cm^3, and the mean susceptibility was 40 x 10^{-6} emu/cm^3. Thus the mean of the vector directions after demagnetization at an AF of 190 oe is a good approximation of the early Jurassic VGP, if the assumption of horizontal orientation is correct.

The samples from Chisik Island, TXD-4, had a mean NRM P that was not in the same direction as the present axial dipole field direction. Demagnetization in an AF of 48 and 95 oe caused a small shift of the mean magnetic vector direction. The samples were too weak to demagnetize at a higher level, as the mean NRM intensity was 4 x 10^{-6} emu/cm^3, and the mean susceptibility was 35 x 10^{-6} emu/cm^3. The results, however, seem to be stable and a good approximation of the upper Jurassic VGP.

SOUTHCENTRAL ALASKA

Over 100 cores were collected at 11 different sites from the Sheep Mountain, Mentasta, and Nabesna areas in southcentral Alaska (Fig. 3-17). Rocks of Permo-Triassic, Jurassic, and Cretaceous age were sampled. The rock types collected were both sedimentary and igneous.

Geologic setting of the Upper Matanuska Valley

Capps' (1927) description of the geology of the upper Matanuska Valley served as the main source of the geological information included here. Waring (1936), Martin and Katz (1912), Capps (1940), and Grantz (1964) describe various aspects of Matanuska Valley geology. More recent geologic maps and cross sections of adjacent areas by Grantz (1960a, b, c; 1961a, b) and Barnes (1962) are also available.

The oldest rocks in the upper Matanuska Valley are early Mesozoic or older, and consist of slates, graywackes, basaltic greenstones, tuffs, and associated mica schists and gneissic rocks. These metamorphic rocks are exposed along the flanks of the Chugach Mountains to the south of the Valley. Throughout the Matanuska Valley the lower Jurassic Talkeetna Formation is a widespread unit that consists of volcanic agglomerate, breccia, and tuff with interbedded minor amounts of sandstone and shale. Although this formation is largely marine, its age has been established from fossil plant remains.

Middle and upper Jurassic rocks are not exposed in the upper Matanuska Valley, although they were deposited in the Talkeetna Mountain portion of the upper Matanuska geosyncline (Grantz, 1961a).

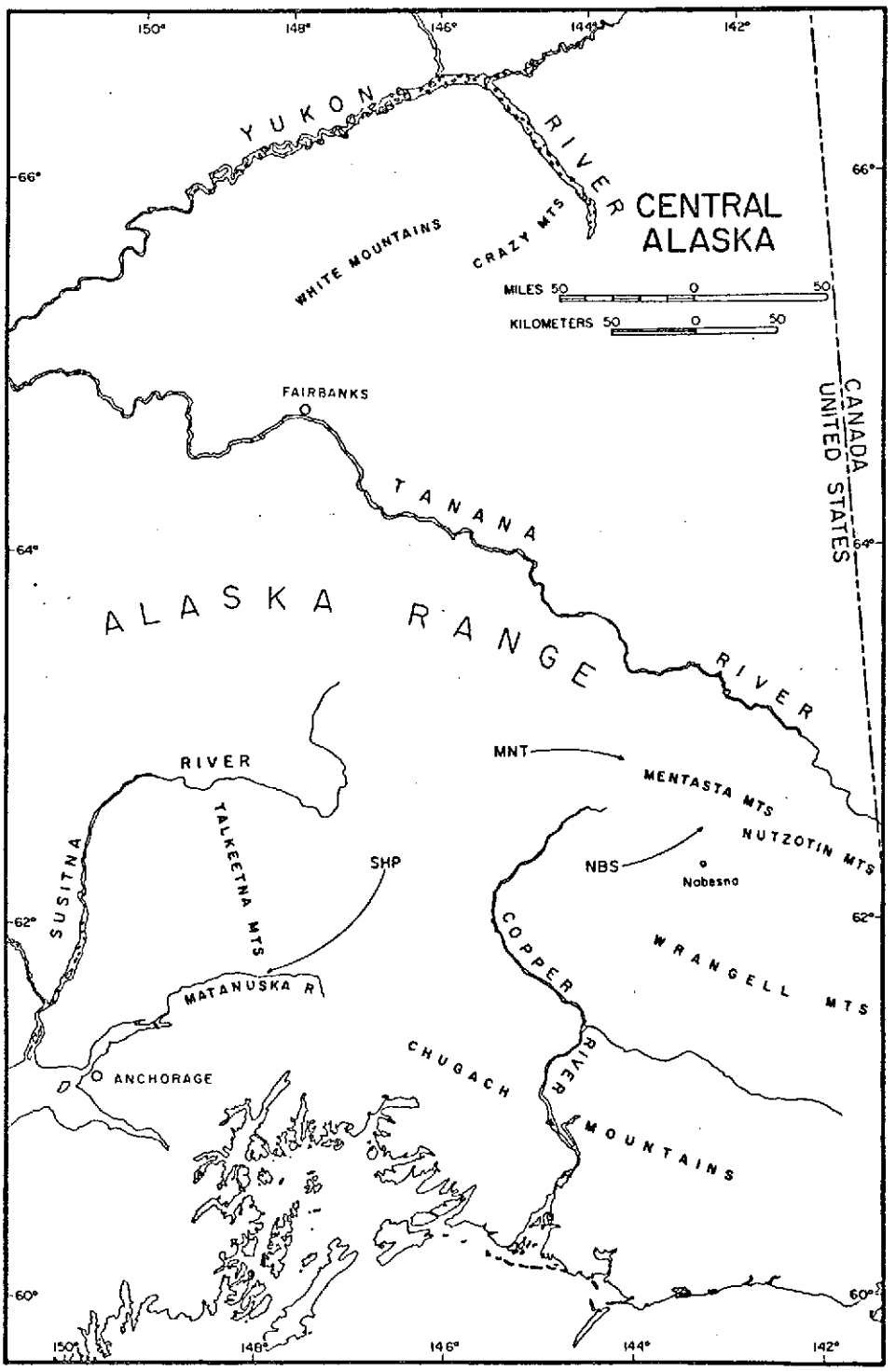

Figure 3-17. Location map for place names and sampling localities in central Alaska.

These rocks are sandstones of the Tuxedni Formation, siltstones of the Chinitna Formation, and siltstones and shales of the Naknek Formation. During the Jurassic or early Cretaceous, a quartz diorite and granodiorite body was intruded into the Talkeetna Formation on the flanks of the Chugach Mountains to the south of the Valley (Grantz, 1961a) and in the Talkeetna Mountains to the north (Capps, 1927). The Arkose Ridge Formation was deposited directly on part of this batholith in the lower Matanuska Valley. In the upper Matanuska Valley during the lower Cretaceous, local deposits of siltstone and sandstone were laid down, which unconformably overlie the Talkeetna Formation, and are themselves unconformably overlain by the Matanuska Formation.

The Matanuska Formation is an extensive unit in the lower Matanuska Valley. Its lower half consists of shale and its upper half of sandstone and shale (Barnes, 1962). In the upper Matanuska Valley however, the Matanuska Formation varies locally in composition. Generally it consists of a basal coarse sandstone, unconformably overlain by sandstone and siltstone, which is unconformably overlain by claystone, siltstone, sandstone, and conglomerate. This formation spans the entire upper Cretaceous, and in the lower Matanuska Valley it is separated from Tertiary arkose and conglomerate by an unconformity. In the upper Matanuska Valley, the basal portion of the overlying early Tertiary coal-bearing sandstone, pebble conglomerate, siltstone, and claystone, called the Chickaloon Formation, is not exposed. Similarly it is impossible to distinguish the Paleocene or early Eocene Wishbone and the Eocene Tsadaka Formations, from the Chickaloon For-

mation conglomerates and sandstones, mapped in the lower Matanuska Valley.

In the Paleocene or Eocene, felsic plugs and dikes of quartz and feldspar porphyries were intruded in rocks to the north of the Matanuska Valley. Eocene mafic dikes, sills, and plugs of diabase, basalt, and gabbro also intrude the rocks to the north. Although the relative number of hypabyssal intrusives is comparatively small, they have a large areal distribution in the eastern Talkeetna Mountains to the north of the Matanuska Valley. Extrusive basalt flows and associated pyroclastic debris of late Eocene and younger age overlie the Tertiary sediments and cap the mountains immediately north of the Matanuska Valley. Quaternary glaciers dissected the area and are responsible for extensive outwash deposits in the Valley proper.

The Matanuska Valley is the northern part of the Cretaceous Matanuska geosyncline, bounded on the south by the Seldovia geanticline and on the north by the Talkeetna geanticline (Payne, 1955). In the upper Matanuska Valley, Mesozoic and Tertiary sediments have been moderately folded, with the fold axes generally parallel to the trend of the valley. Several high-angle normal faults, also parallel to the trend of the Valley, are present in the upper Matanuska Valley. Grantz (1961) believes they define three or four elongate blocks in the Valley. With one exception the upthrown blocks are on the north. The right-lateral strike-slip Caribou fault (Grantz, 1961a) is approximately 10 miles to the north, and it joins the Castle Mountain fault in the lower Matanuska Valley. The majority of the deformation in the Matanuska geosyncline occurred in the mid to late Tertiary.

Sites in the Upper Matanuska Valley

Sheep Mountain (SHP)

To the west of Sheep Mountain at the base of the north end of Anthracite Ridge, 31 cores of the Cretaceous Matanuska Formation were collected from three sites. The sites have a total separation of approximately two miles. Each site represents at least 10 stratigraphic feet, and consists of tan to gray, fine- to coarse-grained sandstone composed of quartz, plagioclase, opaques, and sedimentary rock fragments in an argillaceous matrix. Bedding planes at SHP-1 and 2 dip northwest at 25-30 degrees and at SHP-3, two miles southeast, dip southeast at 53 degrees.

The results of measurements for samples from Sheep Mountain are given in Table 3-7 and plotted in Figure 3-18. The means for NRM P for the three sites were significantly different from the present axial dipole field direction (Fig. 3-18). SHP-3 and SHP-1 and 2 overlapped in the NRM P plots of the means, but when the vector directions were corrected for the orientation of the bedding planes they separated. SHP-1 and 2 had a small scatter, and SHP-3 a very large scatter. Both means shifted upon demagnetization in an AF of 48 oe. SHP-3 scatter was reduced but remained large, and the sample intensity was too weak to demagnetize further. For SHP-3 the mean NRM intensity was 1×10^{-6} emu/cm^3 and the mean susceptibility was 1×10^{-6} emu/cm^3. SHP-1 and 2 were also demagnetized at an AF of 95 oe which decreased the scatter, but did not shift the mean significantly. The mean intensity and susceptibility for samples at SHP-1 and 2 were 2×10^{-6} emu/cm^3

TABLE 3-7

PALEOMAGNETIC DIRECTIONS AND POLE POSITIONS

LOCATION	TREATMENT	N	DIRECTION D	DIRECTION I	DIRECTION A95	DIRECTION K	POLE POSITION LAT	POLE POSITION ELONG	POLE POSITION A95	POLE POSITION K
SHP-1&2 - SHEEP MTN AREA, ALASKA	NRM P	22	281	74	7.7	17.2	54	156		
(61.8N,212.0E)	NRM	22	306	51	8.1	15.6	46	106	9.1	12.6
2 SITES UPPER CRETACEOUS MATANUSKA FM	AF 48 OE	22	350	48	8.8	13.3	58	48	9.4	12.0
	AF 95 OE	22	334	50	6.7	22.7	55	74	7.5	18.3
SHP-3 (61.8N,212.0E)	NRM P	9	226	55	34.5	3.2	14	175		
	NRM	9	192	19	34.5	3.2	-17	201	33.0	3.4
1 SITE	AF 48 OE	9	104	30	29.8	3.9	8	281	32.8	3.4

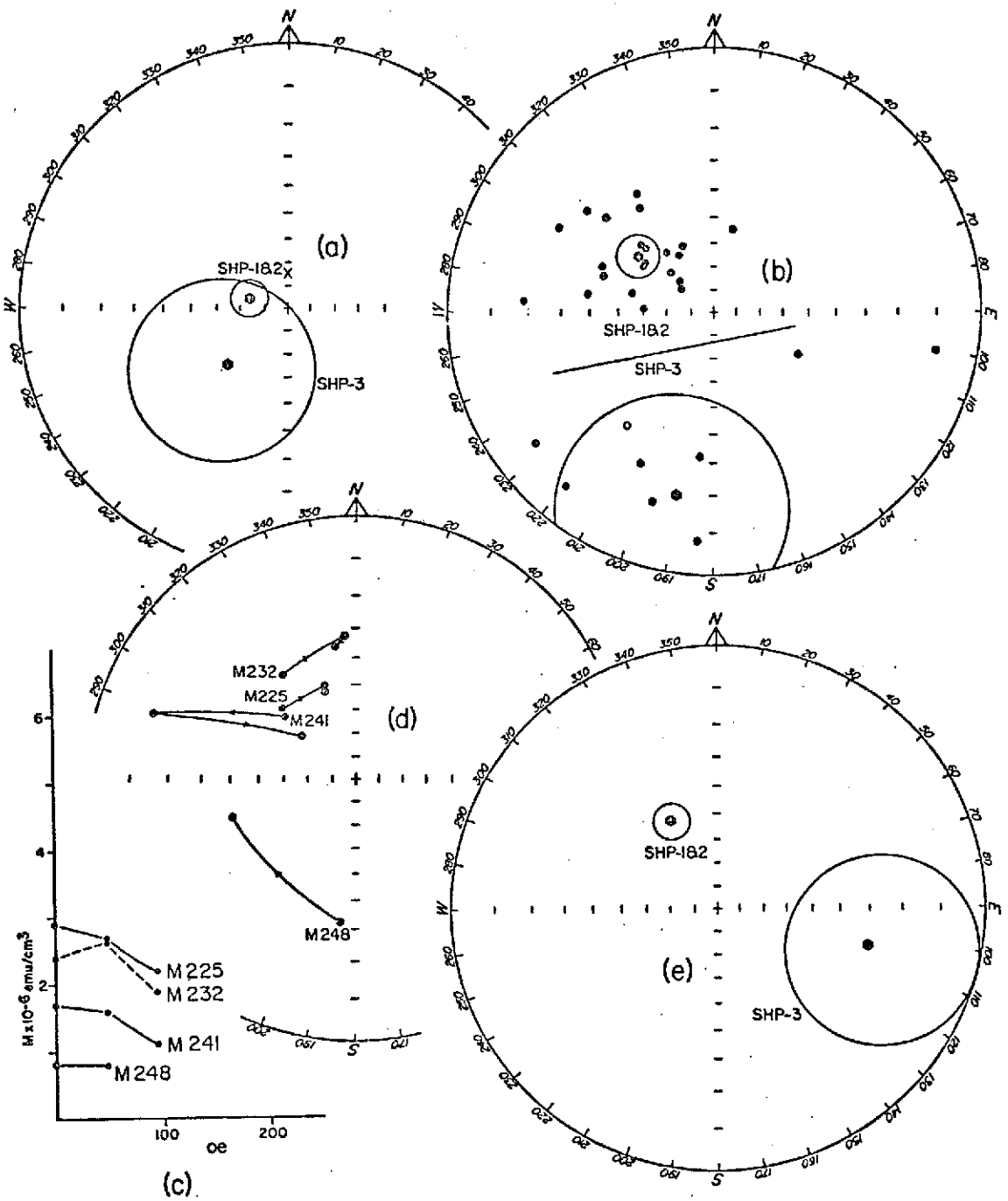

Figure 3-18. Paleomagnetic data for SHP, Sheep Mountain area, Alaska. (a) NRM P. (b) NRM. (c) Magnetic intensity and (d) directions of pilot samples during AF demagnetization. (e) SHP-1 and 2 after demagnetization at 95 oe, and SHP-3 after demagnetization at 48 oe.

and 15 x 10^{-6} emu/cm^3, respectively. Because the mean vector positions for SHP-1 and SHP-2 combined were different than SHP-3, and because SHP-3 also seemed at least potentially unstable, it has been ignored in the final statistics. The mean of SHP-1 and 2 probably represents a fair approximation of the upper Cretaceous VGP.

Geologic setting of the Mentasta Mountains

Most of the geologic history presented here comes from Richter (1967). Reports by F. H. Moffit, who did most of the early work in this area, are summarized and referenced by Richter.

The Mentasta Mountains are divided into two geologic sections by the Denali fault which cuts their northern flanks. To the north of the Denali fault, Paleozoic low-grade regionally metamorphosed sediments and volcanics make up approximately 10,000 feet of section. These rocks consist of quartz mica schist, phyllite limestone, marble, serpentinite, serpentine-chlorite schist, and greenstone. These Paleozoic metamorphic units dip steeply to the southwest. On the south side of the Denali fault relatively non-metamorphosed volcanic and sedimentary units dip at moderate angles to the northeast. The oldest of these units is the Permian Mankomen Formation, which consists of over 2500 feet of argillite, shale, limestone, and chert. The unconformably overlying Triassic-Permian amygdaloidal basalt, called the Slana basalt (Richter, 1967) or the Nikolai greenstone, correlated from the southern Wrangell Mountains (Moffit, 1938), is approximately 8000 feet thick. A massive limestone, limy siltstone and sandstone, known as the Jack limestone, conformably overlies the amygdaloidal basalt and occurs locally with thicknesses up to 600

feet. Diorite, granodiorite, and quartz monzonite bodies intruded the rocks throughout the Mentasta Mountain area in the early Mesozoic. Mafic bodies (dunite) that were intruded into the Denali fault zone can also be found within the Mentasta Mountains.

Up to 9000 feet of upper Jurassic to lower Cretaceous marine sediments unconformably overlie the Triassic limestone. These Jura-Cretaceous marine sediments are part of a unit that extends into the Nutzotin Mountains to the southeast and into areas of the Alaska Range to the northwest. Fairly extensive stream and glacial deposits, developed since the Pleistocene, cover the valleys within and around the Mentasta Mountains.

The Denali fault trends northwest and has probably been active since the middle Mesozoic with most of the offset occurring during early Tertiary time. Right-lateral strike-slip has been the principal direction of motion, but evidence for a vertical displacement can also be observed. South of the Denali fault, folding is only evident close to the fault zone. Richter and Matson (1971) have also described another fault zone in the Mentasta Mountains, the Totschunda fault system, which abuts the Denali fault from the south in the northwestern Mentasta Mountains. The Totschunda fault has had predominantly right-lateral offset and is believed to be no older than 2 million years.

Sites in the Mentasta Mountains

Mentasta (MNT)

Thirty-seven cores of Triassic-Permian greenstone were collected at three sites from outcrops on a large hill 4 1/2 miles northwest of

Mentasta Lake. These Permo-Triassic greenstones are part of the Slana basalt (Richter, 1967) or the Nikolai greenstones (Moffit, 1938) and consist of green-to-maroon amygdaloidal basalt that has been metamorphosed through the pumpellyite-prehnite facies. MNT-1 represents approximately 10 stratigraphic feet; MNT-2, approximately 60 stratigraphic feet; and MNT-3, approximately 50 stratigraphic feet. Bedding orientation measured on vesicle bands at the three sites, which have a separation of about three-quarters of a mile, generally dips northeast at 20 to 60 degrees. These sites are approximately two miles south of the Denali fault zone.

The mean vector directions and pole positions at NRM and demagnetization levels are given in Table 3-8 and are shown in Figure 3-19. The mean NRM P did not lie along the present axial dipole field direction. The mean NRM intensity was 250×10^{-6} emu/cm^3 and the mean susceptibility was 450×10^{-6} emu/cm^3. The moderate amount of alteration observed in thin-section might explain the behavior of the intensities of the pilot samples during stepwise demagnetization, and the widely varying intensity from core to core. The scatter was fairly large, $k < 4$, and often individual samples moved nearly randomly from one demagnetization level to the next. The measurements are repeatable, however. These results are marginal in interpreting the Triassic-Permian VGP.

Nabesna area (NBS)

Samples of the Permo-Triassic greenstone and the Jura-Cretaceous marine sediments were collected in the Nabesna area. Fifteen cores of Triassic-Permian greenstone (described in the Mentasta section)

TABLE 3-8

PALEOMAGNETIC DIRECTIONS AND POLE POSITIONS

LOCATION	TREATMENT	N	DIRECTION D	DIRECTION I	DIRECTION A95	DIRECTION K	POLE POSITION LAT	POLE POSITION ELONG	POLE POSITION A95	POLE POSITION K
MNT - MENTASTA, ALASKA (62.9N,216.0E)	NRM P	37	95	38	24.2	1.9	17	292		
	NRM	37	82	6	22.2	2.1	7	312	19.3	2.5
3 SITES TRIASSIC-PERMIAN GREENSTONE	AF 95 OE	37	69	-11	15.9	3.2	1	327	13.7	3.9
	AF 190 OE	37	70	-11	17.0	2.9	1	326	15.3	3.4
	AF 380 OE	37	76	-21	15.9	3.2	-8	322	14.2	3.7

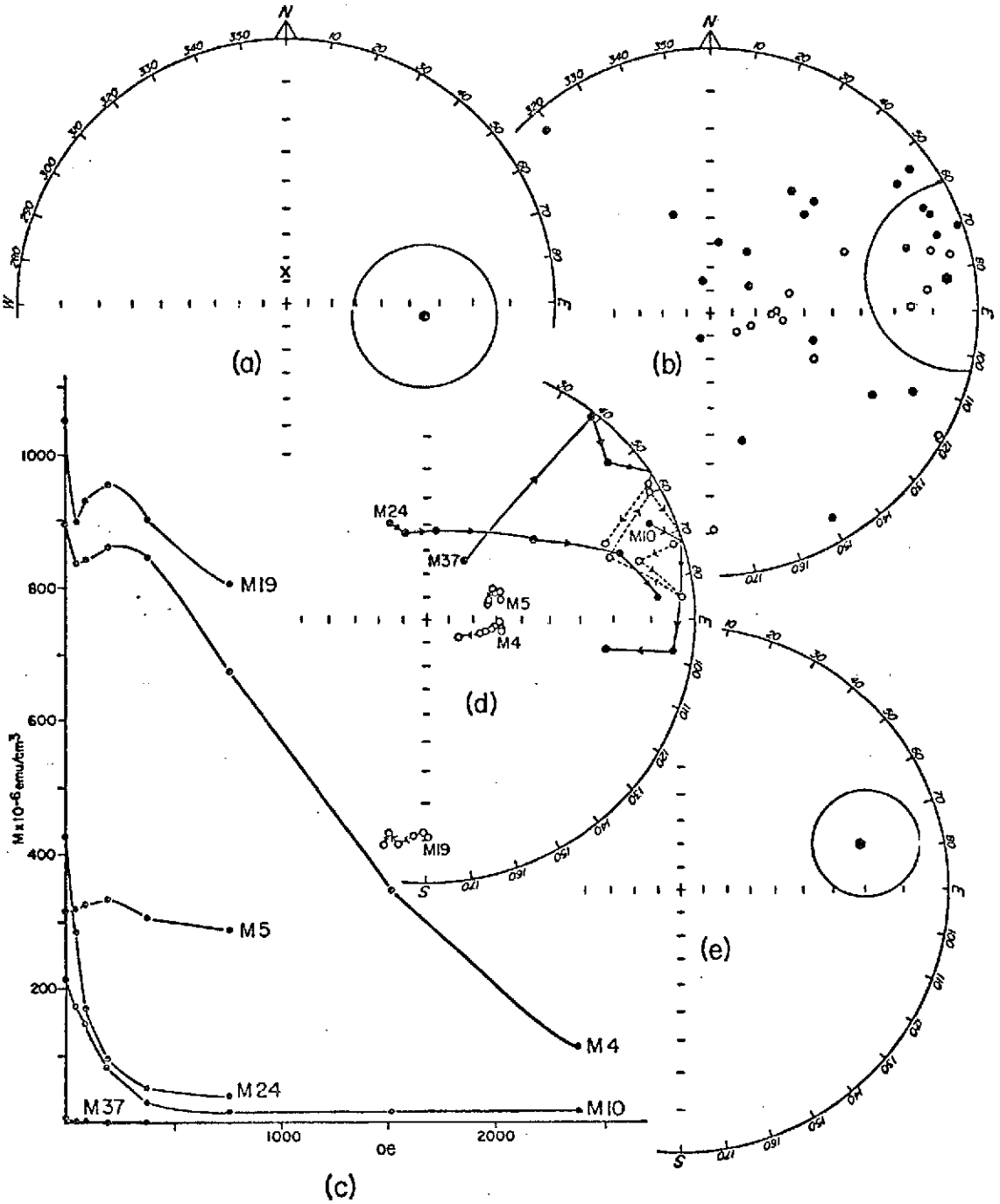

Figure 3-19. Paleomagnetic data for MNT, Mentasta, Alaska. (a) NRM P. (b) NRM. (c) Magnetic intensity and (d) directions of pilot samples during AF demagnetization. (e) After demagnetization at 380 oe.

representing about 25 feet of section were collected on the east side of Lost Creek, about 5 1/2 miles north of the Nabesna Road. The bedding dips northwest at 45 degrees.

Approximately three miles due east of this Lost Creek site, on either side of Platinum Creek, are two sites from which 25 cores of the Jura-Cretaceous marine sediment unit were collected. The samples are fine-grained calcareous sandstone composed of quartz, plagioclase, biotite, and sedimentary and volcanic rock fragments in an argillaceous and calcareous matrix. The sandstone occurs interbedded with siltstone. NBS-1 on the east side of Platinum Creek covers 400 feet of section in beds dipping 10-24 degrees to the east-northeast. On the west side, NBS-3, approximately 50 feet of section is represented in beds that dip northeast at 17 degrees.

The means of the measured paleomagnetic field directions and paleomagnetic pole positions for cores collected in the Nabesna area are shown in Table 3-9 and Figures 3-20 to 3-22. NBS-1, from Jura-Cretaceous marine sediments had a mean NRM P which included the present axial dipole field direction within its 95% confidence limits. This component was removed after demagnetization at an AF of 48 and 95 oe, and the 95 oe level also reduced the scatter. The mean NRM intensity and susceptibility were 10×10^{-6} emu/cm^3 and 35×10^{-6} emu/cm^3, respectively. The mean NRM P vector direction of the Jura-Cretaceous marine sediments from NBS-3 did not lie along the present axial dipole field direction. After demagnetization in an AF of 48 oe and 95 oe, the mean shifted and at the same time the scatter decreased. The mean NRM intensity was 10×10^{-6} emu/cm^3, and the mean susceptibi-

TABLE 3-9

PALEOMAGNETIC DIRECTIONS AND POLE POSITIONS

	LOCATION	TREATMENT	N	DIRECTION D	I	A95	K	POLE POSITION LAT	ELONG	A95	K
NBS-1	NABESNA AREA, ALASKA (62.6N,217.0E)	NRM P	14	10	75	5.2	60.4	85	312		
		NRM	14	55	69	6.9	34.2	61	297	10.2	16.2
	1 SITE JURA-CRETACEOUS MARINE SEDS	AF 48 OE	14	87	62	16.9	6.5	41	281	24.5	3.6
		AF 95 OE	14	63	65	7.4	30.2	54	297	10.6	15.1
NBS-2	(62.6N,216.8E)	NRM P	15	133	43	18.0	5.5	6	259		
		NRM	15	200	69	18.0	5.5	30	200	26.9	3.0
	1 SITE TRIASSIC-PERMIAN GREENSTONE	AF 380 OE	15	159	63	17.5	5.7	24	229	25.0	3.3
		AF 760 OE	15	154	52	15.4	7.1	12	237	20.0	4.6
		AF 1520 OE	15	147	36	13.3	9.2	-2	247	14.1	8.3
NBS-3	(62.6N,217.0E)	NRM P	11	2	61	5.5	69.3	70	33		
		NRM	11	23	31	5.5	69.2	42	7	4.7	94.2
	1 SITE JURA-CRETACEOUS MARINE SEDS	AF 48 OE	11	24	28	7.2	40.7	40	7	6.0	59.3
		AF 95 OE	11	26	40	4.7	93.8	47	1	4.8	91.4

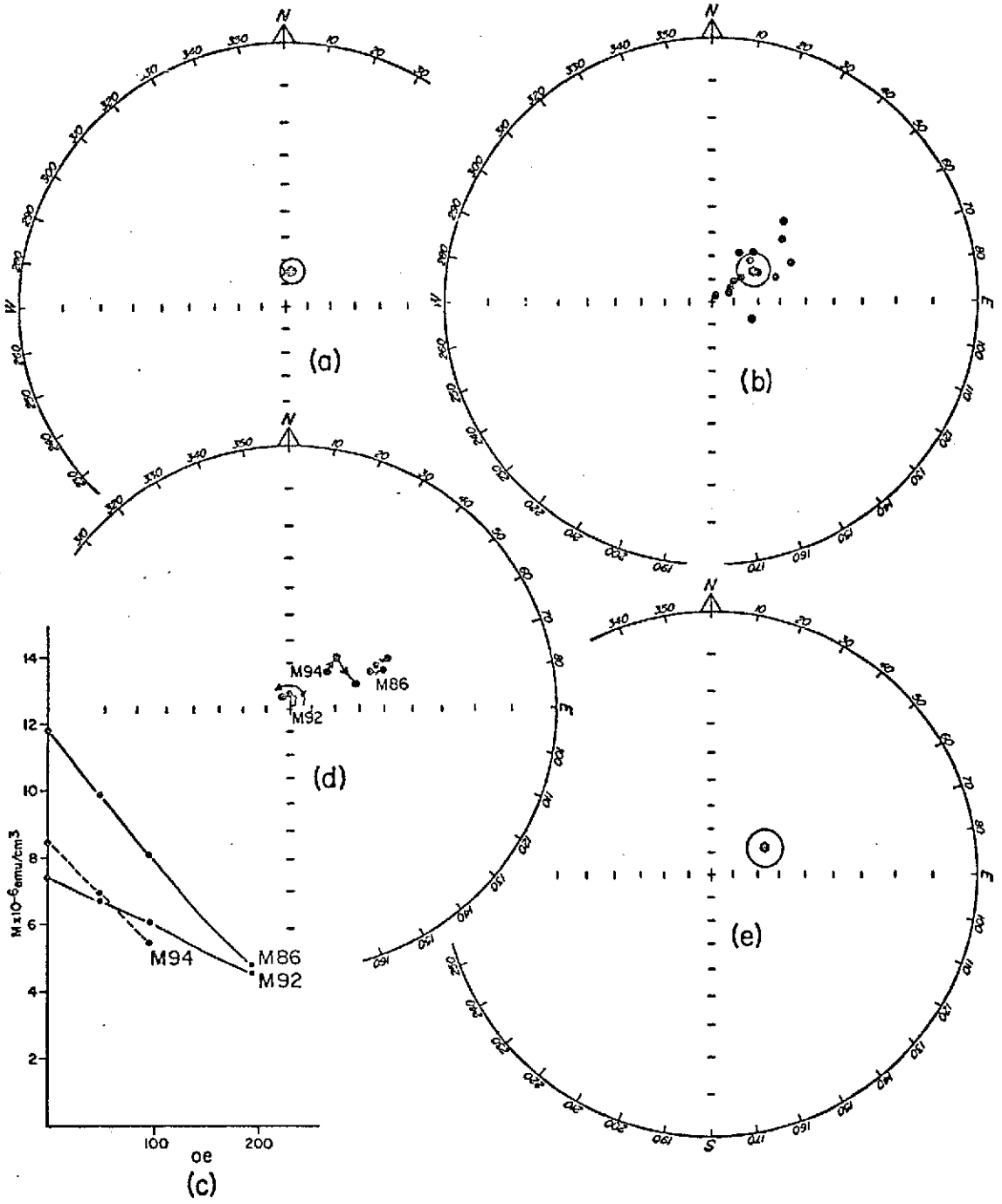

Figure 3-20. Paleomagnetic data for NBS-1, Nabesna area, Alaska. (a) NRM P. (b) NRM. (c) Magnetic intensity and (d) directions of pilot samples during AF demagnetization. (e) After demagnetization at 95 oe.

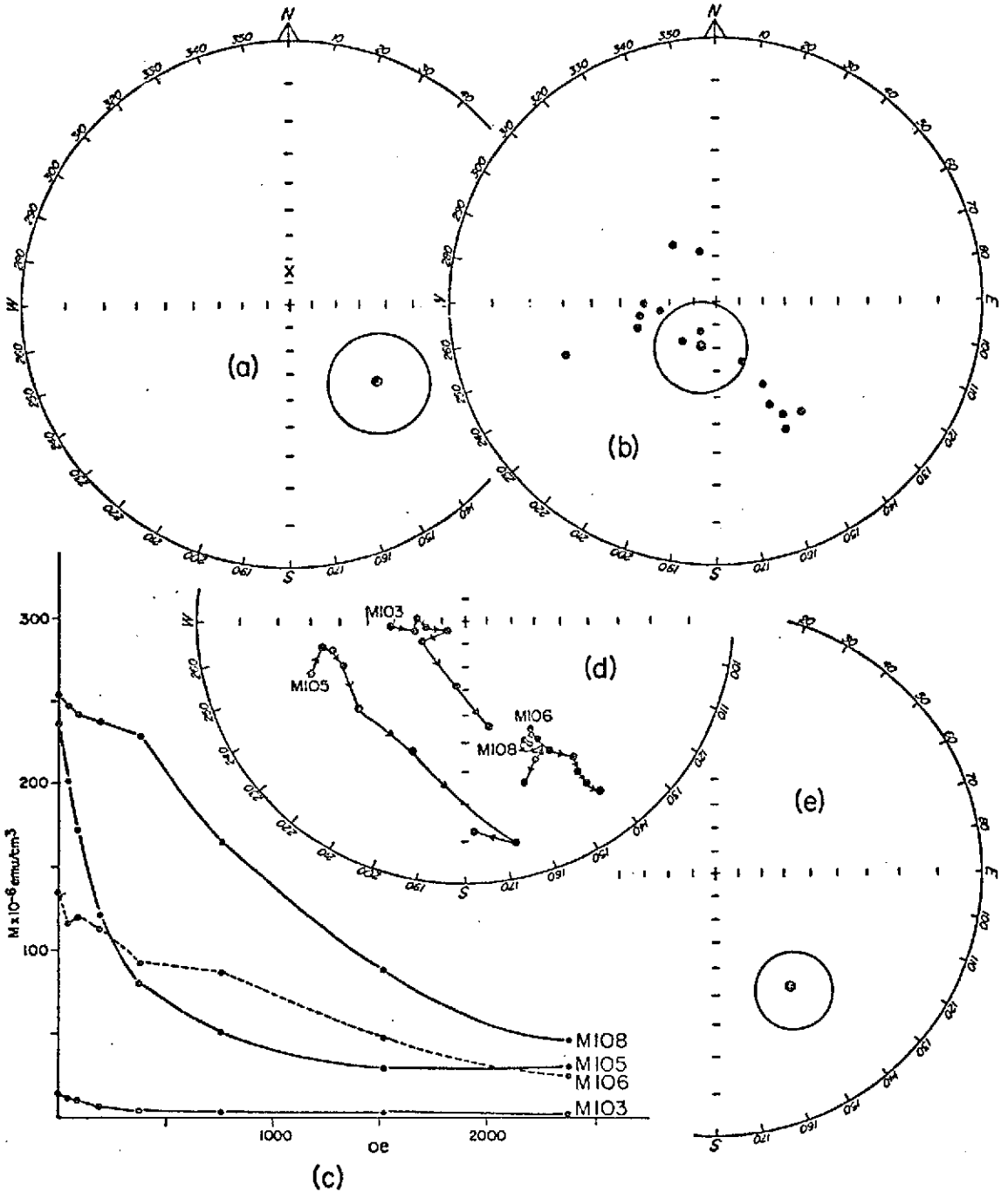

Figure 3-21. Paleomagnetic data for NBS-2, Nabesna area, Alaska. (a) NRM P. (b) NRM. (c) Magnetic intensity and (d) directions of pilot samples during AF demagnetization. (e) After demagnetization at 1520 oe.

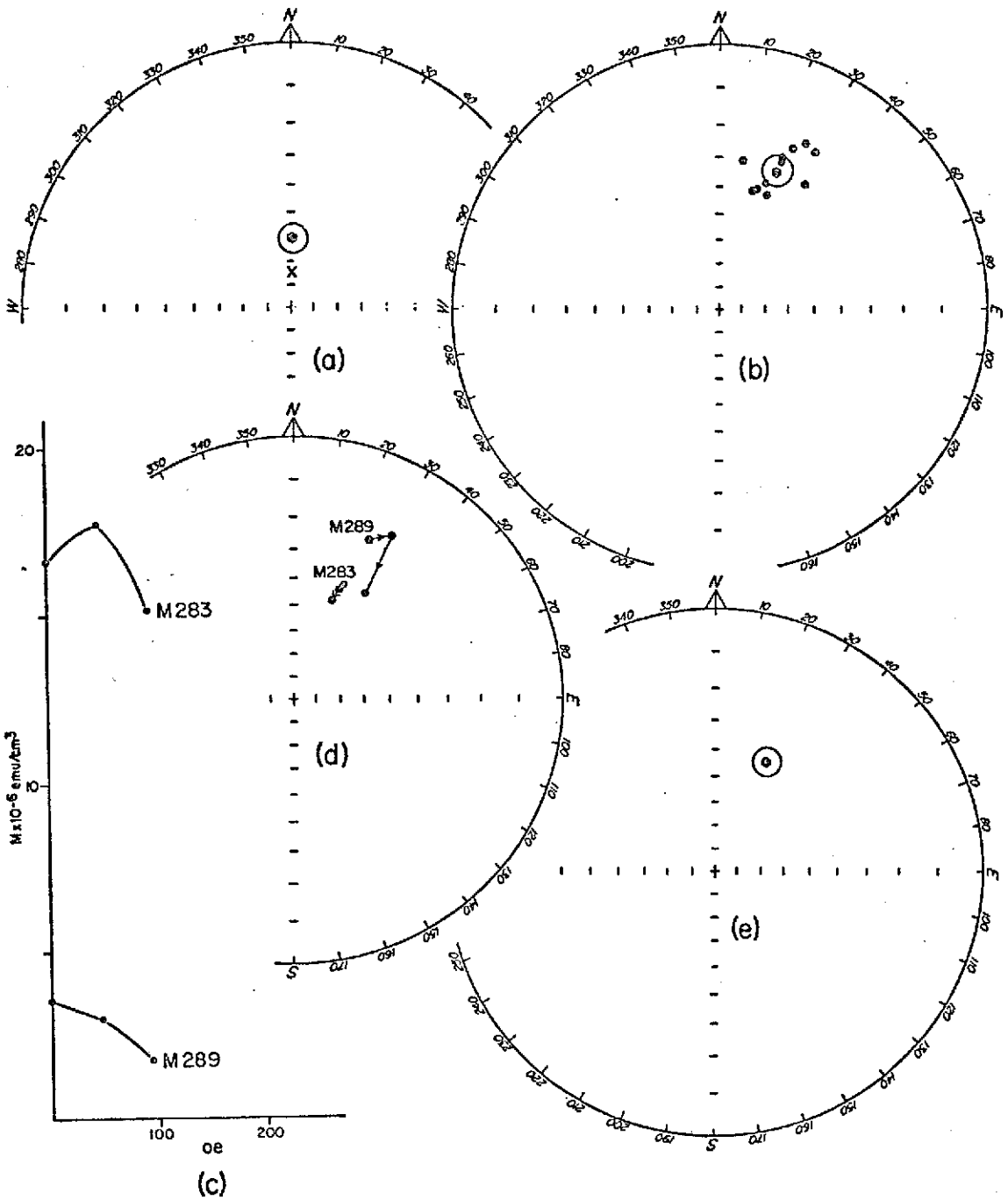

Figure 3-22. Paleomagnetic data for NBS-3, Nabesna area, Alaska. (a) NRM P. (b) NRM. (c) Magnetic intensity and (d) directions of pilot samples during AF demagnetization. (e) After demagnetization at 95 oe.

lity was 30 x 10^{-6} emu/cm^3. The samples from both NBS-1 and 3 had intensities too small to demagnetize further. It would appear that both of these groups of samples arrived at a stable position by the removal of low-coercivity secondary components. The scatter for both sites was extremely small, and they are both good approximations of the Jura-Cretaceous VGP.

The Triassic-Permian greenstone sampled in the Nabesna area had an NRM P that did not lie along the present axial dipole field direction. Demagnetization at an AF of 380, 760, and 1520 oe caused a small shift in the mean vector direction and at the same time reduced the scatter. The mean NRM intensity was 220 x 10^{-6} emu/cm^3, and the mean susceptibility was 630 x 10^{-6} emu/cm^3. The behavior of these samples was nearly the same as those of the same rock type collected at MNT. The scatter was a bit less than MNT, but the secondary components shown in the intensity upon demagnetization and the alteration as seen in thin section were the same. These results, then, are marginal in their representation of the Triassic-Permian VGP.

WHITEHORSE, CANADA

Geologic setting of the Whitehorse area, Canada

The geologic summary presented here is taken from J. O. Wheeler's Geological Survey of Canada Memoir on the Whitehorse map-area, Yukon Territory 105 D, which was published in 1961. His work is an excellent treatment of the geology, glaciation, and economic mineral deposits in the Whitehorse map-area. An attempt has been made to limit the discussion, when possible, to the Takhini Hotspring vicinity where paleomagnetic samples were collected (Fig. 3-23).

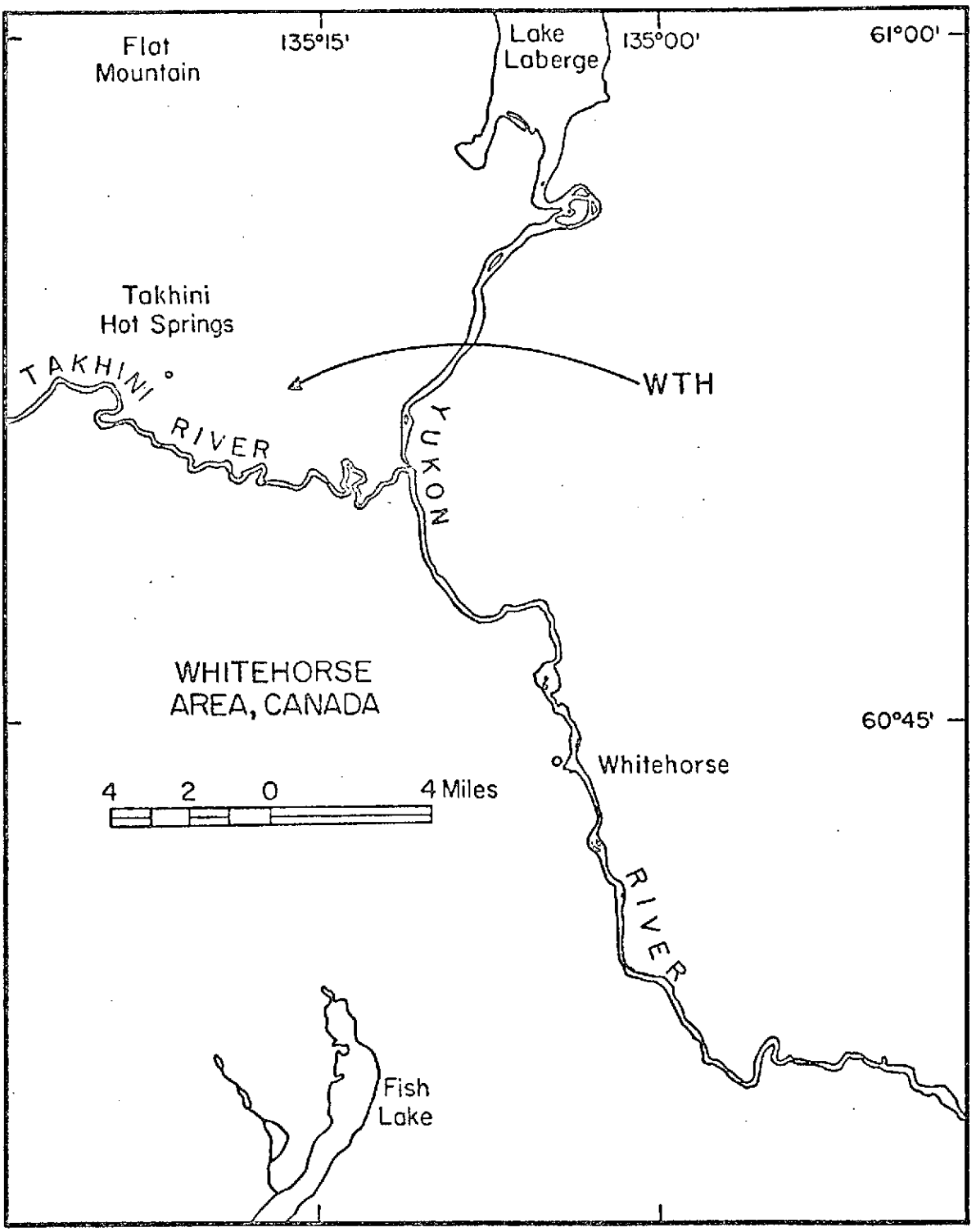

Figure 3-23. Location map for place names and sampling locality in the Whitehorse area, Canada.

The Yukon group, Precambrian and early Paleozoic metamorphics, which are composed chiefly of quartz-mica schist, quartzite, and feldspathic gneiss is the oldest rock unit in the Whitehorse map-area. It outcrops along a northwest trending belt approximately 30 miles southwest of Whitehorse. The Taku group, a massive limestone interbedded with greenstone and chert, is exposed to the southeast of Whitehorse. The age of the Taku group ranges from Pennsylvanian through upper Triassic. The relationship of the Taku group to the upper Triassic Lewes River group is unknown.

The Lewes River group is exposed in the north, central, and eastern parts of the Whitehorse map-area. In the Takhini Hotspring area it is the oldest unit exposed and is composed of interbedded limestone, volcanic graywacke, and maroon sandstone and conglomerate. Generally its composition through 10,000 feet of section ranges from graywacke, siltstone, andesite and basalt flows, limestone, and low-grade metamorphosed volcanic rocks. This assemblage probably represents a trough in which clastic sediments, partly of volcanic origin, were deposited during most of Norian time. In late Norian however, limy muds were deposited throughout the trough. This trough has been called the Whitehorse trough and is part of the Tagish belt, which has been classified as an idiogeosyncline that extends south into British Columbia.

In the Takhini Hotspring area the Lewes River group is disconformably overlain by approximately 9500 feet of a graywacke with interbedded conglomerate and argillite of the early to middle Jurassic Laberge group. To the southwest of Whitehorse, the Laberge

group is in fault contact with the upper Jurassic-lower Cretaceous Tantalus Formation, which is composed of arkose, siltstone, and conglomerate. To the northeast of Takhini Hotspring, the Laberge group is intruded by a mid Cretaceous peridotite body that is highly deformed and lies parallel to the bedding plane.

The Hutshi group, consisting mainly of flows that range in composition from basalt to rhyolite and minor graywacke and argillite, is mid Cretaceous in age. On Flat Mountain to the north of Takhini Hotspring, the Hutshi group is in contact with the Laberge group and the Lewes River group across an angular unconformity. This area was deformed in the early to mid Cretaceous into northeast trending folds. In the Takhini Hotspring area the folding is represented by a broad syncline; however, the intensity of folding increases to the northeast. Minor faulting also occurred during this time. Northward trending right-lateral strike-slip faults are predominant, one occurs in the Takhini Hotspring area. Cross faults, both normal and reverse, are also present.

Intruded into the Hutshi group in the Takhini area is a body of Cretaceous leucocratic granite. This body is a part of a granitic complex known as the Coast Intrusives that outcrop in and underlie well over half of the western portion of the Whitehorse map-area. The rock types in order of abundance in this complex are granodiorite, leucocratic granite, and quartz diorite. Other smaller bodies of quartz monzonite and the Eocene or older Skukum group, an andesitic and basaltic volcanic flow unit with associated pyroclastic debris, are present in the Whitehorse map-area but do not occur in the Takhini

Hotspring area. Minor block faulting accompanied the intrusion of some of the larger granitic bodies.

Extensive glacial deposits from the Cordillerian Ice-sheet of Pleistocene age, recent alpine glacial deposits, and deposits of a small Pleistocene basalt flow and pyroclastics (western Whitehorse map-area) make up the Cenozoic record.

Sites near Whitehorse area, Canada

Whitehorse, Canada (WTH)

Forty-four cores from the upper Triassic Lewes River group were collected from the Takhini Hotspring vicinity approximately twelve miles northwest of Whitehorse. These samples are from two sites, approximately a quarter of a mile apart. The rock consists of tan-to-maroon fine-grained chlorite with minor argillaceous interstitial material. In some area the rocks have been affected by hematite staining that has been preferentially absorbed by the argillaceous fraction. WTH-1 represents approximately 400 stratigraphic feet, and WTH-2 approximately 100 stratigraphic feet. The beds dip east-northeast at 15 to 30 degrees.

The results of measurements on the samples from WTH are presented in Table 3-10 and Figure 3-24. The mean of NRM P was not along the present axial dipole field direction. On demagnetization at an AF of 48 and 95 oe the mean shifted slightly and reduced the scatter of vector directions around it. The mean intensity and susceptibility were 30×10^{-6} emu/cm^3 and 120×10^{-6} emu/cm^3, respectively. It seems that the mean direction of these samples after demagnetization at an

C2

TABLE 3-10

PALEOMAGNETIC DIRECTIONS AND POLE POSITIONS

	LOCATION	TREATMENT	N	DIRECTION D	I	A95	K	POLE POSITION LAT	ELONG	A95	K
WTH -	WHITEHORSE AREA, CANADA	NRM P	44	269	67	11.5	4.5	42	166		
	(60.9N,224.7E)	NRM	44	19	78	11.8	4.3	76	249	16.9	2.6
	2 SITES	AF 48 OE	44	65	60	10.1	5.6	50	306	12.9	3.8
	UPPER TRIASSIC LEWES RIVER GROUP	AF 95 OE	44	73	61	9.3	6.4	47	299	11.4	4.5

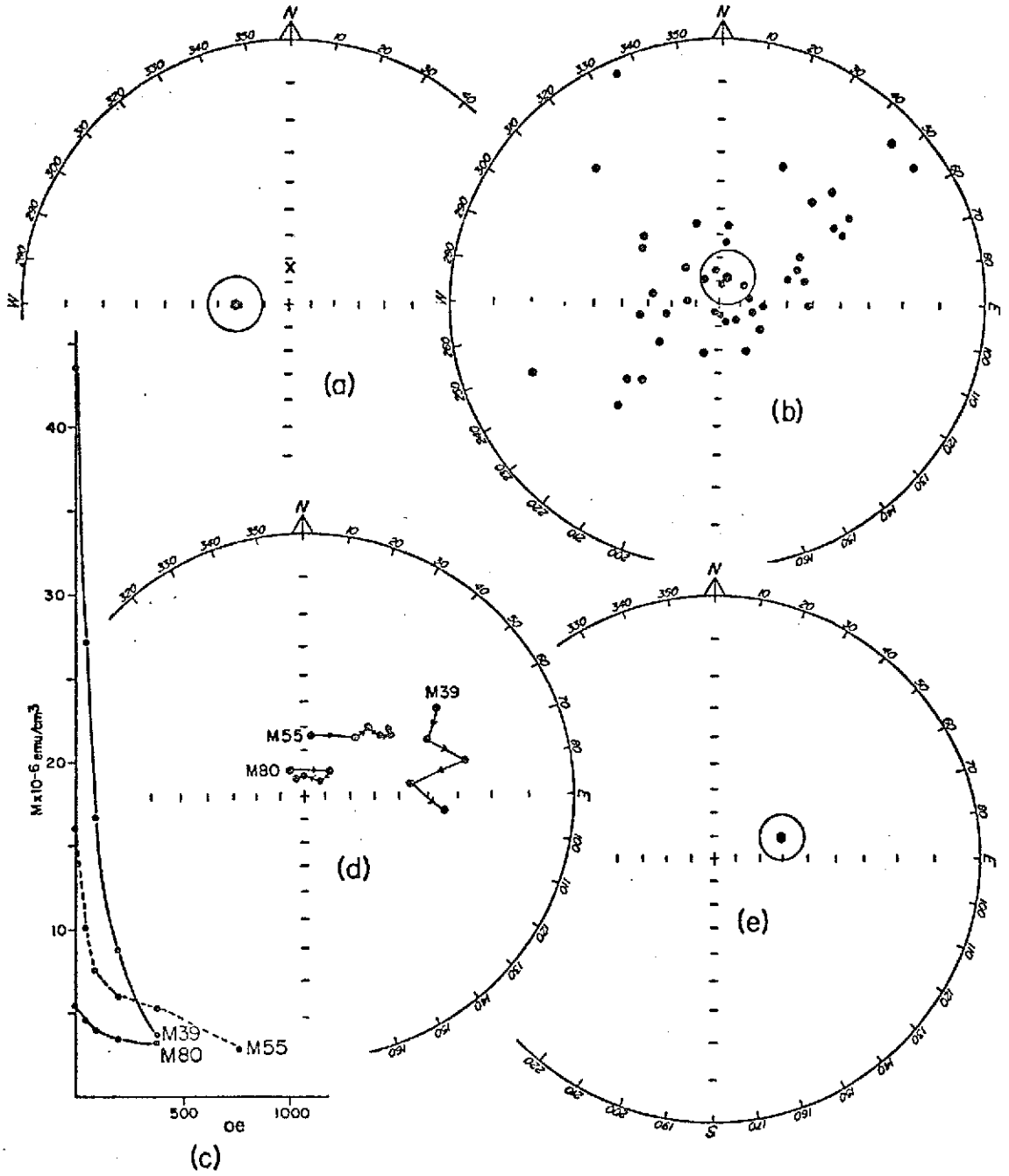

Figure 3-24. Paleomagnetic data for WTH, Whitehorse area, Canada. (a) NRM P. (b) NRM. (c) Magnetic intensity and (d) directions of pilot samples during AF demagnetization. (e) After demagnetization at 95 oe.

AF of 95 oe represents a stable field and a good approximation of the upper Triassic VGP for this area.

IV. ALASKAN MAGNETIC DECLINATIONS AND VIRTUAL GEOMAGNETIC POLES

A summary of the results from Chapter III is presented in Figures 4-1 to 4-3. The mean virtual geomagnetic poles (VGP's) for NRM P (NRM with respect to present horizontal), NRM (NRM with respect to ancient horizontal), and demagnetization levels are plotted for all sites except KTM-3, which was unstable. Selection criteria were applied to the "good" results (see Chapter III), as indicated in Figures 4-1a, 4-2a, and 4-3a, by discarding any results having a $k < 5$, namely CHL-3 and KTM-1. Also rejected was the mean pole from TXD-2 because it is displaced from the mean of the other Jurassic samples by more than 90 degrees. There appears to be no simple explanation for this divergence in terms of magnetic stability, local rotation, or tilting. The most plausible explanation is probably that of a large field excursion.

These selected VGP's and their 95% circles of confidence are plotted in Figures 4-1b, 4-2b, and 4-3b, and listed in Table 4-1. Although there are other ways of combining the apparently stable results from individual sites by choosing different selection criteria, etc., they do not significantly alter the mean paleomagnetic pole position. The particular approach used here is the most viable paleomagnetically and geologically. A two-tier analysis (Watson and Irving, 1957) was not applied to the data because the variances, k, are unequal, and because the products, $K_i N_i$, vary widely (McElhinny, 1967; and Bingham, 1971).

For the Triassic the only stable result is WTH. No obvious explanation can be found for the divergence between the two apparently mag-

Explanation to Figures 4-1 to 4-3

(a) Plots of mean VGP's for NRM P (NRM with respect to present horizontal) shown as ⊷, NRM (NRM with respect to ancient horizontal) shown as ⊡⊷, and demagnetization levels for both stable and marginal results from Chapter III shown as ⊷. The best demagnetization level for stable results is shown as ⊷◎.

(b) Stable results shown within 95% circles of confidence. VGP's not included in mean if $k < 5$, or divergent (indicated by ?). Mean is shown as ⊡.

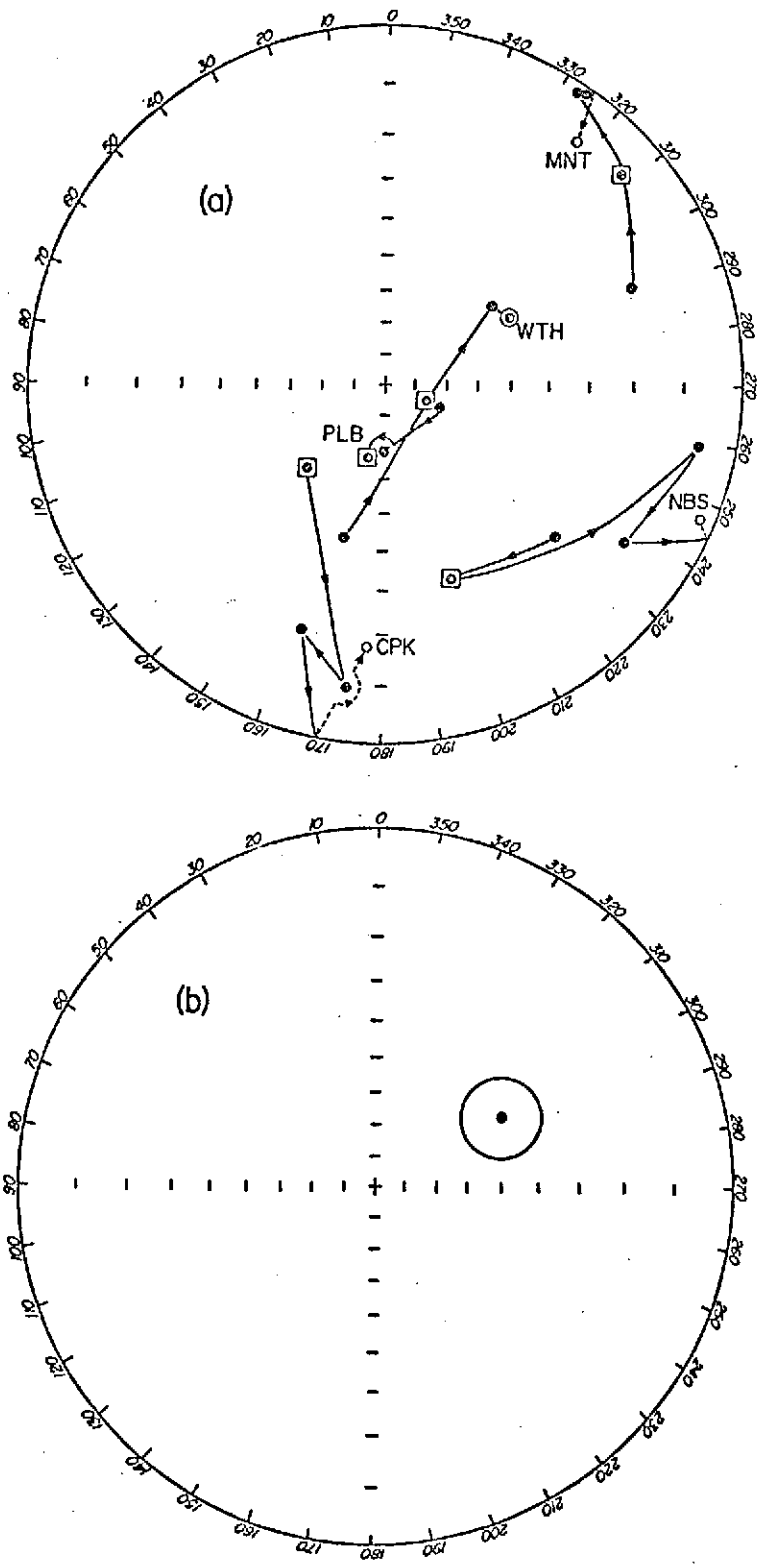

Figure 4-1. (a) Mean VGP's for Triassic and Permian sites. (b) Mean of stable results. (Explanation on preceding page.)

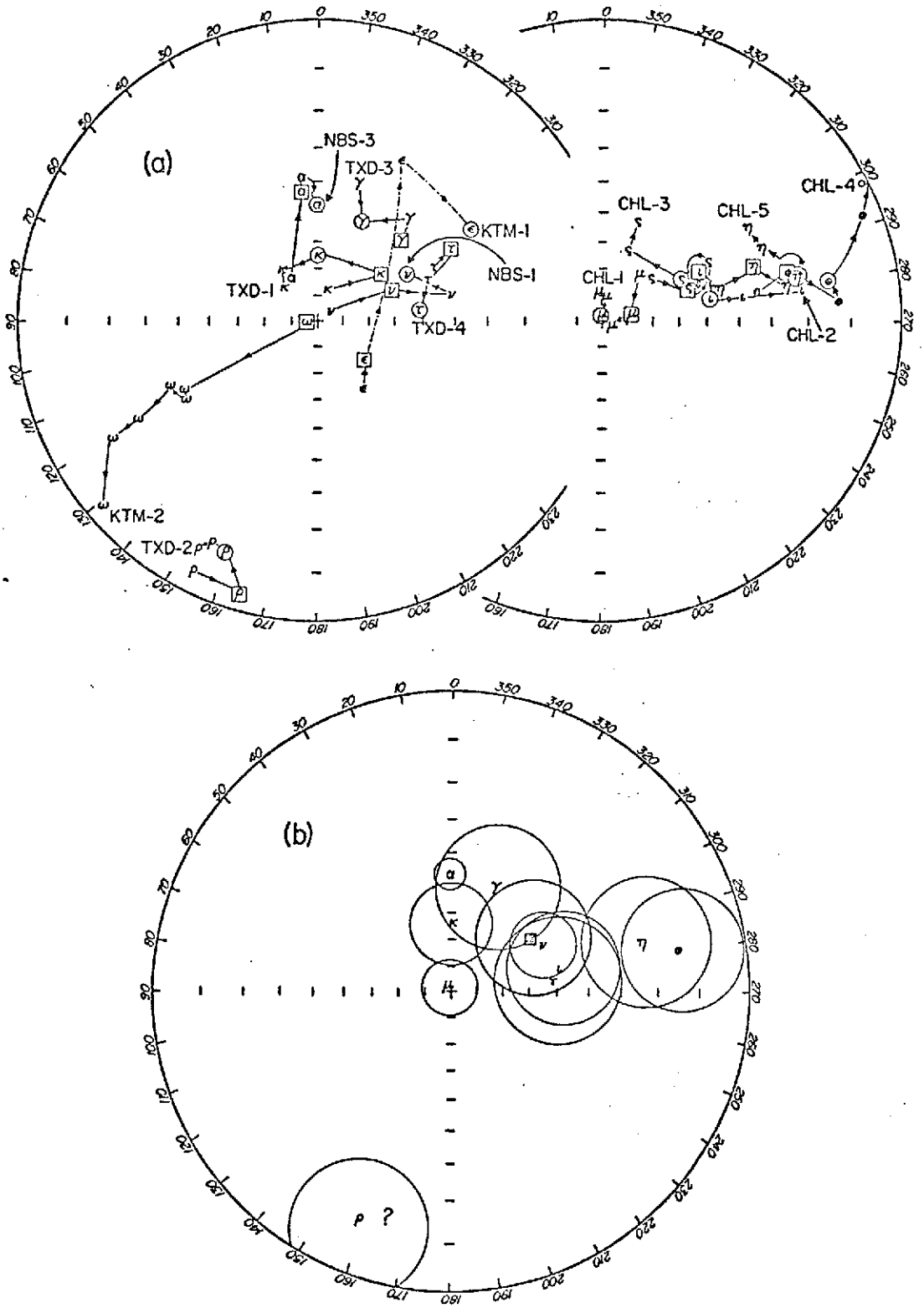

Figure 4-2. (a) Mean VGP's for Jurassic sites. (b) Mean of stable results. Separate symbols are used for each site for clarity. (Explanation precedes Fig. 4-1.)

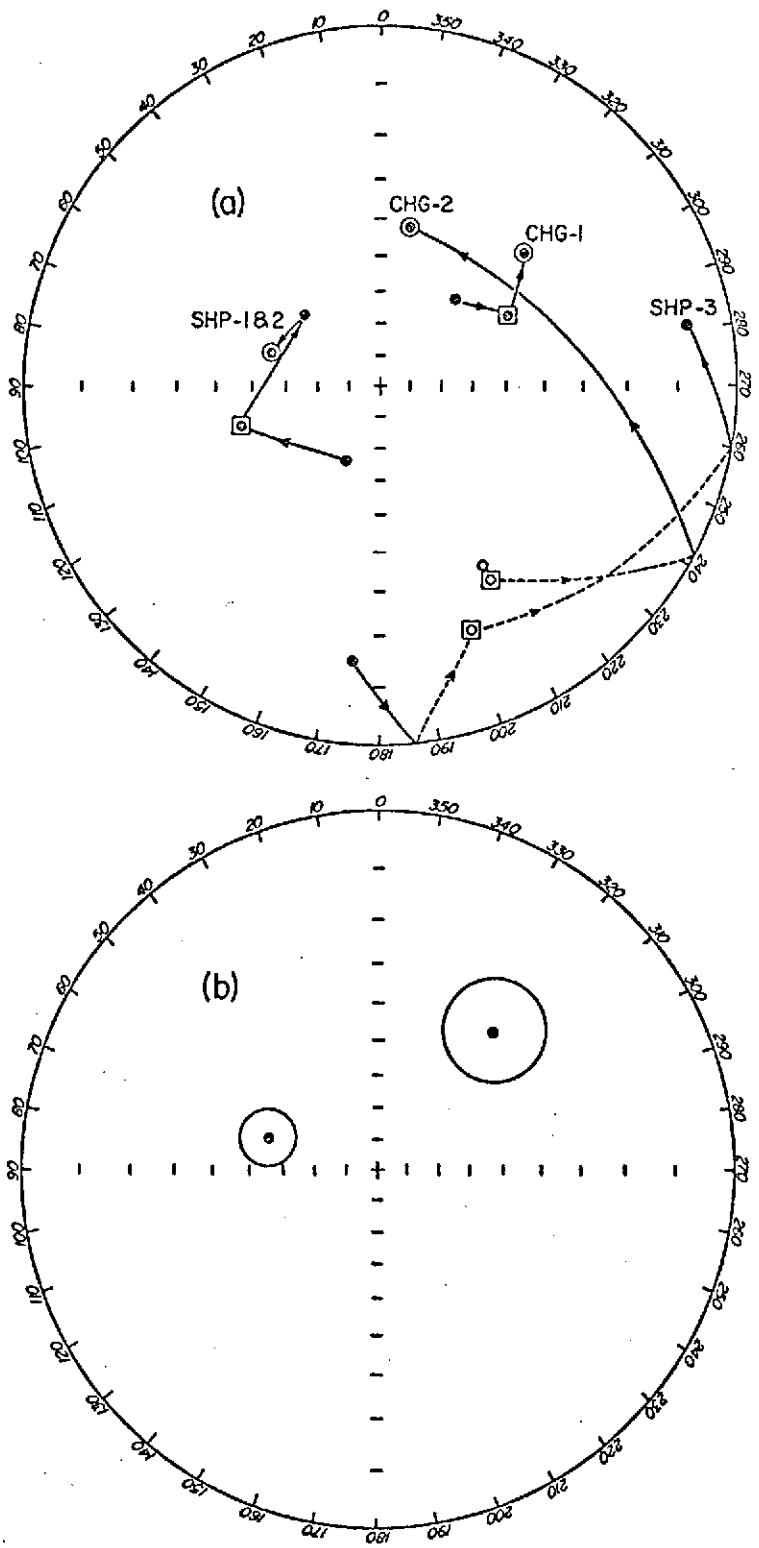

Figure 4-3. (a) Mean VGP's for Cretaceous sites. (b) Mean of stable results. CHG-1 and 2 combined (see Chap. III). (Explanation precedes Fig. 4-1.)

TABLE 4-1

PALEOMAGNETIC DIRECTIONS AND POLE POSITIONS

	SITE	TREATMENT	N	DIRECTION D	I	A95	K	POLE POSITION LAT	ELONG	A95	K
TRIASSIC	WTH	AF 95 OE	44	73	61	9.3	6.4	47	299	11.4	4.5
JURASSIC	CHL-1	AF 95 OE	10	1	70	6.8	51.2	89	339	10.8	21.0
	CHL-2	AF 95 OE	10	62	61	13.5	13.8	49	282	19.5	7.1
	CHL-4	AF 95 OE	9	90	32	23.1	5.9	15	280	19.3	8.1
	CHL-5	AF 95 OE	12	81	39	16.6	7.8	23	284	18.0	6.8
	TXD-1	AF 95 OE	15	14	53	15.2	7.3	65	0	15.2	7.3
	TXD-3	AF 190 OE	10	36	45	18.4	7.8	50	336	20.5	6.5
	TXD-4	AF 95 OE	9	71	66	15.8	11.5	52	276	20.4	7.3
	NBS-1	AF 95 OE	14	63	65	7.4	30.2	54	297	10.6	15.1
	NBS-3	AF 95 OE	11	26	40	4.7	93.8	47	1	4.8	91.4
	MEAN		9					54	303	20.3	7.4
CRETACEOUS	CHG-1&2	AF 48 OE	17	48	31	13.1	8.4	37	319	13.5	7.9
	SHP-1&2	AF 95 OE	22	334	50	6.7	22.7	55	74	7.5	18.3

netically stable Cretaceous results from CHG-1 and 2 from SHP-1 and 2. Without other measurements from these same general areas and from southern Alaska, no firm conclusion can be drawn as to the true position of the southern Alaskan Triassic and Cretaceous paleomagnetic poles. It is interesting to note, however, that the mean VGP's of Cretaceous CHG-1 and 2, the stable Triassic WTH, and the Alaskan mean Jurassic pole all have 95% circles of confidence which overlap. Also interesting is the fact that the mean VGP's of the Cretaceous SHP-1 and 2 and the Cretaceous Taylor Highway site of Chantry-Price's study (1967) have α_{95} circles that overlap.

The mean pole position of the nine remaining Jurassic VGP's have a k equal to 7.4 and an α_{95} of 20.3 degrees (Table 4-1). The data are a good representation of the paleomagnetic field on the basis that it comes from sites that have a geographic spread of over 700 miles, and have a varied lithology which includes sandstones, siltstones, and granitic intrusives. The Jurassic period is also adequately represented by rocks that range in age from lower to upper Jurassic. Thus, although α_{95} and k indicate a fair amount of scatter, the results are certainly significant. Because of the inconclusive Cretaceous and Triassic data, the Jurassic results have been used to test the orocline.

ALASKAN OROCLINE

Workers attempting to define oroclines in the past have worked mainly with declinations (see Irving, 1964), because inclinations add still another variable. In Figure 4-4 the declinations for the

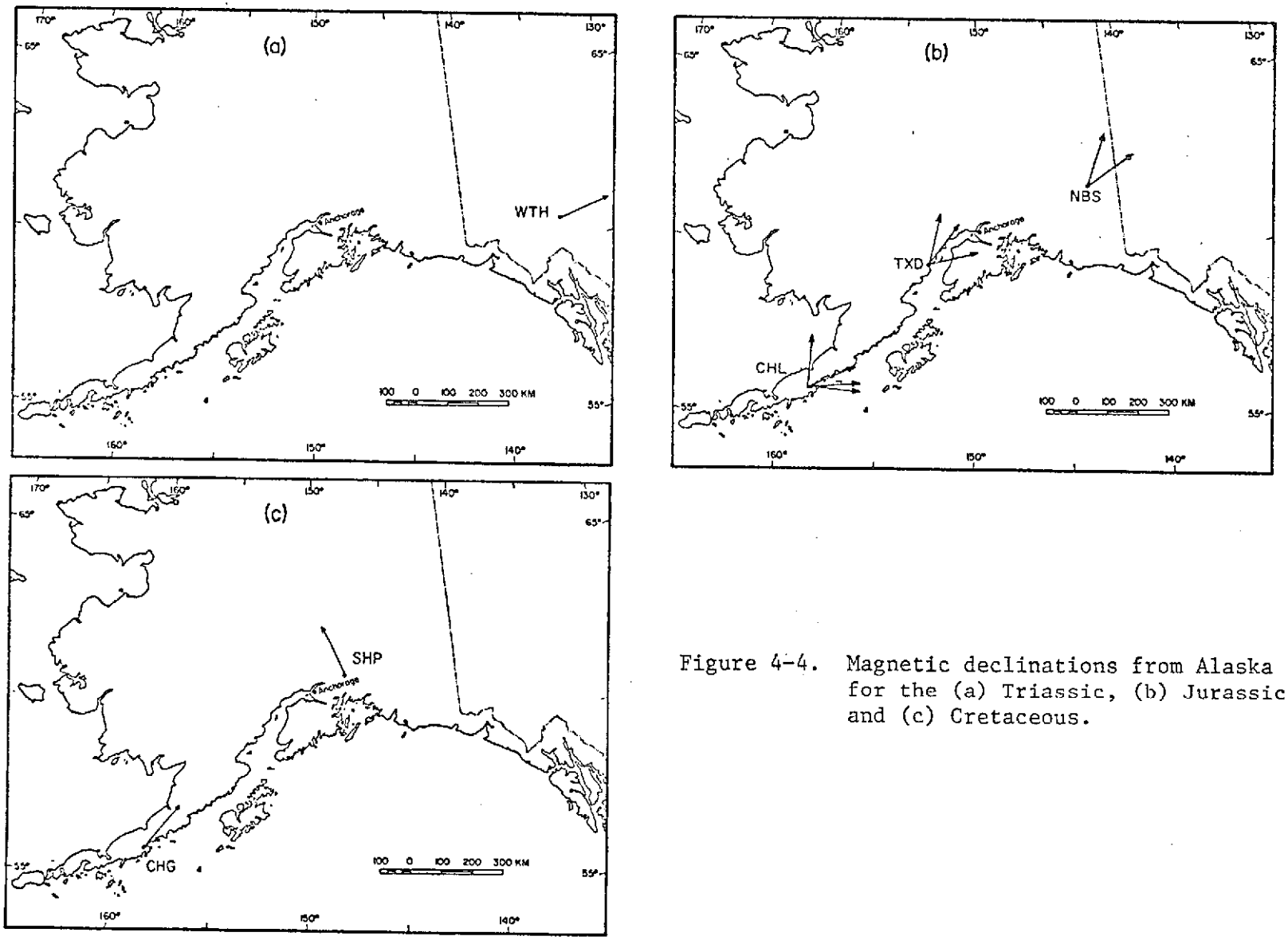

Figure 4-4. Magnetic declinations from Alaska for the (a) Triassic, (b) Jurassic, and (c) Cretaceous.

stable results for the Triassic, Jurassic, and Cretaceous are shown. Figure 4-5 shows the declination for the Jurassic after "unbending" according to both Carey's and Grantz's models of the orocline.

Grantz (1966) modeled the Alaskan orocline as a series of rigid bodies rotating about pivots along a north-south line in mid-Alaska (see Chapter 1). The rotation he estimated for the Alaska Peninsula was 40 degrees. A simple rotation of 30 degrees has also been shown for Carey's (1958) model of the orocline (Fig. 4-5). This representation is not precisely correct, because an orocline is a 'fold', and points near the axis would undergo relatively lesser amounts of rotation. In practice, this would only increase the scatter of the declinations for Carey's model, because as can be seen from Figure 4-5, the largest declinations are farthest from the pivot points.

In Figure 4-5d, the mean vector directions and their standard deviations indicate that the two models are not significantly different from the present; thus it is impossible to say for sure whether or not oroclinal bending has occurred. This is in part due to the moderately large scatter, and hence large standard deviations, about the means of the various models, and in part due to the fact that not enough resolution can be obtained from the two sites on the North American or eastern limb of the Alaskan orocline. In order to establish a fixed point from which to determine relative motion between the two limbs, it will be necessary to collect more samples from the eastern limb. If the VGP's from the western limb are compared with those from elsewhere in North America, as is explained in more detail in the next section, they are displaced from each other in the wrong direction to be explained by the Alaskan orocline.

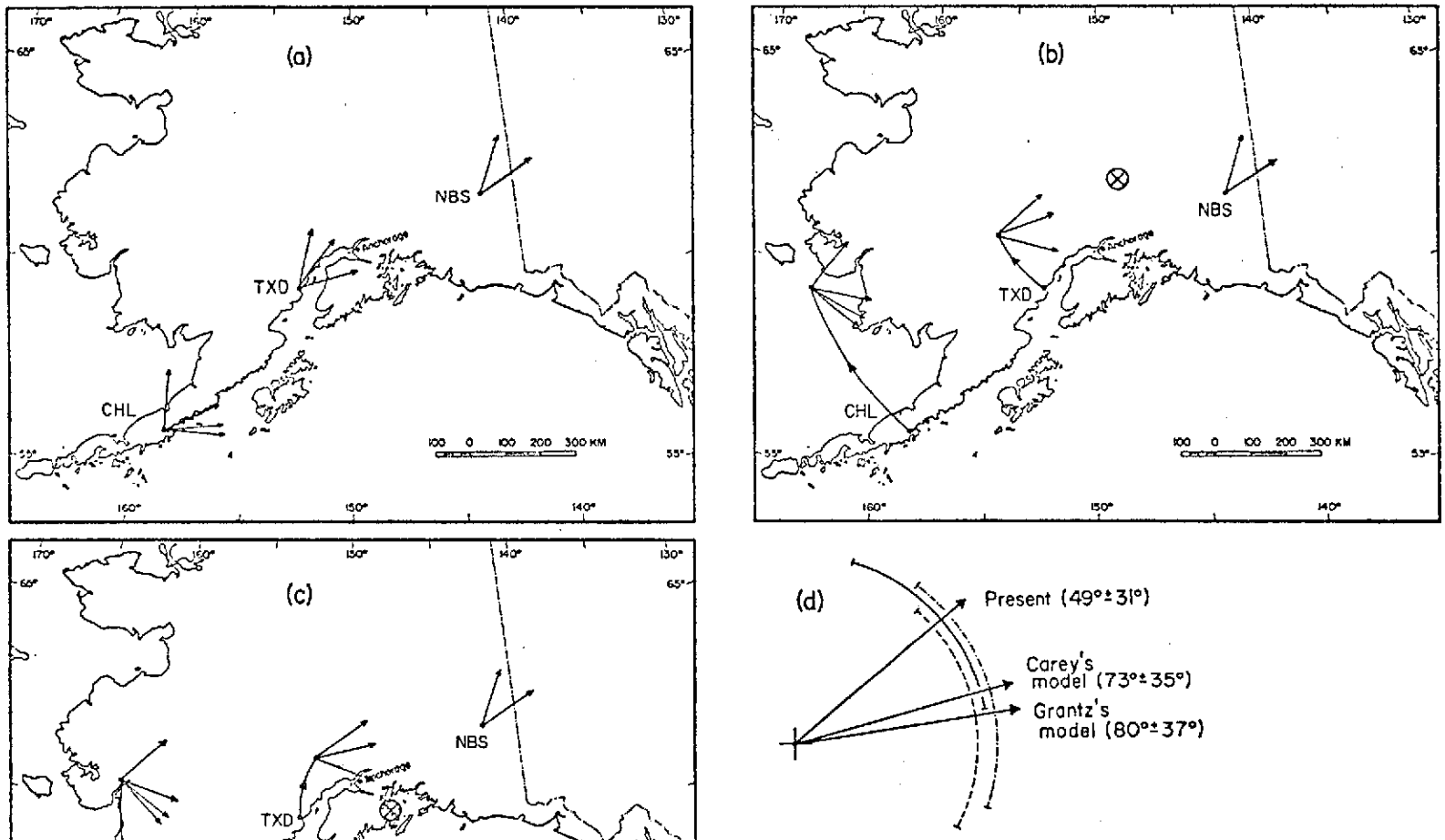

Figure 4-5. Magnetic declinations for Alaskan Jurassic results showing (a) present position, (b) after rotation of 30° about ⊗ for Carey's model, and (c) after rotation of 40° about ⊗ for Grantz's model. (d) Mean magnetic declinations ± standard deviations.

In summary, the relative positions of the Jurassic poles for Alaska and North America represent relative motion in a sense opposite that suggested by Carey. Thus it would seem unlikely that Carey's concept of an Alaskan orocline is valid.

ALASKAN PALEOMAGNETIC POLES

For the purposes of comparing Alaskan data with the continents surrounding the Arctic Ocean, a compilation of paleomagnetic poles was made, and is given in the Appendix. The mean paleomagnetic pole for the Jurassic from southern Alaska is shown in Figure 4-6 along with selected Jurassic paleomagnetic poles for North America and their mean (see next section). The Jurassic paleomagnetic pole from southern Alaska is significantly different from the present magnetic dipole and from the Jurassic paleomagnetic pole for North America.

Alaska's Jurassic orientation and latitude with respect to the present has been determined from the Jurassic mean paleomagnetic pole position (Table 4-1). Employing the common paleomagnetic assumption of a mean geocentric axial dipole (see Chapter II), the latitude and orientation for any given "reference site" can be found by spherical trigonometry from the paleomagnetic pole position, which is latitude independent. For convenience, a "reference site" has been defined to be located at 60 degrees north latitude and 207 degrees east longitude, which is the location of Tuxedni Bay and also nearly the median of the Jurassic sampling areas. The paleolatitude of the reference site during the Jurassic has been determined to be 42 degrees north, com-

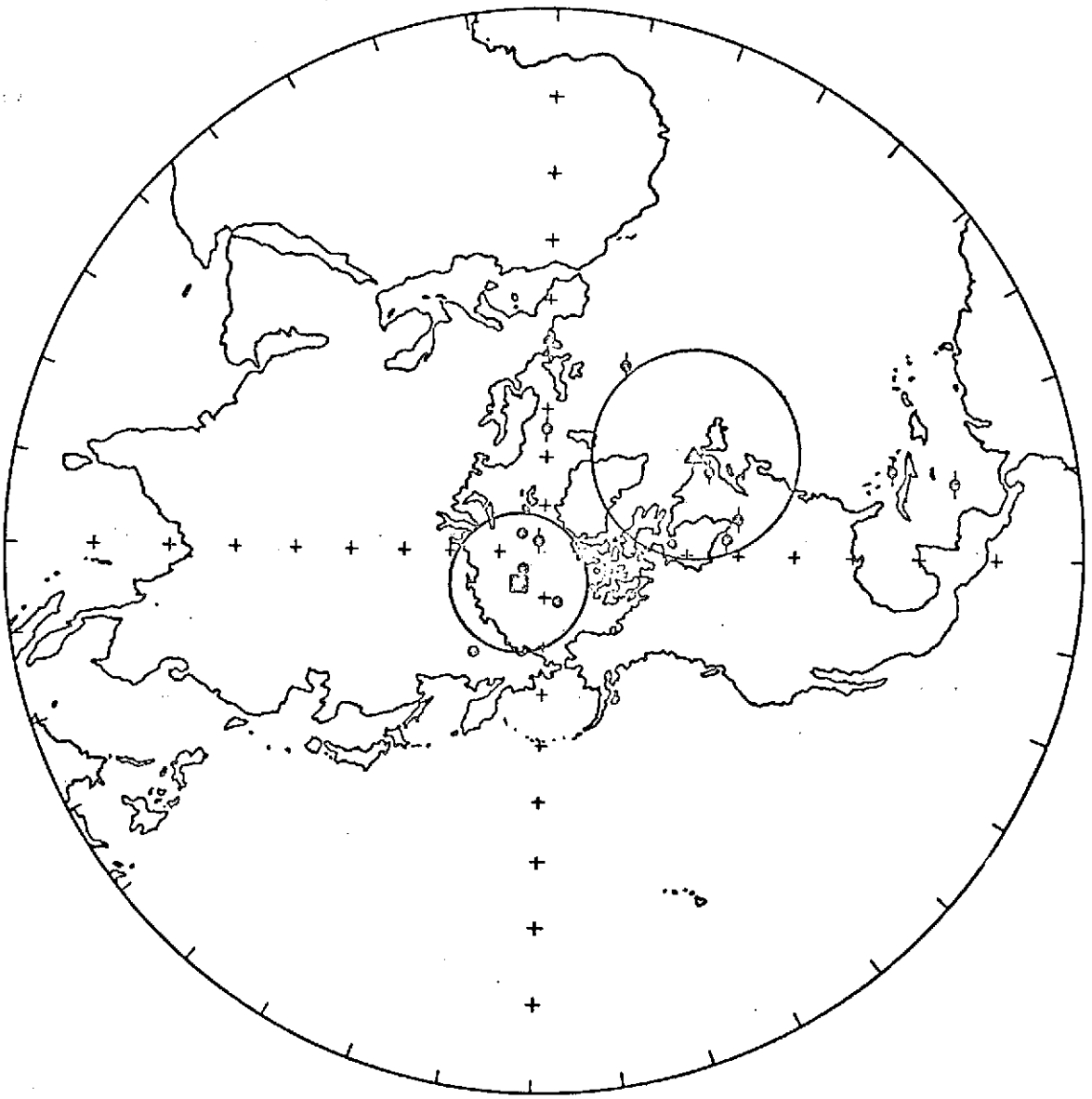

Figure 4-6. Selected North American paleomagnetic poles ● , and their mean □ . Mean VGP's ϕ and their mean Δ for Jurassic results from southern Alaska. Circles are 95% confidence limits.

pared with the present latitude of 60 degrees north, thus requiring a position approximately 18 degrees further south for Jurassic times. A counterclockwise rotation equal to 52 degrees is also required to place Alaska in its Jurassic orientation. Applying the 95% confidence limits, Alaska could have been as far north as 62 degrees north latitude and as far south as 23 degrees north latitude. The 95% confidence limits would allow a rotation of at least 29 degrees with a maximum of 68 degrees. At lesser confidence levels, however, say the 63% confidence level, these limits are reduced by nearly half, i.e. there is a higher probability of the true pole position being nearer the center of the error limits than at its edges.

Alaska's Jurassic latitude with respect to North America may also be found by superimposing the Jurassic paleomagnetic poles for the two blocks. Relative to the Jurassic North American pole, southern Alaska must have had a paleolatitude equivalent to that of Oregon, the continental margins of the Alaska Peninsula and Washington-Oregon being approximately parallel. If Alaska and Washington-Oregon were together in the Jurassic, then the required motion, determined graphically, could be described in terms of an opening of approximately 97 degrees about an Euler pole at 59 degrees north, 236 degrees east. The paleolongitude of southern Alaska, however, is indeterminable from a single paleomagnetic pole position.

Unfortunately the Jurassic paleomagnetic pole for North America is not well defined because there are only four poles from sites east of the Sierra Nevada Mountains. Poles from west of the Sierra Nevada Mountains indicate either a complex tectonic history, a very erratic

magnetic field during the Jurassic, or undetected magnetic instability (see next section).

POLAR WANDERING CURVES

The Appendix is a compilation of Permian, Triassic, Jurassic and Cretaceous paleomagnetic poles for North America, Asia, and Europe taken from compilations by Irving (1964) and McElhinny (1968a, b; 1969; 1970) and recently published pole positions.

An attempt was made to list every Mesozoic mean paleomagnetic pole position for the United States, Canada, China, Union of Soviet Socialist Republics, and European countries, available in scientific journals in English, with the exception of results from areas in southern Europe. These are not listed because of the complex tectonic history of the area. The paleomagnetic pole positions are listed systematically by longitude within each country, starting with the USA and working west to England. It was also the practice to list the extremes of latitude and longitude when samples for the same study were collected over a large region. In a few cases many formations of the same age were collected from a given region, and their poles have been listed separately if so reported. This is more effective in averaging secular variation. Care was taken to avoid duplication of results that have been superceded by further study; however, different studies of the same rock unit in adjacent areas are included separately.

In calculating the overall mean paleomagnetic pole, pole positions that were extremely divergent (> 40 degrees) from a visual mean of the greatest density of points were excluded. Also excluded from

the mean were those poles mentioned in the original publications as having undergone local rotation or tectonic movement. The mean paleomagnetic pole position for a given age follows the list of the individual determinations used. Any poles of that age which were not included for any of the above reasons are given after the mean for that section.

Figures 4-7 to 4-18 are derived from the Appendix. The pole positions and collecting sites are both shown and are connected together when the pole is divergent from the mean and in other cases of interest. The mean paleomagnetic pole position for each continent by age is listed in Table 4-2. A brief explanation of some of the mean paleomagnetic pole positions in Figures 4-7 to 4-18 follows.

There appears to be a difference between Permian poles determined from eastern Asian sites and western Asian sites; a mean pole position from the eastern sites would not be well defined (Fig. 4-7). Hamilton (1970) cites paleomagnetic evidence to support a hypothesis that the Siberian and Russian platforms were separated until the Permian or Triassic, but it has not been possible to review all of the Russian data he used.

Jurassic pole positions from North America (Fig. 4-13) show a distinct division between those from sites east of the Sierra Nevada Mountains and those from sites west of the Sierra Nevada Mountains. Poles 120 and 121 are west coast batholiths, and 122 and 123 are peridotite and dunite respectively, from the Franciscan Formation. Pole 124 represents 'divergent' results from both the peridotite and the dunite. Pole 125 is from a number of sedimentary sections within

Explanation to Figures 4-7 to 4-18

- • sites from which samples were collected.
- ⊕ pole positions included in the mean.
- ⊗ poles not included in the mean.
- ⊡ mean pole position, within its 95% circle of confidence.

All data taken from Appendix.

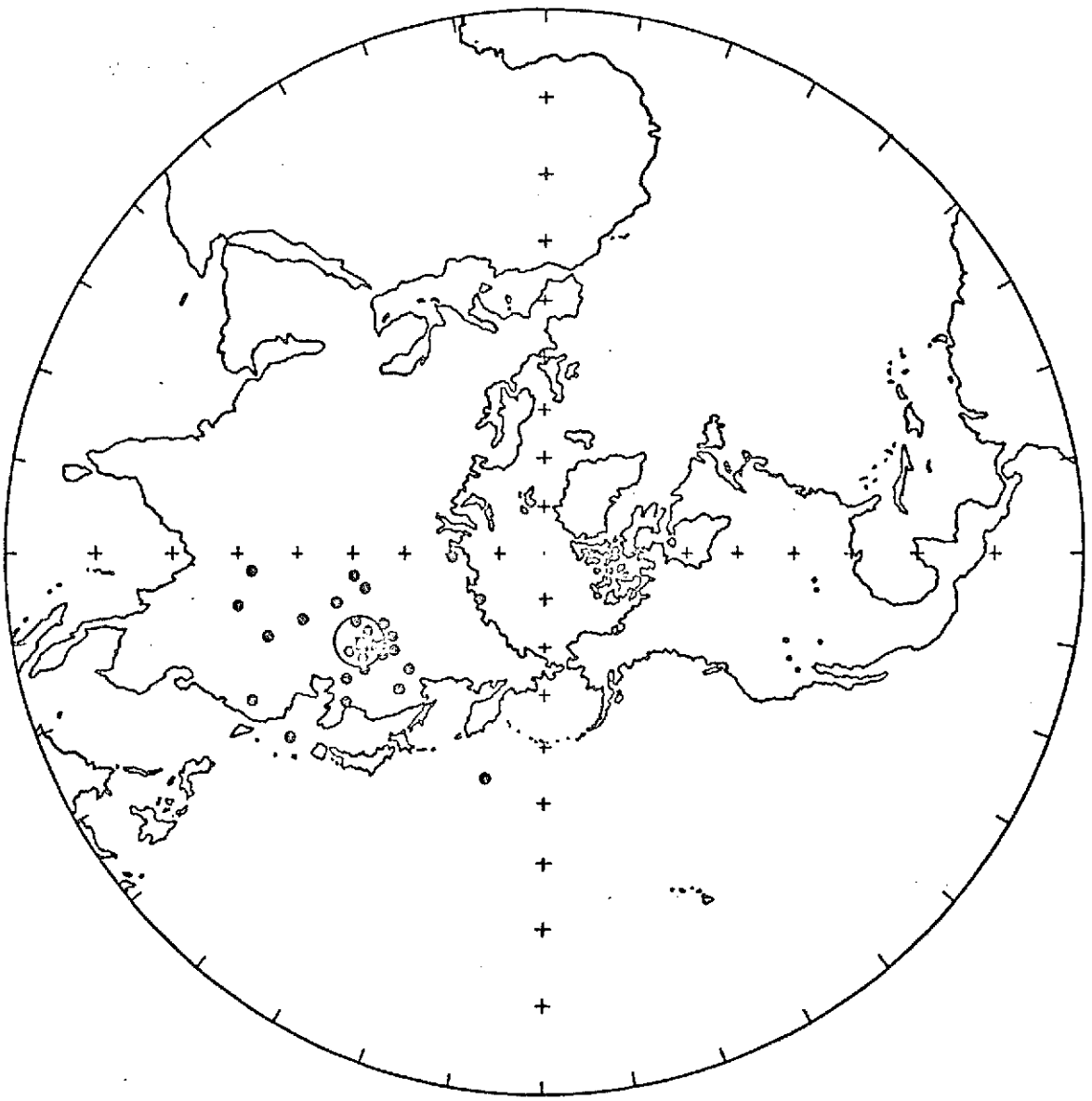

Figure 4-7. Permian paleomagnetic poles from North America. (Explanation on preceding page.)

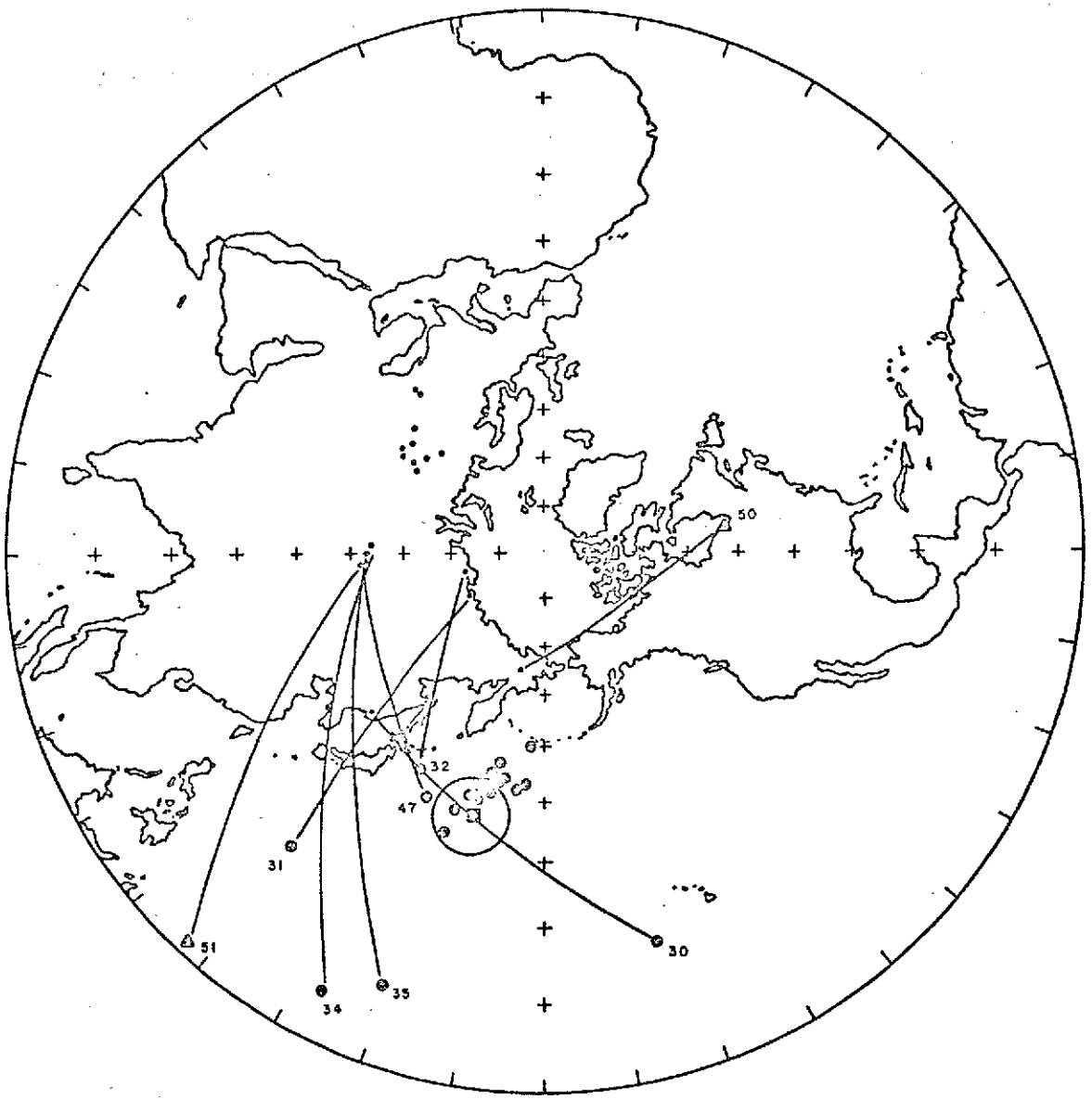

Figure 4-8. Permian paleomagnetic poles from Asia.
(Explanation precedes Fig. 4-7.)

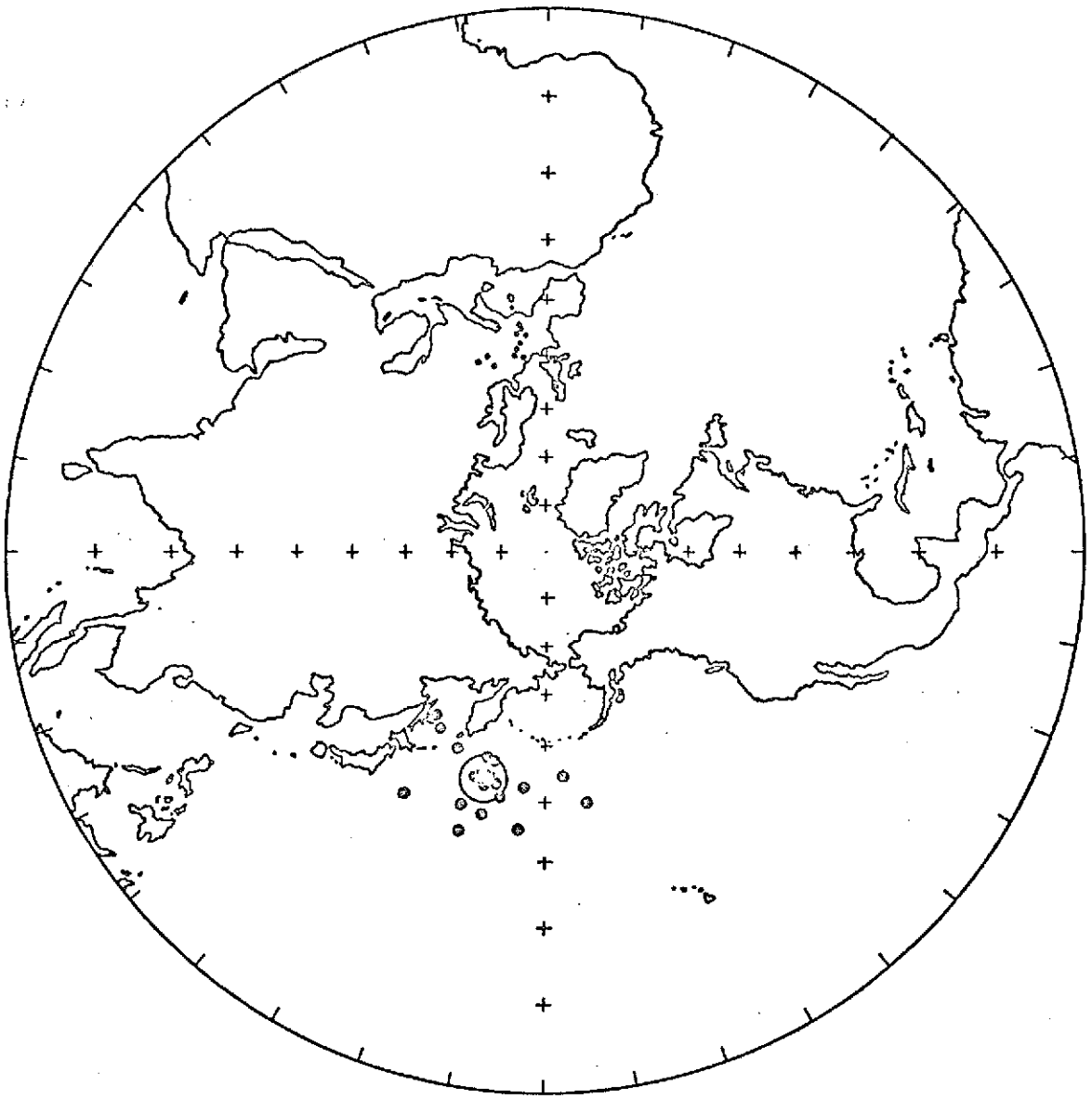

Figure 4-9. Permian paleomagnetic poles from Europe.
(Explanation precedes Fig. 4-7.)

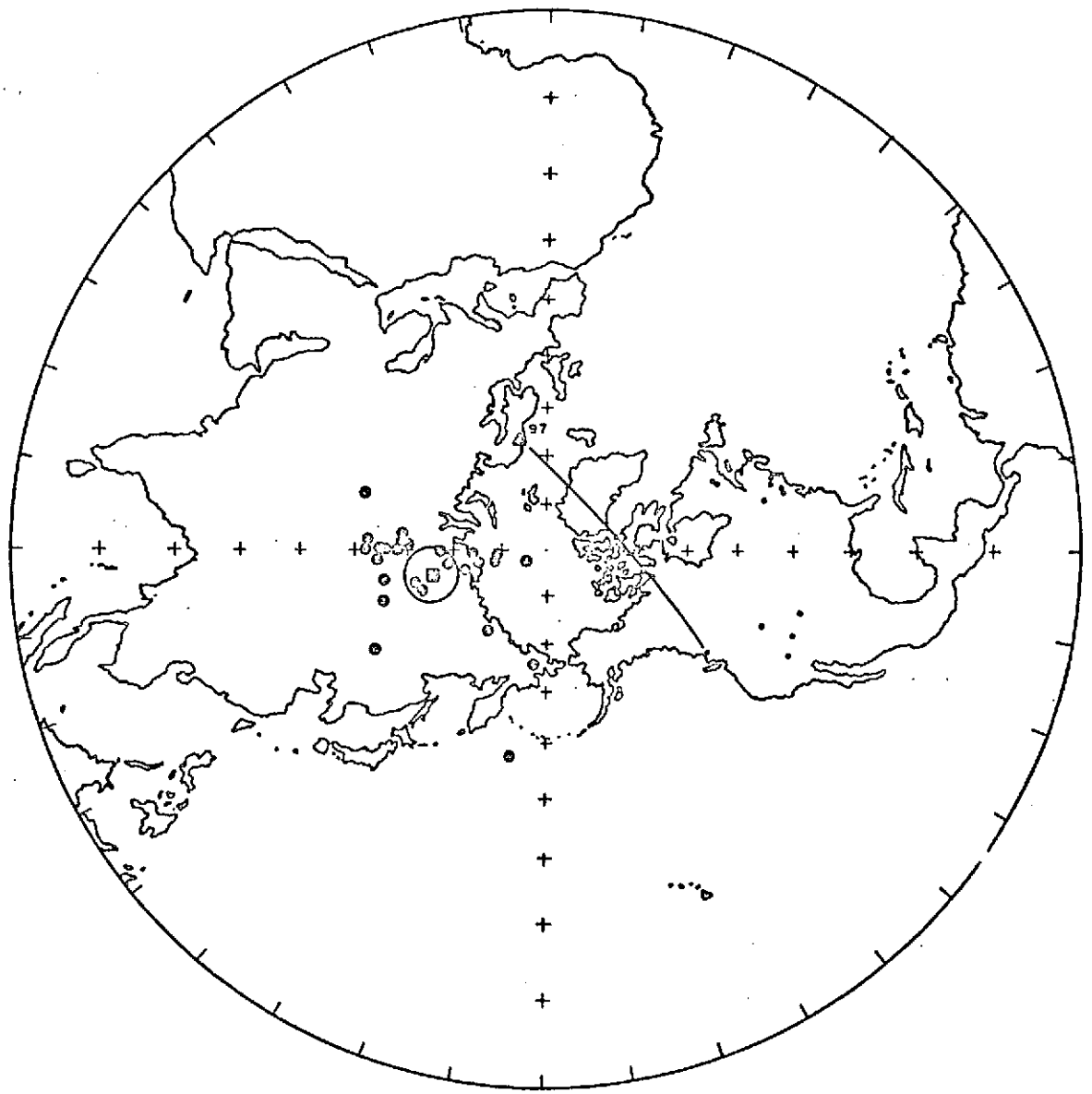

Figure 4-10. Triassic paleomagnetic poles from North America. (Explanation precedes Fig. 4-7.)

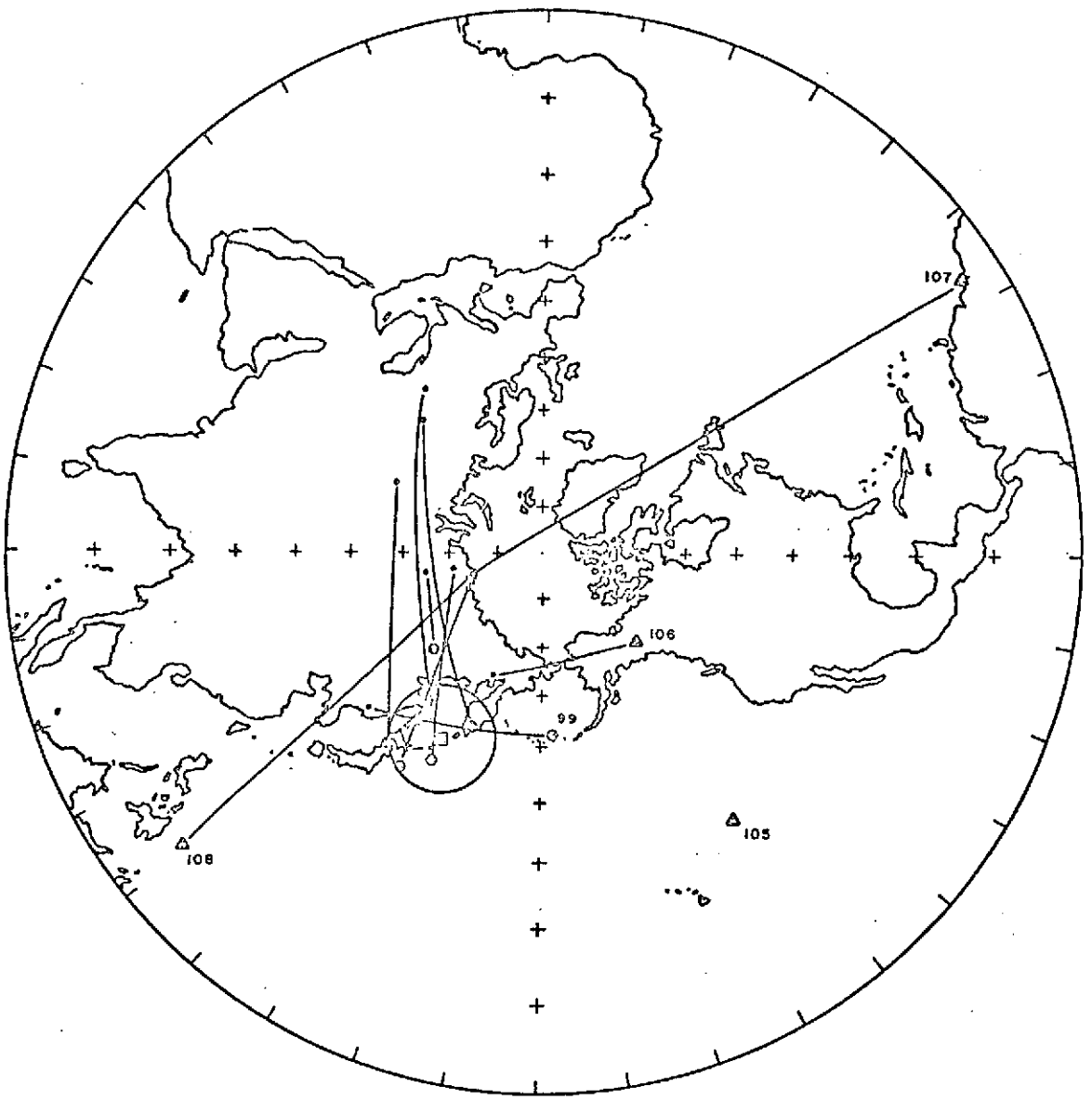

Figure 4-11. Triassic paleomagnetic poles from Asia. (Explanation precedes Fig. 4-7.)

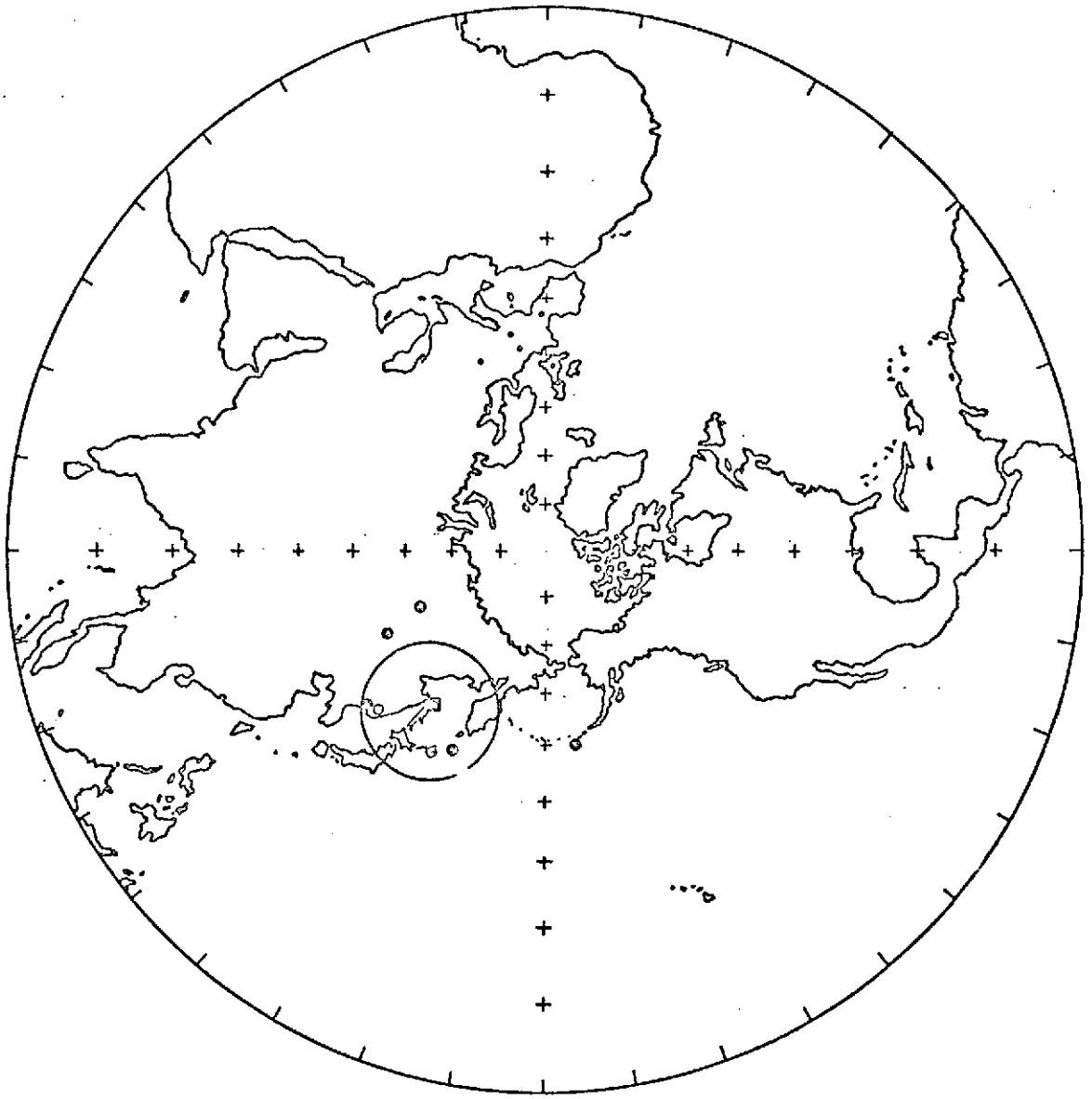

Figure 4-12. Triassic paleomagnetic poles from Europe. (Explanation precedes Fig. 4-7.)

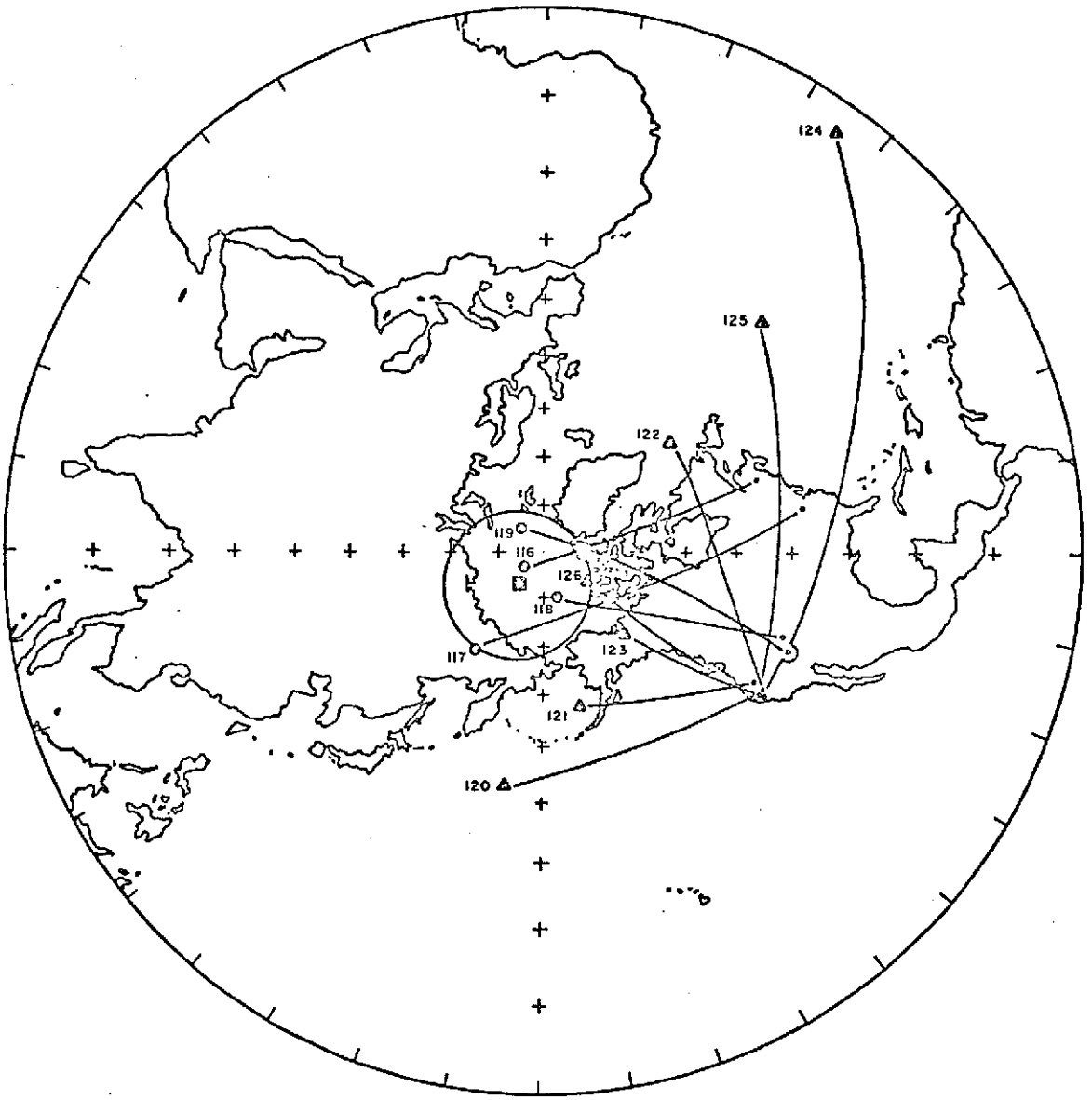

Figure 4-13. Jurassic paleomagnetic poles from North America. (Explanation precedes Fig. 4-7.)

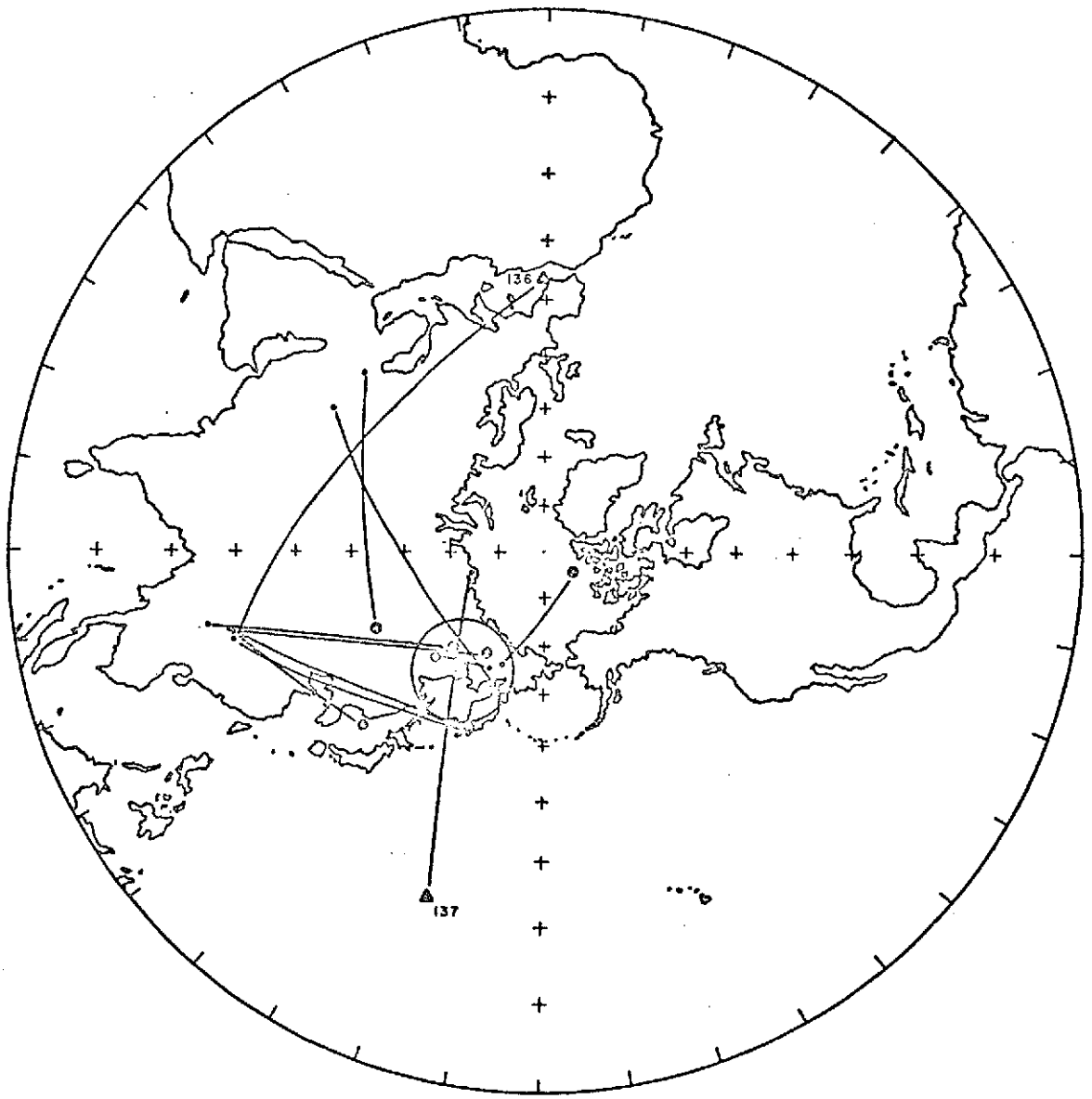

Figure 4-14. Jurassic paleomagnetic poles from Asia.
(Explanation precedes Fig. 4-7.)

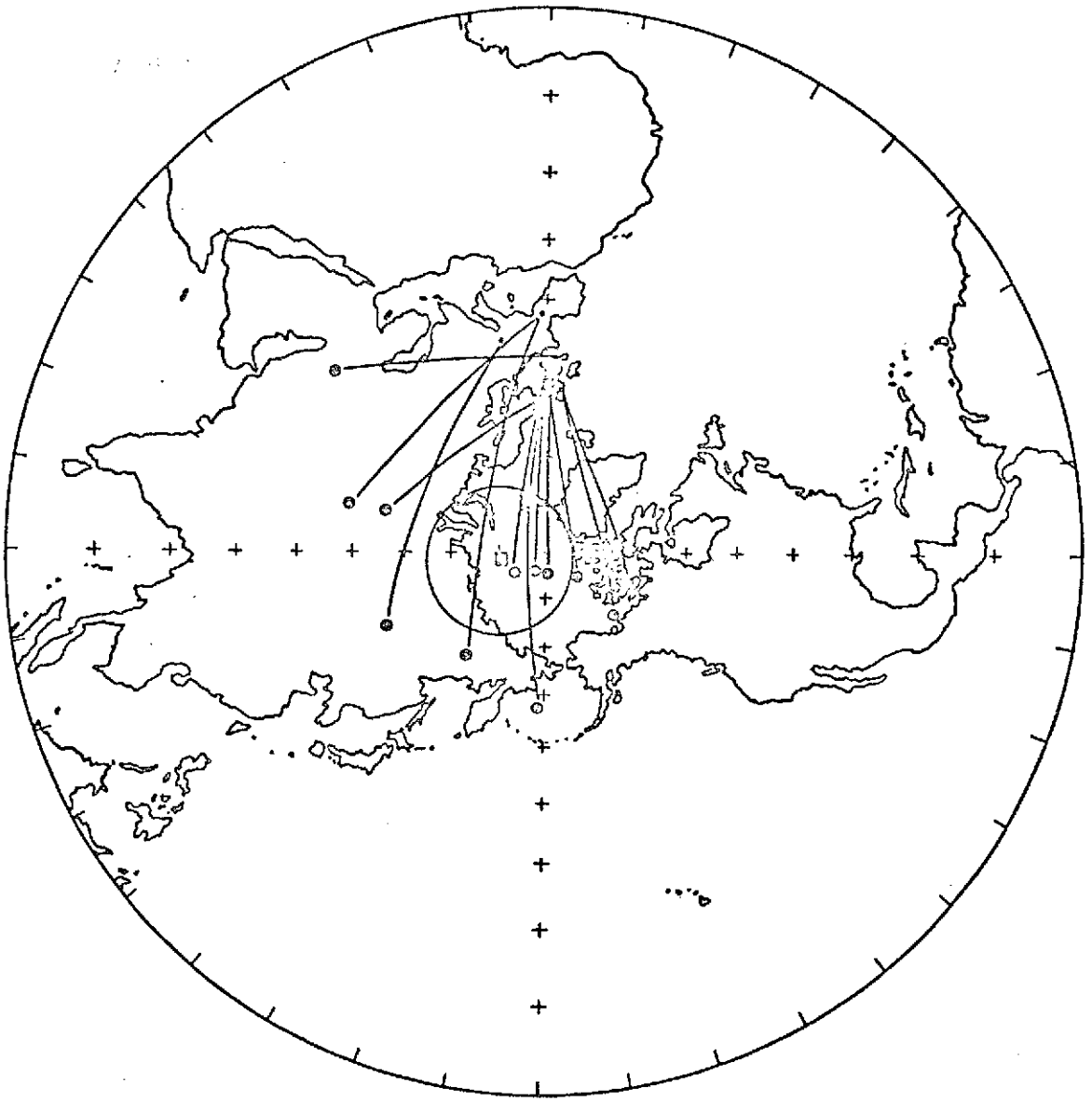

Figure 4-15. Jurassic paleomagnetic poles from Europe. (Explanation precedes Fig. 4-7.)

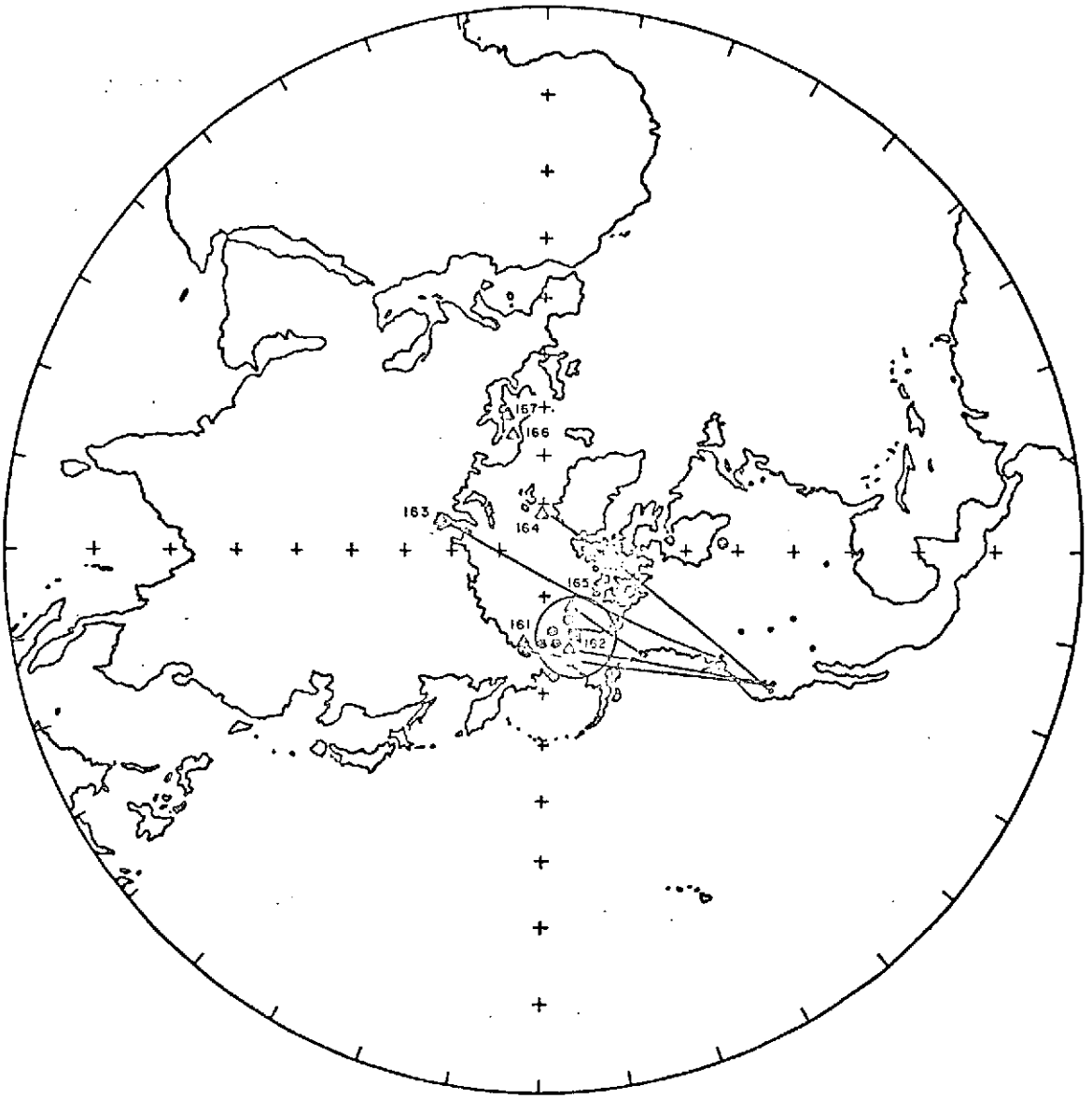

Figure 4-16. Cretaceous paleomagnetic poles from North America. (Explanation precedes Fig. 4-7.)

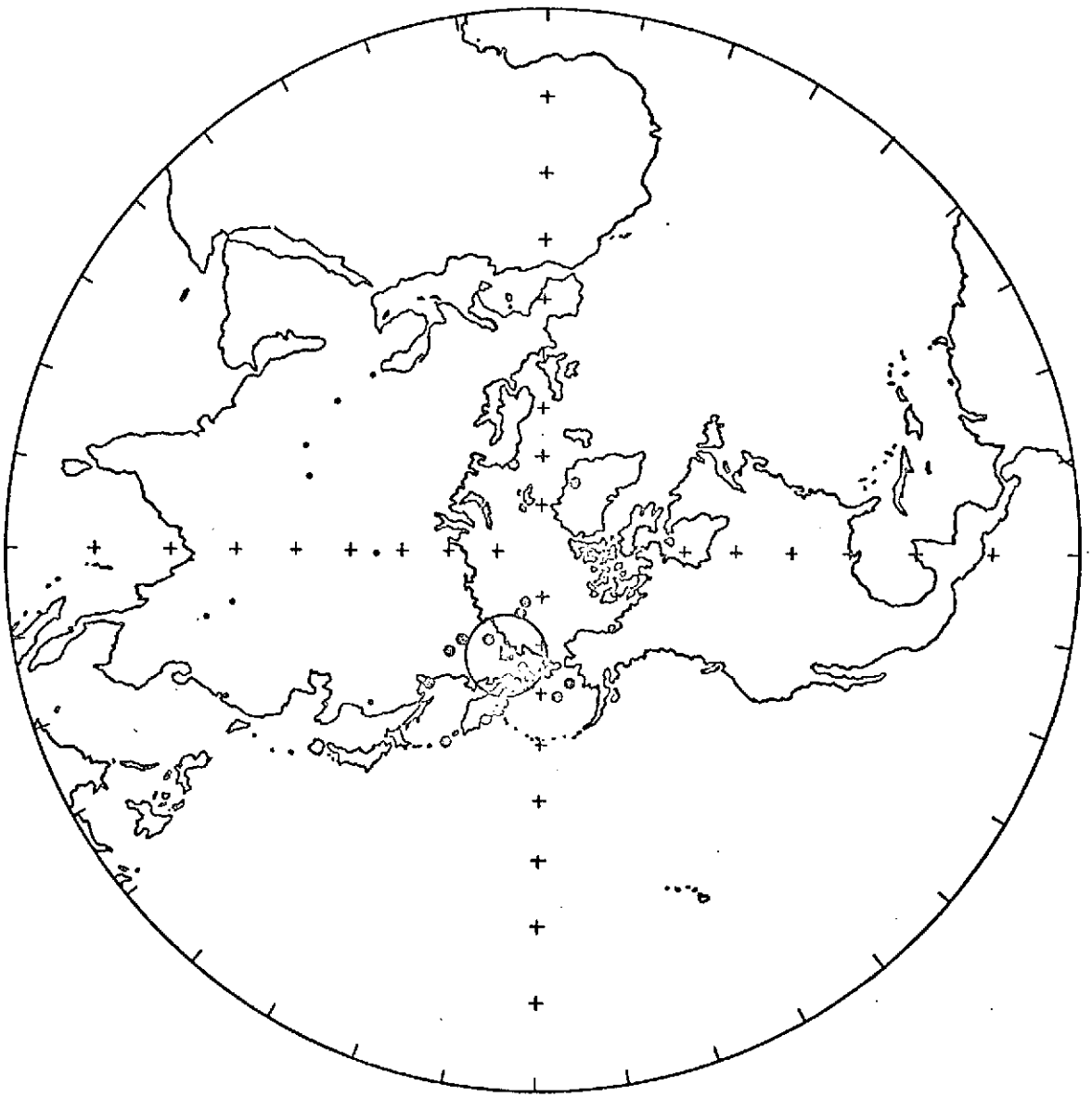

Figure 4-17. Cretaceous paleomagnetic poles from Asia. (Explanation precedes Fig. 4-7.)

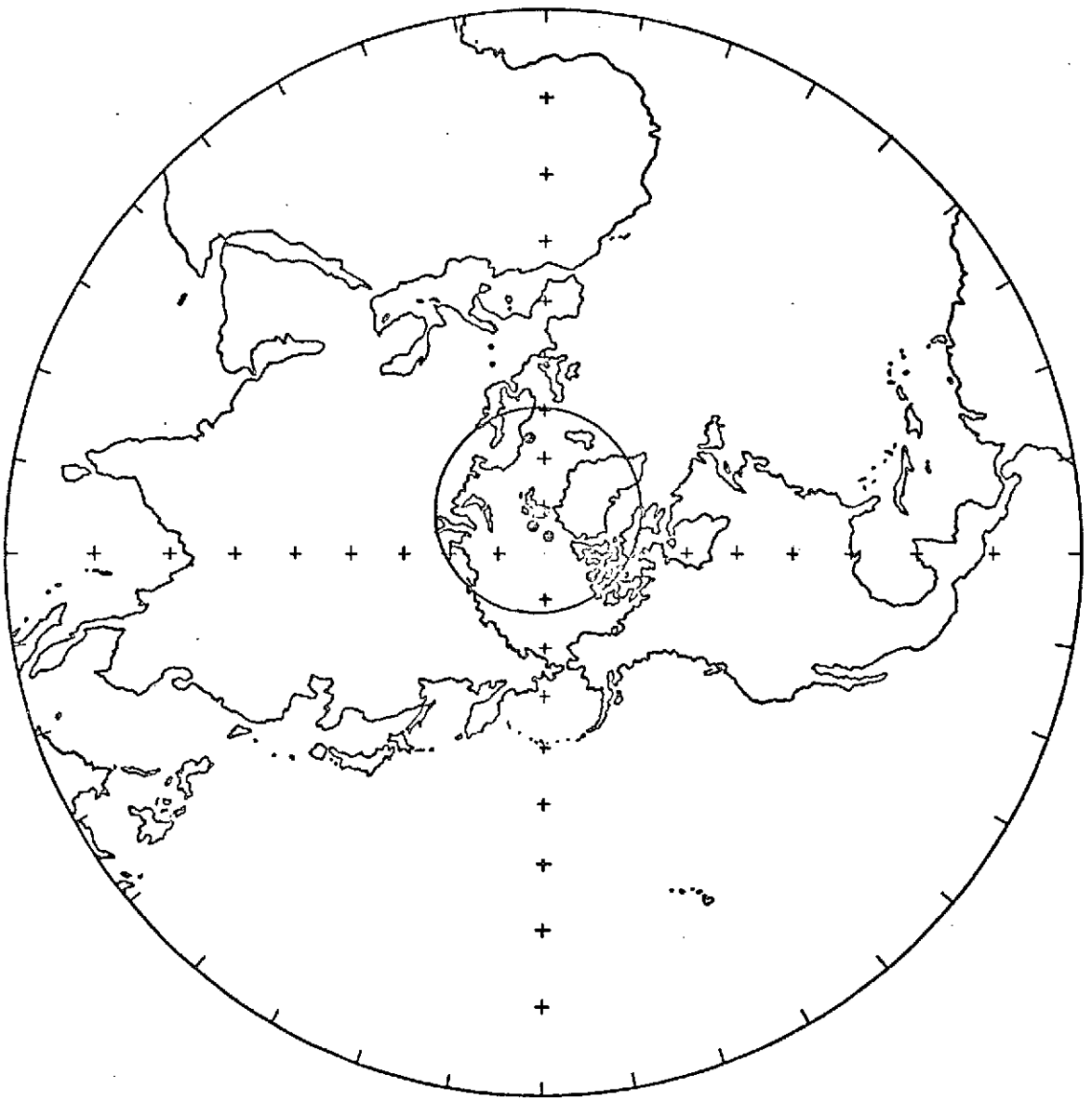

Figure 4-18. Cretaceous paleomagnetic poles from Europe. (Explanation precedes Fig. 4-7.)

TABLE 4-2

MEAN PALEOMAGNETIC POLE POSITIONS

	N	NLAT	ELONG	A95	K
PERMIAN					
MEAN OF NUMBERS 1-29, NORTH AMERICA	29	49	116	5	33
MEAN OF NUMBERS 30-49, ASIA	20	37	164	7	26
MEAN OF NUMBERS 50-72, EUROPE	19	43	165	4	68
TRIASSIC					
MEAN OF NUMBERS 71-96, NORTH AMERICA	26	66	102	5	30
MEAN OF NUMBERS 98-104, ASIA	7	48	152	10	37
MEAN OF NUMBERS 109-115, EUROPE	7	51	143	13	22
JURASSIC					
MEAN OF NUMBERS 116-119, NORTH AMERICA	4	82	145	15	41
MEAN OF NUMBERS 127-135, ASIA	9	60	146	11	25
MEAN OF NUMBERS 138-150, EUROPE	13	80	101	15	9
CRETACEOUS					
MEAN OF NUMBERS 151-160, NORTH AMERICA	10	71	203	8	34
MEAN OF NUMBERS 168-185, ASIA	18	67	162	7	24
MEAN OF NUMBERS 186-189, EUROPE	4	81	352	21	21

the Franciscan Formation. Pole 126 comes from the Island Intrusives on Vancouver Island. It is interesting to note that the poles from west of the Sierra Nevada Mountains are spread out along a great circle. There is no obvious explanation for this, and any explanation must take into account the diverse rock types, northerly geographic spread of sites, and the time span represented.

The Cretaceous paleomagnetic poles for North America (Fig. 4-16) have been divided into those from sites east of the Sierra Nevada Mountains, because the Cretaceous results are probably influenced by whatever affected the west coast Jurassic results. Pole 163 from Cretaceous plutonic rocks in Washington indicates a paleolatitude 25 degrees south of its present position (Beck and Noson, 1972). It is of interest to note here that the Triassic Guichon batholith in western British Columbia gives a similarly anomalous pole (pole 97, Fig. 4-10). Other west coast Cretaceous poles (161, 162, 164, 165) do not indicate such a large displacement. Poles 166 and 167 from the northeast Pacific have been determined for the Great Magnetic Bight (Vine, 1968) and the Hawaiian seamounts (Francheteau et al., 1970), respectively, and are displaced in the same general direction as the Alaskan data. Tertiary seamounts in the northeast Pacific have poles which lie on the trend between the Cretaceous and the present geographic pole (Francheteau et al., 1970).

Polar wandering curves have been constructed (Figs. 4-19 to 4-21) from the data listed in the Appendix. Unfortunately most pole positions are not well enough defined at the 95% confidence level to show small movements of the poles, but all accurately portray the

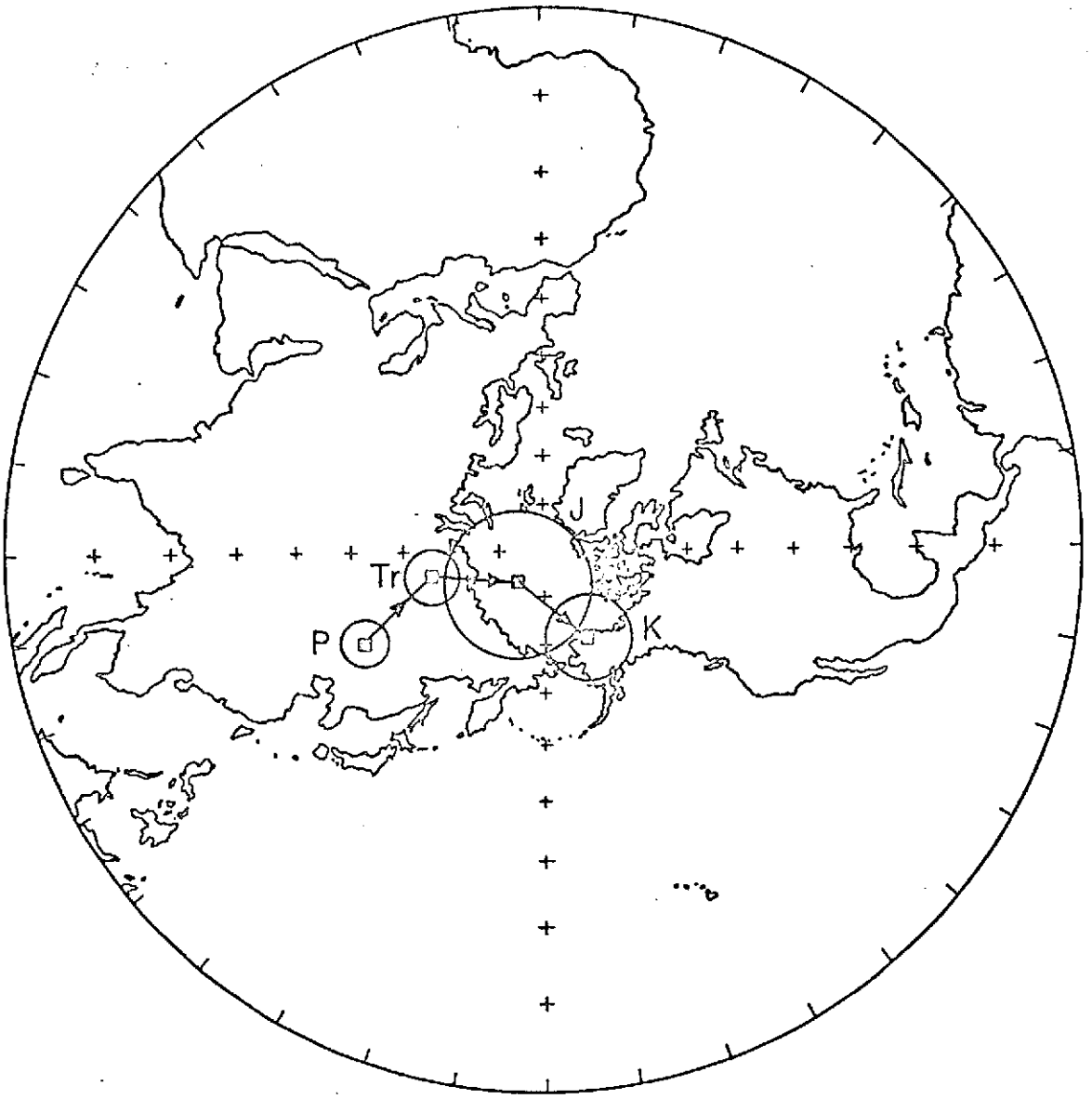

Figure 4-19. Polar wandering curve for North America. Mean paleomagnetic poles within 95% circles of confidence.

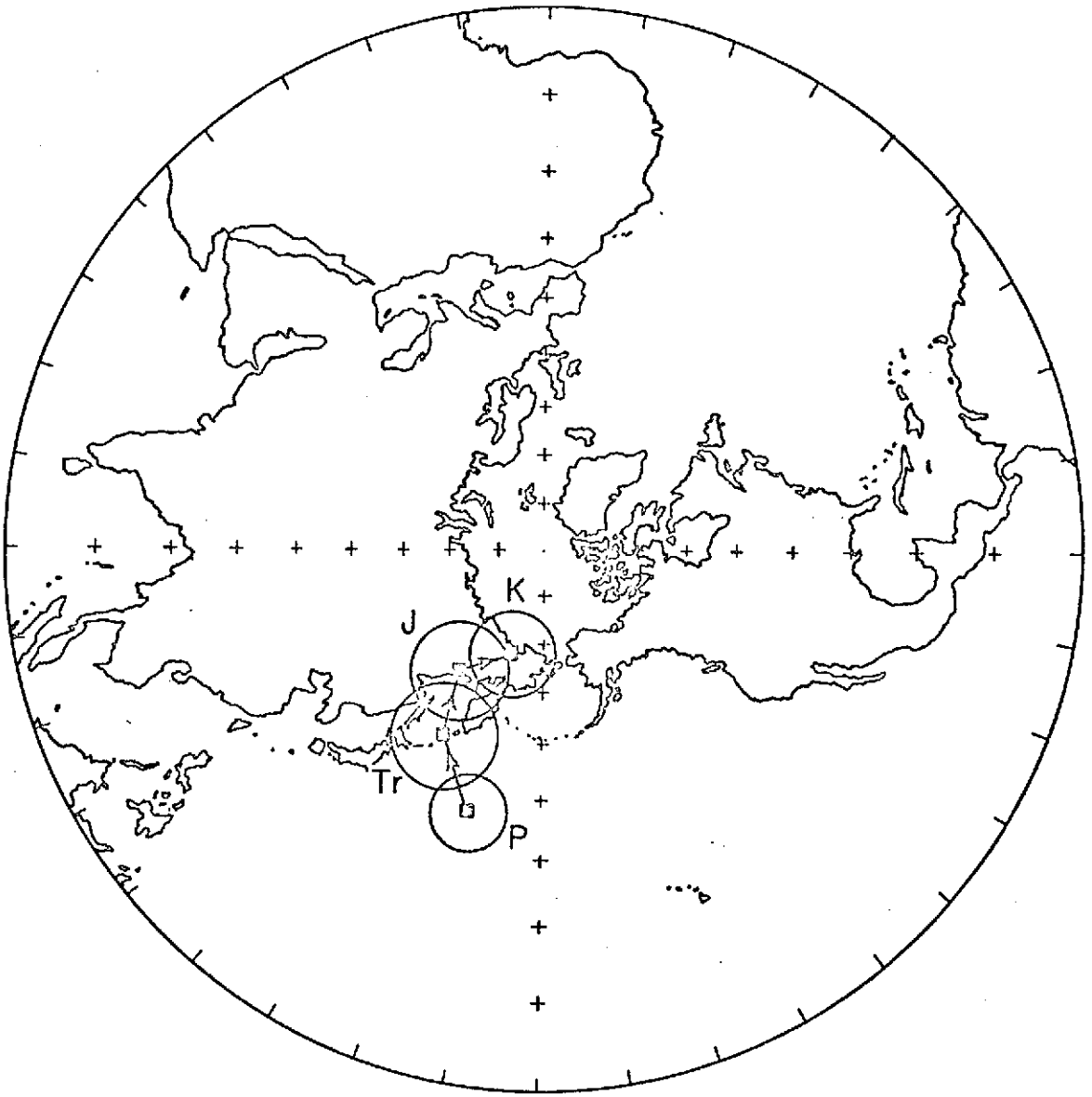

Figure 4-20. Polar wandering curve for Asia. Mean paleomagnetic poles within 95% circles of confidence.

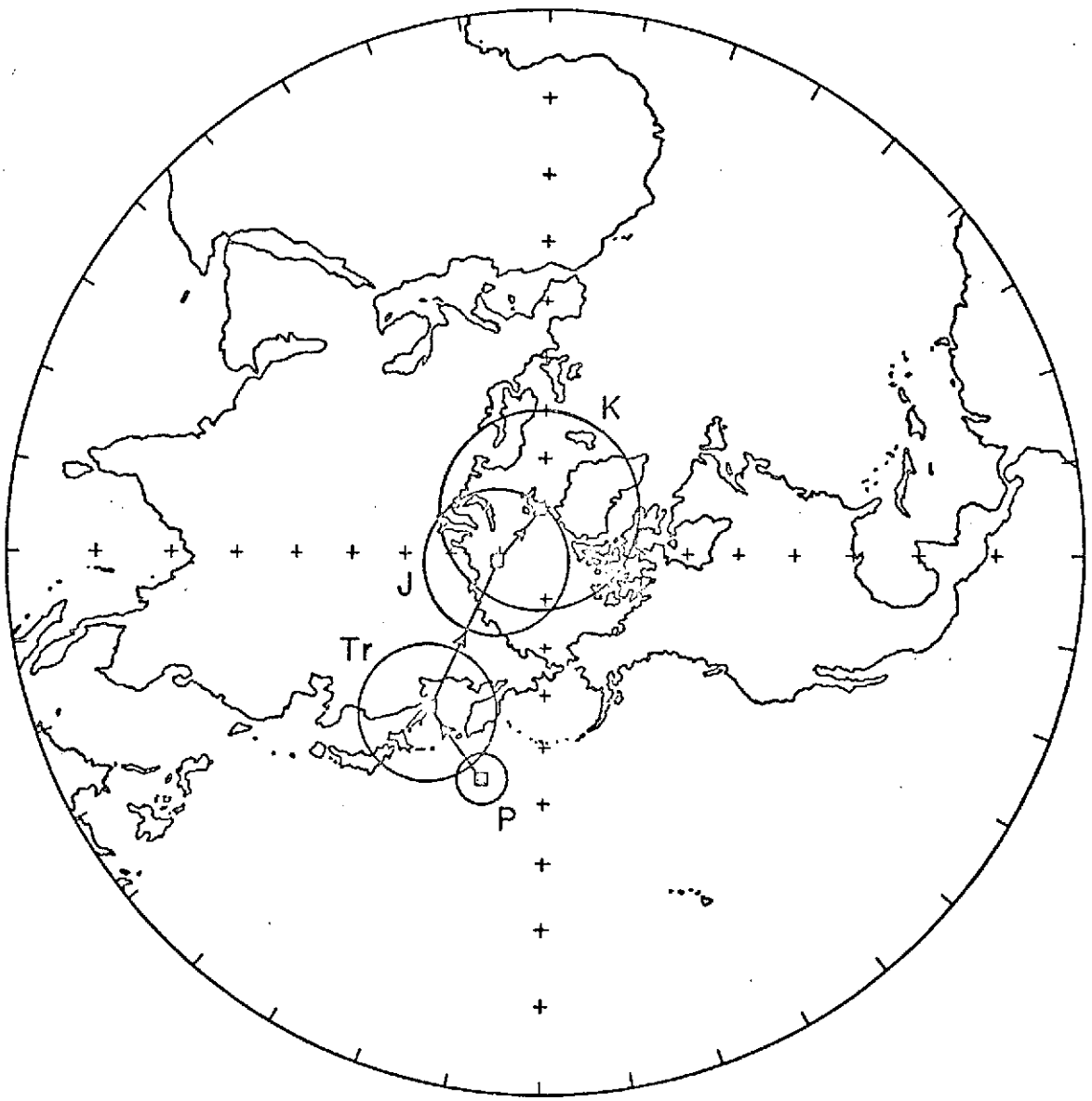

Figure 4-21. Polar wandering curve for Europe. Mean paleomagnetic poles within 95% circles of confidence.

trends of the motions involved. A schematic picture (Fig. 4-22) combining these polar wandering trends clearly indicates a contrast between the Jurassic pole from southern Alaska and the poles for Permian through Cretaceous from North America, Asia, and Europe. In fact, assuming the Alaskan Cretaceous pole lies between the Jurassic pole and the present magnetic dipole, the southern Alaskan results have the same trend as the results from the northeast Pacific.

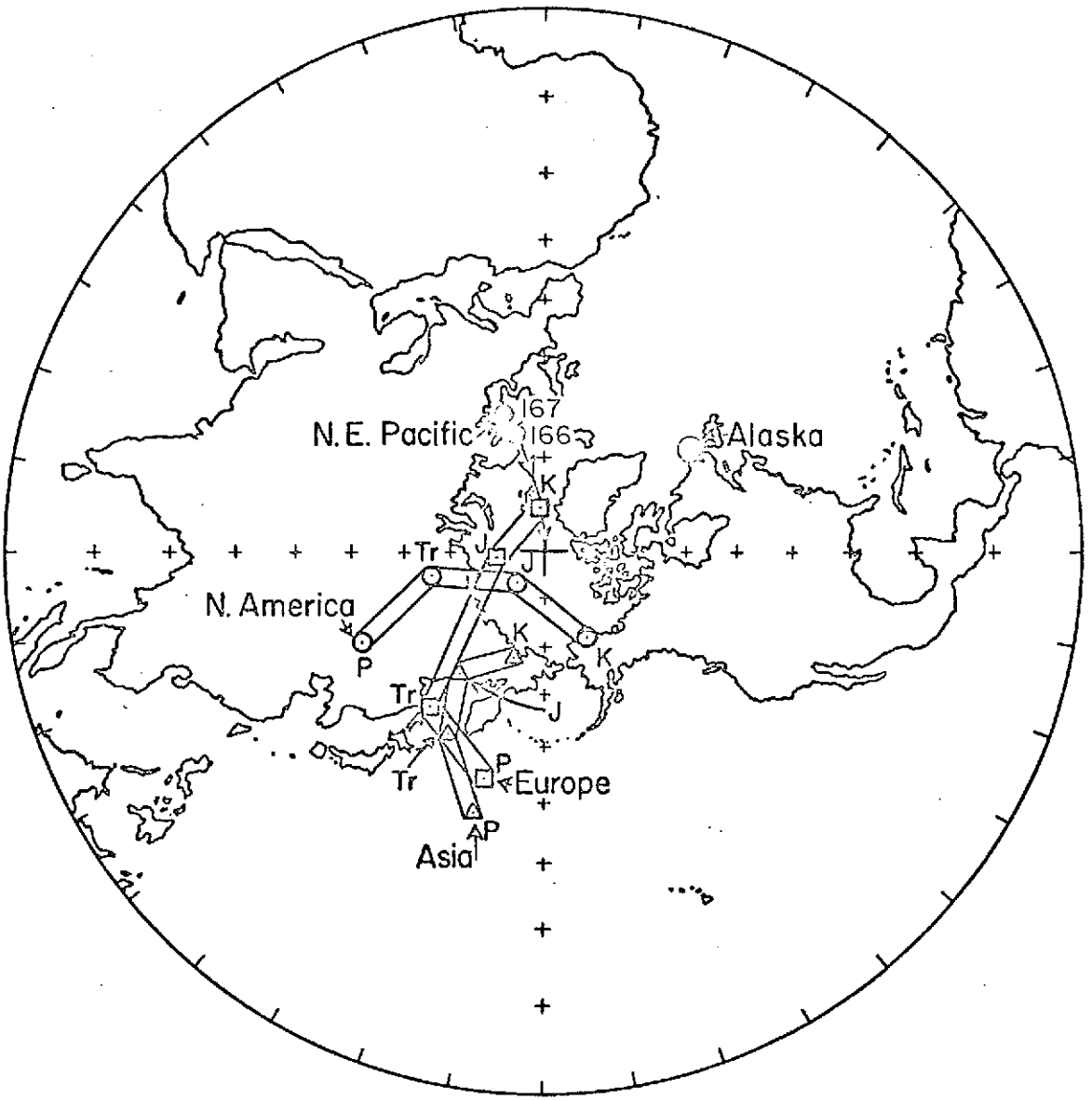

Figure 4-22. Schematic representation of polar wandering curves for North America ⊙, Asia △, and Europe ⊡. Northeast Pacific Cretaceous poles ○ from the Appendix with trend ⟶. Mean Jurassic paleomagnetic pole ◯ for Alaska.

V. TECTONIC IMPLICATIONS OF ALASKAN PALEOMAGNETIC DATA

SUMMARY AND CONCLUSIONS

For the purpose of defining the Alaskan orocline, over 400 oriented cores of Permian, Triassic, Jurassic, and Cretaceous sedimentary and igneous rocks were collected from 34 sites at 10 areas throughout southern Alaska. After magnetic 'cleaning' in successively higher alternating fields 179 samples were considered to be stable and give statistically consistent results within each site and age group. Due to lack of a sufficient number of stable samples, the results from Permian, Triassic, and Cretaceous aged rocks are inconclusive. The nine remaining Jurassic sites represent 100 samples from three general areas in southern Alaska.

The major conclusion is that the southern Alaskan Jurassic paleomagnetic pole is significantly different from the North American Jurassic pole. These poles indicate that since the Jurassic, southern Alaska must have moved approximately 18 degrees north and rotated 52 degrees clockwise to reach its present position.

The mean paleomagnetic declinations calculated with respect to the present, and with respect to Carey's and Grantz's models of the possible bending of Alaska are not significantly different from one another, and do not show any systematic change along the strike of the orocline. Also, the paleomagnetic poles for the Jurassic from Alaska are separated in the wrong direction to be explained by the Alaskan orocline. The Alaskan orocline as Carey defined it, therefore, does not appear to be a valid concept.

TECTONIC IMPLICATIONS

The above conclusions have obvious implications for any tectonic interpretation of the geologic history of Alaska and the northeast Pacific, because the Alaskan Jurassic pole position is significant and must be accounted for in some way in any explanation of the geologic history of Alaska. The Jurassic pole could be the result of many local rotations, but due to the internal consistency of the data and the overall indication of northward movement, this explanation seems implausible. As a result, it seems worthwhile to present a possible first attempt at a reconstruction, as an idea of what must be done to incorporate the results of this paleomagnetic study into the general understanding of the geology of Alaska.

The geologic history of Alaska is extremely complex, and no clear understanding of what took place is yet available. It seems that a reasonable picture can be constructed that explains many features; however, the following explanation is in no way to be considered the final explanation, but rather a speculative attempt to combine geologic and geophysical features from Alaska and the northeast Pacific.

SPECULATIVE RECONSTRUCTION

For the Jurassic, the paleomagnetic pole for southern Alaska with respect to the North American pole indicates a latitude equivalent to that of Oregon-Washington, and an orientation such that the continental margins are approximately parallel. Although longitude is indetermi-

nate from a single pole, it might be worthwhile to assume that in Jurassic time the southern part of Alaska was attached to the Jurassic west coast of North America. Because rocks from the western edge of North America, i.e. west of the Sierra Nevada Mountains, give discordant pole positions (see Chapter IV and Figs. 4-13 and 4-16), some indicating a clockwise rotation and/or a more southerly latitude in the past, direct matching of geologic features between the two areas is not likely.

In the Jurassic, the west coast of North America is thought to have been generally characterized by a subduction zone. If the reconstruction presented here is correct, then an explanation of the Permian and Triassic volcanics, tuffs, pillow lavas, limestones, cherts, and volcanic breccias found on the northwestern shore of Kodiak Island requires a small basin or gulf in which spreading and shallow marine deposition were taking place. A comparable feature today might be the Gulf of California and Baja California. Jurassic sediments were deposited around the edges of this gulf also, and make up the shallow water deposits such as the Naknek and Tuxedni Formations of the present Alaska Peninsula (see Chapter III). The subduction zone could also have generated the Jurassic Aleutian Range batholiths on the Alaska Peninsula.

Lack of a mid Cretaceous sedimentary record on the Alaska Peninsula indicates a short period of uplift, possibly representing the end of subduction at least locally, and the time that southern Alaska became attached to the Pacific plate. The lower to mid Cretaceous also appears to correspond to a new plate tectonic regime in the Pacific.

This is based on the central and northern Pacific magnetic anomaly pattern which seems to have originated during the magnetically quiet late Cretaceous. The east-west oriented anomalies of the north Pacific, and presumably the ridge generating them appear to have formed at a site now represented by the Chinook trough (Naugler and Rea, 1970; Erickson, 1969). Because this occurs in the magnetically quiet zone, it cannot be dated accurately, but all indications point to a late Cretaceous age.

The mid Cretaceous uplift and erosion also mark the beginning of rapid deposition of the mid to upper Cretaceous flysch deposits of Kodiak Island. These deposits, as described by Moore (1972), formed in a trough in which the direction of the paleocurrent was parallel to the present coastline and flowing in what is now a southwesterly direction. He implies that a gulf situation would best describe the depositional features. On the Alaska Peninsula, the upper Cretaceous Chignik and Hoodoo Formations, composed of a basal coal member, siltstones, and sandstones, were deposited in large basin-like areas (see Chapter III).

By the end of the Cretaceous, Alaska was attached to the Pacific plate, had undergone at least some rotation, and was moving north on it. The direction of motion of the Pacific plate and hence southern Alaska may well be represented by "hot spot" trails (Morgan, 1972). Morgan, on the basis of several lines of seamounts generated by "hot spots", calculated Euler poles about which the Pacific has moved. Over the past 40 million years, a rotation of 34 degrees about a pole at 67 degrees north and 73 degrees west describes the movement, and for the

period from 40-100 million years ago the motion can be represented by a 45 degree rotation about a pole at 23 degrees north, 100 degrees west. A trend that ends today at the Cobb seamount is seen in the Gulf of Alaska. By graphical methods, the 40 million year point, or the bend in the Cobb or Gulf of Alaska seamount line is placed just to the south of Kodiak Island. It should perhaps be noted that Jackson et al. (1972) have dated the bend in the Hawaiian-Emperor Chain at approximately 25 million years, compared with the 40 million year date of Morgan (1972). The different dates have little effect on the reconstruction presented here, because of its ill-defined time scale.

In terms of other evidence for motions of the Pacific plate, from the reconstruction presented it is not possible to decide between the models presented by either Atwater (1970) or Hayes and Pitman (1970). This is largely due to the fact that southern Alaska must have been essentially in its present position by the time the Kula ridge disappeared.

On the basis of Churkin's (1970a) geologic correlations of the geology between Siberia and North America (see Chapter I) and Stoneley's (1971) note on Alaska's geologic evolution, it is likely that the Brooks range was separated from southern Alaska in the Jurassic because of southern Alaska's Jurassic paleolatitude. The compression created by southern Alaska's northward motion must have been taken up on the north side of the southern Alaska block. Since all the required motion could not have been taken up on the large thrust faults present in the Brooks Range today (Tailleur and Brosge, 1970), a subduction

zone is required. It seems likely that this zone must have been located between the Brooks Range and the Alaska Range, and is possibly represented today by the Tintina and Kobuk systems in Alaska, and the Koryak Mountain system in eastern Siberia. Perhaps an ocean basin extended eastward, almost to the Canadian border, and this ocean, (the Yukon Ocean!) together with the present Bering Sea, would have been part of the Kula or North Pacific plate, as the Aleutian subduction zone had not yet formed.

By latest Cretaceous or early Eocene time the Yukon Ocean was closing rapidly, and imposing severe restraints on the motion of southern Alaska. As a result of the increased resistance a new trench system on the south margin of the southern Alaska block began to form. The line of weakness formed by this new trench propagated out from the North American continental edge to Unimak Island and on across to the Kamchatka Peninsula. The ancestral western Aleutian trench and arc were formed, thereby cutting off the Bering Sea, and effectively shortcircuiting the Koryak Trench. The oldest rocks on the eastern Aleutian Islands are lower Cretaceous to Eocene (Coats, 1956), and the oldest rocks on the western islands, the Komandorsky's, are Oligocene (Vaslov, 1967), perhaps indicating development from the east.

One line of evidence for the time of onset of the eastern Aleutian subduction might be found in the upper Paleocene-lower Eocene Shumigan batholiths, which are exposed in the Shumigan Islands and on the northwest shore of Kodiak Island. These intrusives were probably formed at a time when the trench dipped at a steep angle, therefore generating the batholiths close to the trench. As the dip of the subduction zone

became shallower, another group of batholiths was intruded to the northwest, and is exposed along the southeastern shore of the present Alaska Peninsula. These batholiths, exposed at many bays along the length of the Alaska Peninsula, are thought to be Oligocene or Miocene in age.

By middle Eocene the paleogeography must have been roughly similar to that seen today, although it is likely that the change from largely north-south to northwest-southeast motion as suggested by the 0-40 million year "hot spot" trails (Morgan, 1972) further widened the Gulf of Alaska. It is also unlikely that Kodiak was above sea level until after the large-scale deformation and uplift that took place in the Pliocene.

Much of the faulting pattern observed in Alaska today might possibly be explained as the result of the closing of the Yukon Ocean. It was postulated by Grantz (1966) that the faulting in the western half of Alaska could possibly be the result of compressional stress along an axis running west-northwest to east-southeast, and that the fault patterns represent conjugate faulting (see Chapter I). There is conjugate faulting in the Yukon Delta region, and the Iditarod-Nixon Fork and the Aniak-Thompson Creek faults may be part of this pattern. The north striking part of the Denali fault system, the Chatham Strait fault, was probably associated with the transform fault system along which Alaska moved north. The western Denali faults, the Holitna and Togiak-Tikchik faults, must be the result of interaction between the southern Alaska and central Alaska blocks upon collision.

The paleomovements of the central block (the portion of Alaska between the Denali and the Tintina-Kaltag fault systems) and the northern block (essentially the Brooks Range) have not been defined paleomagnetically due to a lack of data. One site from the Devonian of the western Brooks Range (Stone, unpublished data) indicates a more northerly latitude with respect to North America, although the exact position is uncertain.

RECOMMENDATIONS FOR FUTURE WORK

Further collection of the Jurassic on the Alaska Peninsula would reduce the scatter of the results presented in this study, although it would be unlikely to change the pole position significantly. Paleomagnetically, it is most important to sample thoroughly and systematically the several sections of Cretaceous and Cenozoic rocks exposed on the Alaska Peninsula. These samples would facilitate a better time resolution, a greater time span, and allow a polar wandering curve to be constructed.

To further investigate Carey's orocline, Mesozoic rocks from the eastern limb need to be collected. It would appear that a good study of the many dated batholiths in western Canada could yield worthwhile results, assuming the geology is well enough known to make a reasonable guess at the ancient horizontal.

It is also important to paleomagnetically collect from the Brooks Range, the northern block, and from the central block, in an attempt to distinguish the role each has played in the tectonic history of Alaska. Samples, which gave consistent results, from the Paleozoic

sections of the Brooks Range have been collected by Humble Oil and Refining Company. In this area it is moderately easy to find suitable limestones, shales, and sandstones, although access to the region is difficult.

Samples from the central or interior portion of Alaska, especially the western segment, hold the least chance of giving successful results because of the intense deformation throughout most of the area. Exposures are also extremely small and little can be determined about the overall structure. Intrusive complexes are probably the logical choice, if their age and ancient horizontal are well known.

APPENDIX

Paleomagnetic Directions and Pole Positions

Permian, Triassic, Jurassic, and Cretaceous age rocks from selected sites in North America, Asia, and Europe.

Column 1 gives the map reference number of poles used in text and figures.

Column 2 gives the location of the sampling sites by country and geographical coordinates.

Column 3 gives name of the rock unit sampled and in some cases specific locations. An asterisk followed by a number refers to a special note listed at the end of the table. Abbreviations used are: combined - CMB; rocks - RX; sedimentary rocks - SEDS.

Column 4 gives relative age of the rock unit studied according to the following symbols: Permian (P), Triassic (TR), Jurassic (J), and Cretaceous (K), followed by U, M, or L, meaning Upper, Middle, or Lower portion of that geologic age.

Column 5 gives population used in statistical computations--usually the number of samples (pieces of rock oriented individually), but in a few cases, the number of specimens cut from these oriented rocks.

Columns 6 and 7 give the mean declination, in degrees east of true north, and mean inclination, in degrees below (+) or above (-) horizontal, after correction for known local tectonic movement.

Columns 8 and 9 give the radius in degrees of the α_{95} circle of confidence about the mean paleofield direction and the Fisher (1953) parameter, k.

Columns 10 and 11 give the coordinates of the paleomagnetic pole position in degrees north latitude and east longitude.

Columns 12 and 13 give the estimates of error, in degrees, of the pole position in either DM, DP, the semi-axes of the elliptical error at the 95% confidence level, or A95, the radius of the circular error at the 95% confidence level--whichever was listed in the literature.

Column 14 gives the number of the reference from which these data were taken, listed after the notes at the end of this table.

For further explanation and remarks, see Chapter IV.

PALEOMAGNETIC DIRECTIONS AND POLE POSITIONS

NO		LOCATION	ROCK NAME	AGE	N	DIRECTION D	I	A95	K	POLE POSITION NLAT	ELONG	(DM,DP)	A95	REF
PERMIAN														
1	USA	39.5N,81W	DUNKARD SERIES	PL	57	164	8	4	177	44	122	2,4		17
2	USA	35.5N,105.2W	YESO FM	PL-M		143	-1	3	99	41	127	2,3		14
3	USA	35N,107W	ABO FM CMB	PL		153	32			30	100			14
4	USA	38N,109W	CUTLER FM CMB	P		130	20			34	107			14
5	USA	36.1N,112.2W	TOROWEAP FM GRAND CANYON	P	11	157	3	7	36	47	103	4,7		20
6	USA	36.1N,112.2W	HERMIT SHALE GRAND CANYON	P	4	161	-7	8	76	53	101	4,8		20
7	USA	36.1N,112.2W	CUTLER GROUP	P	14	151	-11	6	54	49	117	3,6		20
8	USA		CUTLER FM, UTAH	P						44	166			8
9	USA	27-37N,97-132W	SUPAI FM, OAK CREEK	PL	50	163	1	8	40	51	96			23
10	USA	27-37N,97-132W	SUPAI FM, HERMIT TRAIL	PL	5	152	13			40	105			23
11	USA	27-37N,97-132W	CUTLER FM-2 MEMBERS	PL	16	134	9	9	17	30	126			23
12	USA	27-37N,97-132W	CUTLER FM-HALGAITO MBR	PL	14	151	-11	6	54	49	117			23
13	USA	27-37N,97-132W	ABO FM	PL	33	152	2	8	77	46	116			23
14	USA	27-37N,97-132W	HENNESSEY SHALE	PM	5	157	-10			53	122			23
15	USA	27-37N,97-132W	TOROWEAP ALPHA MBR	PM	6	154	-20	7	36	55	117			23
16	USA	27-37N,97-132W	GARBER FM	PM	7	348	41			74	125			23
17	USA	27-37N,97-132W	WELLINGTON FM	PM	11	159	-6			51	118			23
18	USA	27-37N,97-132W	HERMIT SHALE	PM	6	158	32			33	93			23
19	USA	27-37N,97-132W	CUTLER-ORGAN ROCK MBR	PM	12	138	21	12	14	28	117			23
20	USA	27-37N,97-132W	DEWEY LAKE FM	PU	4	336	5			52	119			23

PALEOMAGNETIC DIRECTIONS AND POLE POSITIONS (CONTINUED)

NO		LOCATION	ROCK NAME	AGE	N	DIRECTION D	I	A95	K	POLE POSITION NLAT	ELONG	(DM,DP)	A95	REF
PERMIAN														
21	USA	27-37N,97-132W	ELK CITY FM	PU	22	157	-10	4	56	53	122			23
22	USA	27-37N,97-132W	DOXEY FM	PU	5	153	-2			47	123			23
23	USA	27-37N,97-132W	CLOUD CHIEF FM	PU	6	357	33			72	90			23
24	USA	27-37N,97-132W	YATES FM	PU	6	331	16			54	130			23
25	USA	27-37N,97-132W	SEVEN RIVERS FM	PU	13	147	-13	7	33	50	133			23
26	USA	27-37N,97-132W	MARLOW FM	PU	7	159	-11			54	119			23
27	USA	27-37N,97-132W	DOG CREEK FM	PU	4	156	-1			48	119			23
28	USA	27-37N,97-132W	BLAINE FM	PU	3	160	-5			51	115			23
29	CANADA	46N,64W	BASIC SILL	PU	24	182	-16		70	50	111			18
		MEAN OF NUMBERS 1-29, NORTH AMERICA		P	29					49	116		5	
30	USSR	43N,132E	KALUZINA & YUZAGOL SUITES	P		94	50	10		16	196	9,14		19
31	USSR	76N,111E	SANDSTONES	PU-TRL	60	149	51			19	139	7,10		17
32	USSR	72N,102E	ULTRABASICS	PM-U		295	-68	5		40	150	7,8		14
33	USSR	53N,92E	COAL-FREE SUITE	PL		264	-64			37	155			18
34	USSR	54N,87E	IL'YINSKI SUITE	PU	11	102	39	11	10	6	153	8,12		19
35	USSR	54N,87E	YERUNAKOVA SUITE	PU	7	108	42	21	8	10	159	17,25		19
36	USSR	58N,56E	SEDS, KAMA RIVER	PU	12	230	-44		23	42	167			18
37	USSR	57N,55.5E	UFIMIAN CMB	PU		224	-39			43	173			14
38	USSR	55N,55E	SEDS, BELAGA RIVER	PU	33	231	-39		16	40	165			18

PALEOMAGNETIC DIRECTIONS AND POLE POSITIONS (CONTINUED)

NO	LOCATION	ROCK NAME	AGE	N	DIRECTION D	I	A95	K	POLE POSITION NLAT	ELONG	(DM,DP)	A95	REF
PERMIAN													
39 USSR	57N,55E	KAZANIAN CMB	PU		227	-43			45	170			14
40 USSR	57N,54E	SEDS, KAMA RIVER	PU	54	233	-42		22	40	163			18
41 USSR	55N,53E	SEDS	PU	7	40	37	13	21	44	176	11,17		17
42 USSR	54N,53E	SEDS, ZAVOLZH'E	PU	44	227	-39		41	42	167			18
43 USSR	59N,50E	SEDS, VYATKA RIVER	PU	15	228	-41		9	42	165			18
44 USSR	55N,49E	SEDS, VOLGA RIVER	PU	23	215	-44		20	51	178			18
45 USSR	53-61N,46-54E	TARTARIAN CMB	PU		42	44	4	189	47	169	4,4		14
46 USSR	60N,45E	SEDS, SUKHONA RIVER	PU	81	222	-43		16	45	167			18
47 USSR	48N,38E	SAKMAR	PL	82	219	-19		33	41	165			18
48 USSR	48N,38E	DONBASS RED SEDS	PL		225	-9			33	161			14
49 USSR	49N,38E	DONBASS	PL	151	223	-20		37	37	161			18
	MEAN OF NUMBERS 30-49, ASIA		P	20					37	164		7	
50 USSR	63N,159.3E	SEDS * 1	P	12	39	52	8	30	52	279			22
51 USSR	54N,88E	VOLCANICS	PL	13	306	-42	17	6	2	137	14,20		19
52 POLAND	50N,20E	VOLCANICS	PL	41	205	-16	8	35	43	165	4,8		17
53 POLAND	51N,15.5E	LOWER SILESIA VOLCANICS	PL	60	196	-4	11	15	43	175	6,11		20
54 CZECH	49.5N,16.6E	SANDSTONES	P	15	216	-9			36	150	4,4		17
55 FRANCE	43.5N,6.8E	ESTEREL IGNEOUS RX CMB	P		201	-18		14	50	146			14

PALEOMAGNETIC DIRECTIONS AND POLE POSITIONS (CONTINUED)

NO	LOCATION		ROCK NAME	AGE	N	DIRECTION D	I	A95	K	POLE POSITION NLAT	ELONG	(DM,DP)	A95	REF
PERMIAN														
56	FRANCE	43.5N,6.8E	ESTEREL IGNEOUS & SEDS	P		207	-16	5	59	47	145	3,5		14
57	FRANCE	48N,6E	NIDECK PORPHYRY	PM		193	-7	5	22	43	168	3,5		14
58	FRANCE	53.9N,5.7E	VOLCANICS, NIDECK-DONON	P		193	-13	4	134	41	169	2,4		14
59	FRANCE	46.5N,4.5E	MONTCENIS SANDSTONE	PM		197	6	4	93	38	162	2,4		14
60	W GERMANY	50N,8E	NAHE IGNEOUS RX CMB	P		195	-10			43	167			14
61	W GERMANY	48-49N,7-8E	ROTLIEGENDE SEDS & LAVA	PL		177	1	18	27	40	190	14,14		14
62	W GERMANY	49.5N,7E	ST WENDEL SANDSTONE	PL		181	-9	4	27	45	185	2,4		14
63	BELGIUM	50.3N,6.0E	RED CONGLOMERATE	P	58	194	-14	5	129	46	166	3,5		18
64	ENGLAND	51N,4W	EXETER TRAPS	PL		189	-9	20	15	43	164	10,20		14
65	ENGLAND	51N,4W	EXETER LAVAS	PL	30	198	-25	7		50	149	4,8		18
66	ENGLAND	51N,4W	EXETER LAVAS	PL	66	188	-13	7	19	46	165	4,7		18
67	SCOTLAND	55.4N,4.5W	MAUCHLINE LAVAS	P		180	-4	8	9	36	175	4,8		14
68	SCOTLAND	55.4N,4.5W	MAUCHLINE SEDS	P		187	-6	12	5	37	167	6,12		14
69	SCOTLAND	55.4N,4.5W	AYRSHIRE KYLITES	P		190	2	12	5	34	163	6,12		14
70	NORWAY	59.7N,10.4E	IGNEOUS COMPLEX	PL		204	-36	1	21	47	157	1,2		14
	MEAN OF NUMBERS 52-70, EUROPE			P	19					43	165		4	

PALEOMAGNETIC DIRECTIONS AND POLE POSITIONS (CONTINUED)

NO		LOCATION	ROCK NAME	AGE	N.	DIRECTION D	I	A95	K	POLE POSITION NLAT	ELONG	(DM,DP)	A95	REF
TRIASSIC														
71	USA	36-45N,65-80W	INTRUSIVES & SEDS	TRU	682					68	91	6,6		18
72	USA	41.5N,72-7W	HOLYOKE VOLCANIC UNIT	TRU	150	12	25	3	146	60	83	2,3		6
73	USA	41.5N,72-7W	TALCOTT VOLCANIC UNIT	TRU	111	18	12	4	185	51	72	4,8		6
74	USA	41.5N,72-7W	HAMPDEN VOLCANIC UNIT	TRU	146	4	43	4	102	73	92	3,5		6
75	USA	41.5N,72-7W	WEST ROCK GIANT DIKE	TRU	40	9	29	4	136	63	89	3,6		6
76	USA	41.5N,72-7W	HAMPDEN VOLCANIC UNIT	TRU	54	0	49	7	34	79	106	7,9		6
77	USA	41.5N,72-7W	MT CARMELL SILL	TRU	67	10	26	4	32	61	87	3,6		6
78	USA	41.5N,72-7W	CHESHIRE DIKES	TRU	41	1	47	4	31	76	103	4,5		6
79	USA	42N,72.5W	MASSACHUSETTS LAVAS	TRU		10	16	10	41	55	88	6,11		14
80	USA	42N,73W	CONN VALLEY ROCKS	TRU		12	14	15		54	86	8,15		14
81	USA	40.5N,74.9W	NEWARK GROUP, NJ	TRU		359	25	4	49	63	108	3,4		14
82	USA	40N,76.5W	DIABASE, PENNSYLVANIA	TRU	95	0	23	3	102	62	105	2,3		17
83	USA	40N,77W	NEW OXFORD FM	TRU		334	48	7	36	66	174	6,8		14
84	USA	35-39N,105-111W	CHINLE FM CMB	TRU						55	93			14
85	USA	39.6N,106.6W	UPPER MAROON FM	TRL	48	346	16			56	100			19
86	USA	43N,108.5W	CHUGWATER FM (REVERSED)	TRL	116	142	-31	6	5	48	171	4,7		18
87	USA	43N,108.5W	CHUGWATER FM (NORMAL)	TRL	47	348	39	7	10	70	143	5,8		18
88	USA	38.6N,108.9W	MOENKOPI FM	TRL	318	346	17	5	85	57	89	3,5		20
89	USA	36.1N,112.2W	HOSKINNINI TONGUE	TRL	18	150	-16	7	23	50	121	4,7		20
90	USA	37N,113W	SPRINGDALE SANDSTONE	TRU		338	16			55	107			14

PALEOMAGNETIC DIRECTIONS AND POLE POSITIONS (CONTINUED)

NO		LOCATION	ROCK NAME	AGE	N	DIRECTION D	I	A95	K	POLE POSITION NLAT	ELONG	(DM,DP)	A95	REF
TRIASSIC														
91	CANADA	55.9N,63.4W	MISTASTIN LAKE VOLCANICS	TRU	73	180	-68	2		86	118	3,3		20
92	CANADA	44.9N,65.4W	NORTH MTN BASALT	TRU	40	4	47	5	33	73	104	5,7		19
93	CANADA	44.5N,66.5W	GRAND MANAN IS LAVAS	TRU	8	3	55	16	12	80	100	17,24		19
94	CANADA	44N,66W	DIABASE DIKE	TRU	22	7	41	5	94	69	98	4,6		17
95	CANADA	52N,68W	MANICOUAGAN STRUCTURE	TRL	82	12	42			60	88	4,6		18
96	CANADA	51.5N,68.5W	MANICOUAGAN DACITE	TRL	24	12	36	10	49	57	89	6,11		18
		MEAN OF NUMBERS 71-96, NORTH AMERICA		TR	26					66	102		5	
97	CANADA	50N,120-121W	GUICHON BATHOLITH * 2	TRU	184	20	51	10	12	66	13			27
98	USSR	75N,108E	RED SANDSTONE, TAIMYR	TR		130	68	6		40	147	8,10		14
99	USSR	43N,132E	SEDS, LIANGCHI RIVER	TRM		56	70	10		53	184	15,17		19
100	USSR	71N,101E	SIBERIAN PLATFORM RX CMB	TR		115	63		264	34	153			14
101	USSR	63-67N,88-114E	SIBERIAN TRAPS CMB	TR						60	133	11,11		14
102	USSR	56N,65E	VOLCANICS	TR		66	59	9		44	142	11,14		19
103	USSR	48-59N,38-52E	TRL SUITES CMB	TRL						51	159			14
104	USSR	49N,38E	SEDS, DONBASS	TRL	7	42	46	18	13	51	146	14,22		17
		MEAN OF NUMBERS 98-104, ASIA		TR	7					48	152		10	
105	CHINA		DOLERITE, PEKING * 3	TR		63	18	32		27	217			14
106	USSR	63-65N,159-159.3E	SEDS * 1	TR	5					63	228			22

PALEOMAGNETIC DIRECTIONS AND POLE POSITIONS (CONTINUED)

NO	LOCATION	ROCK NAME	AGE	N	DIRECTION D	I	A95	K	POLE POSITION NLAT	ELONG	(DM,DP)	A95	REF
TRIASSIC													
107	USSR 76N,111E	SANDSTONES	TRM	98	168	18			4	303	4,8		17
108	USSR 76N,111E	SANDSTONES	TRL	160	161	39			9	129	6,10		17
109	CZECH 48.9N,19.2E	WERFENIAN STRATA	TRL	21	6	19			51	190	3,3		17
110	GERMANY 46.4N,11-7E	LADINIAN VOLCANICS	TRM	8	24	14			46	155			19
111	FRANCE 48.5N,7E	VOSGE SANDSTONE CMB	TRL		25	16			44	151			14
112	FRANCE 43N,1.3E	VOLCANICS	TRU	26	29	47	7	69	62	114	8,8		19
113	ENGLAND 53N,2W	KEUPER MARLS	TRU		33	27	12	18	43	131	6,12		14
114	ENGLAND 50.7N,3.2W	KEUPER MARLS (SIDMOUTH)	TRU		30	23			44	134			14
115	SCOTLAND 55.6N,5.3W	NEW RED SANDSTONE, ARRAN	TR		214	-48	21	3	54	118			14
	MEAN OF NUMBERS 109-115, EUROPE		TR	7					51	143		13	

PALEOMAGNETIC DIRECTIONS AND POLE POSITIONS (CONTINUED)

NO		LOCATION	ROCK NAME		AGE	N	DIRECTION D	I	A95	K	POLE POSITION NLAT	ELONG	(DM,DP)	A95	REF
JURASSIC															
116	USA	44N,71W	WHITE MTN VOLCANICS		JL	130	358	59	4	110	85	126	5,6		21
117	USA	33.5-41.5N,72-83.5W	DIKES, APPALACHIANS	* 4	J	223					66	145	3,3		5
118	USA	39N,109W	CARMEL FM		J		349	63	9	10	80	200	11,14		3
119	USA	37N,111.5W	KAYENTA FM		JL	146	4	50		36	83	39			3
		MEAN OF NUMBERS 116-119, NORTH AMERICA			J	4					82	145		15	
120	USA	37.5N,120W	GUADELOUPE MTN IGNEOUS		JU-KL	56					43	171	27,27		12
121	USA	39.9N,121.3W	BUCKS BATHOLITH		JU-KL	116					58	195	8,8		12
122	USA	37.4N,121.5W	FRANCISCAN PERIDOTITE		JU-KU	41	44	59	4	302	56	310	4,6		25
123	USA	37.4N,121.5W	FRANCISCAN DUNITE		JU-KU	18	350	75	6	144	66	228	11,12		25
124	USA	37.4N,121.5W	DIVERGENT FRANCISCAN	* 5	JU-KU	17	90	11	27	9	3	324	14,27		25
125	USA	38N,122.5W	FRANCISCAN FM		JU-KL	127	74	42	8	13	29	316	7,11		10
126	CANADA	48-50N,123-127W	VANCOUVER INTRUSIVES	* 6	JM	65					79	240	10,11		28
127	CHINA	29N,105E	REDBEDS, XICHUAN PROV		J		46	64	31		51	157	40,50		2
128	CHINA	29N,105E	REDBEDS, XICHUAN PROV		J		54	69	17		41	135	22,28		2
129	CHINA	28.5N,104.6E	REDBEDS, XICHUAN PROV		J		22	64	8		66	153	10,13		16
130	CHINA	28.5N,104.6E	REDBEDS, XICHUAN PROV		J		44	64	17		51	154	22,27		16
131	CHINA	25N,102.2E	REDBEDS, YUNNAN PROV		J		21	64	33		64	139	43,53		16
132	USSR	64-65N,158-159E	SEDS	* 1	JL	2					81	238			22
133	USSR	62-67N,156-166E	SEDS	* 1	JM-U	7					60	135			22

PALEOMAGNETIC DIRECTIONS AND POLE POSITIONS (CONTINUED)

NO	LOCATION	ROCK NAME	AGE	N	DIRECTION D	I	A95	K	POLE POSITION NLAT	ELONG	(DM,DP)	A95	REF
JURASSIC													
134	USSR 39.5N,54.5E	TURKMENIAN SEDS	JM-U		32	40			59	165			14
135	USSR 40N,45E	ARMENIAN PORPHYRIES CMB	J		50	61		58	53	115			14
	MEAN OF NUMBERS 127-135, ASIA		J	9					60	146		11	
136	CHINA 29N,106E	DARK RED HEMATITE	J		261	34		54	1	37			14
137	USSR 76N,111E	SANDSTONES	JM-U		123	49			22	162	7,10		17
138	AUSTRIA 47.6N,12.6E	ALPINE SEDS CMB	JL-M		42	50			54	115			14
139	FRANCE 43.0N,1.6E	PYRENEAN TUFFS	JL		55	59	6	17	49	77	6,9		14
140	FRANCE 43N,1.3E	VOLCANICS	JL	26	16	39	7	70	65	143	6,6		19
141	ENGLAND 54.5N,0.5W	BLEA WYKE BEDS 1	JL		10	67	4	46	82	124	5,7		14
142	ENGLAND 54.5N,0.5W	BLEA WYKE BEDS 2	JL		349	66	9	18	81	232	12,14		14
143	ENGLAND 52N,1W	NORTHANTS IRON-STONE	JM		341	56			70	227			14
144	ENGLAND 54N,1W	YORKSHIRE SEDS	J		3	67	5	88	85	150	6,8		14
145	ENGLAND 51N,2.5W	BRIDPORT SANDS	JL		23	60	5	73	71	249	6,8		14
146	ENGLAND 51N,2.5W	YEOVIL SANDS	JL		359	64	6	57	85	185			14
147	ENGLAND 51N,2.5W	MIDFORD & COTSWOLD CMB	JL		91	67			36	50			14
148	SCOTLAND 57.5N,5W	SEDS	JL		234	-66	7	33	56	76	9,11		14
149	NORWAY 78.3N,16.2E	DIABASE DIKE, SPITZBERGEN	JU	8	198	-65	8	38	58	178	14,18		19
150	NORWAY 78N,14-16E	DOLERITES, SPITZBERGEN	JU-KL	37	25	-76	13	22	53	358	23,25		19
	MEAN OF NUMBERS 138-150, EUROPE		J	13					80	101		15	

PALEOMAGNETIC DIRECTIONS AND POLE POSITIONS (CONTINUED)

NO	LOCATION	ROCK NAME	AGE	N	DIRECTION D	DIRECTION I	DIRECTION A95	DIRECTION K	POLE POSITION NLAT	POLE POSITION ELONG	POLE POSITION (DM,DP)	POLE POSITION A95	REF
CRETACEOUS													
151 USA	43.5N,72.5W	MT ASCUTNEY GABBRO	KL	24	150	-54			64	187			21
152 USA	34.5N,92.8W	BATHOLITHIC COMPLEXES	KL	47	329	54	9		65	187	9,12		20
153 USA	33.3N,104.6W	NIOBRARA FM, PUEBLO COLO	KU	100					70	240			26
154 USA	41N,109W	MESAVERDE GROUP SED	KU	427	327	69	13	4	65	198	22,24		20
155 USA	34N,110W	DAKOTA SANDSTONE	K		164	-62			75	200	9,11		14
156 USA	46N,112W	MAFIC DIKE, MONTANA	KU	13					53	273	7,7		13
157 USA	46N,112W	ELKHORN MTN VOLCANICS	KU						73	190	8,8		13
158 CANADA	45.5N,71W	MT MEGANTIC INTRUSIVES	KL		157	-52	7	44	69	172	7,10		14
159 CANADA	45.3N,72.8W	MONTEREGIAN HILLS	KL	147	156	-59	2		71	190	2,3		15
160 CANADA	78.7N,103.7W	ISACHEN DIABASE	K		284	80	8	20	69	180	14,14		14
MEAN OF NUMBERS 151-160, NORTH AMERICA			K	10					71	203		8	
161 USA	37.8N,119.6W	GRANITE PLUTONS	KU		335	61	4	202	70	171	8,10		4
162 USA	38N,120W	SIERRA NEVADA PLUTONS	KU	80					69	195	10,10		11
163 USA	48.6N,121W	STEVENS PASS GRANITE * 7	KU	4	357	49	11	73	71	68		13	1
164 USA		SAN MARCOS GABBRO * 8	KM						81	357		4	9
165 USA	56N,133W	ULTRAMAFICS, SE ALASKA	KM						77	206		15	9
166 NE PACIFIC		GREAT MAGNETIC BIGHT * 9	KU						65	13	7,11		29
167 NE PACIFIC		HAWAIIAN SEAMOUNTS * 10	KU	9					61	16	8,8		7

PALEOMAGNETIC DIRECTIONS AND POLE POSITIONS (CONTINUED)

NO		LOCATION	ROCK NAME	AGE	N	DIRECTION D	I	A95	K	POLE POSITION NLAT	ELONG	(DM,DP)	A95	REF
CRETACEOUS														
168	CHINA	23.3N,114.3E	REDBEDS, CANTON PROV	KU		43	67	18		47	155	25,30		16
169	CHINA	23.3N,114.3E	REDBEDS, CANTON PROV	KU		14	65	16		66	140	23,27		16
170	CHINA	23.3N,114.3E	REDBEDS, CANTON PROV	KM		30	56	4		61	170	4,6		16
171	CHINA	23.3N,114.3E	REDBEDS, CANTON PROV	K		33	55			54	162			16
172	CHINA	23.3N,114.3E	REDBEDS, CANTON PROV	K		21	60	6		54	141	7,9		16
173	CHINA	29.5N,111.3E	DONGHU SANDSTONE, HUBEI	K		20	64	8		68	151	11,13		16
174	CHINA	25N,102.2E	REDBEDS, YUNNAN PROV	K		33	45	18		60	186	14,23		16
175	USSR	61-65N,164-179E	SEDS * 1	KU	4					64	172			22
176	USSR	61-66N,156-179E	SEDS * 1	K	7					56	165			22
177	USSR	43N,132E	SUCHAN SUITE	KL		25	81	11		61	138	21,21		19
178	USSR	70-73N,98-114E	SEDS	KL						63	174			24
179	USSR	56N,92E	ILIKSKAYA & SIMONVAYA FM	KU	93	330	72			74	18	16,18		17
180	USSR	41N,73E	SEDS, SENONIAN & TURONIAN	KU	13	18	32	20	5	62	192	12,22		19
181	USSR	41N,73E	SEDS, CENOMANIAN	KU	52	342	56	3	35	75	332	3,4		19
182	USSR	38N,67E	SEDS, SW AISSAR CHAIN	KL		17	55	5	110	76	162	5,5		17
183	USSR	39.5N,55E	SEDS	KU		32	42			60	165			14
184	USSR	39.5N,54.5E	SEDS	KL						62	169			14
185	USSR	41N,45E	VOLCANICS, GEORGIA	K		13	54	22		78	165	22,31		14
		MEAN OF NUMBERS 168-185, ASIA		K	18					67	162		7	

PALEOMAGNETIC DIRECTIONS AND POLE POSITIONS (CONTINUED)

NO	LOCATION	ROCK NAME	AGE	N	DIRECTION D	I	A95	K	POLE POSITION NLAT	ELONG	(DM,DP)	A95	REF
CRETACEOUS													
186	CZECH 46.9N,14.9E	SPECULARITE, WALDENSTEIN	KU	22	158	-85	15	5	56	8	29,30		17
187	CZECH 50.2N,14.6E	SANDSTONES	KU	12	358	69			87	347	4,8		17
188	ENGLAND 50.5N,1.5E	WEALDEN SEDS	KL		345	63	2	260	79	245	2,3		14
189	ENGLAND 51N,0.5E	IRON GRIT, SUSSEX	KL	120	2	72			84	11			17
	MEAN OF NUMBERS 186-189, EUROPE		K	4					81	352		21	

Footnotes to Appendix

*1. For the most part the VGP's given are means of means. It was not always possible to determine from the article (Reference 22) just which listings were repeated in other listings, which were new listings, as well as other important information. Therefore these VGP's should be used with caution.

*2. This pole indicates a clockwise rotation of 40 degrees ± 10 degrees for the southern part of the interior plateau, British Columbia (Reference 27).

*3. Samples are from the western hills near Peking, China; the exact location is not given (Reference 14).

*4. These dikes are stratigraphically dated as upper Triassic to lower Cretaceous. The Jurassic age is based in part on the paleomagnetic pole position (Reference 5).

*5. This pole includes 'divergent' sites from both dunite and peridotite of the Franciscan Formation (Reference 25).

*6. Author states that the anomalous pole position may be explained by approximately 15 degrees of clockwise rotation and by north-eastward tilt of less than or equal to 5 degrees (Reference 28).

*7. Pole is from samples of the Stevens Pass granites from central Washington and probably indicates a 25 degree northward movement relative to cratonic North America (Reference 1).

*8. Samples are from the San Marcos gabbro in western California, but precise location and number of samples or sites not given (Reference 9).

*9. Magnetic field directions and VGP's determined for seamounts by combining magnetic anomalies and seamount topography (Reference 29).

*10. Magnetic field directions and VGP's determined from ratio of amplitudes of anomalies on north-south to east-west limbs of the Great Magnetic Bight (Reference 7).

REFERENCES

1. Beck, M. E. and Linda Noson, Anomalous paleolatitudes in Cretaceous granitic rocks, Nature, 235, 11-13, 1972.

2. Chen Zhiqiang, Wang Cenghang and Deng Xinghui, Some rusults of paleomagnetic research in China, in The Present and Past of the Geomagnetic Field, Nauka Press, Moscow, pp. 309-311, 1965 (translated by E. R. Hope, Directorate of Scientific Information Services, DRB Canada, T 462 R, 1966).

3. Collinson, D. W. and S. K. Runcorn, Polar wandering and continental drift: evidence of paleomagnetic observations in the United States, Bull. Geol. Soc. Amer., 71, 915-958, 1960.

4. Currie, R. G., C. S. Gromme, and J. Verhoogen, Remanent magnetization of some Upper Cretaceous granitic plutons in the Sierra Nevada, California, J. Geophys. Res., 68, 2263-2279, 1963.

5. deBoer, J., Paleomagnetic-tectonic study of Mesozoic dike swarms in the Appalachians, J. Geophys. Res., 72, 2237-2250, 1967.

6. _____, Paleomagnetic differentiation and correlation of the Late Triassic volcanic rocks in the central Appalachians (with special reference to the Connecticut Valley), Bull. Geol. Soc. Amer., 79, 609-626, 1968.

7. Francheteau, Jean, C. G. A. Harrison, J. G. Slater, and M. L. Richards, Magnetization of Pacific seamounts: a preliminary polar curve for the northeastern Pacific, J. Geophys. Res., 75, 2035-2061, 1970.

8. Gose, W. A. and C. E. Helsley, Paleomagnetic and rockmagnetic studies of the Permian Cutler and Pennsylvanian Rico formations, Utah (abstract), EOS Trans. Amer. Geophys. Union, 52, 189, 1971.

9. Gromme, C. S. and G. B. Dalrymple, Paleomagnetism and K-Ar ages of Cretaceous plutonic rocks (abstract), Fourth U.S.-Japan Seminar on Paleomagnetism, R. R. Doell, organizer, Honolulu, Hawaii, 1970.

10. Gromme, C. S. and H. J. Gluskoter, Remanent magnetization of spilite and diabase in the Franciscan formation, western Marin County, California, J. Geol., 73, 74-94, 1965.

11. Gromme, C. S. and R. T. Merrill, Paleomagnetism of late Cretaceous granitic plutons in the Sierra Nevada, California: further results, J. Geophys. Res., 70, 3407-3420, 1965.

12. Gromme, C. S., R. T. Merrill and J. Verhoogen, Paleomagnetism of Jurassic and Cretaceous plutonic rocks in the Sierra Nevada, California, and its significance for polar wandering and continental drift, J. Geophys. Res., 72, 5661-5684, 1967.

13. Hanna, W. F., Paleomagnetism of Upper Cretaceous volcanic rocks of southwestern Montana, J. Geophys. Res., 72, 595-610, 1967.

14. Irving, E., Paleomagnetism and its Application to Geological and Geophysical Problems, Wiley and Sons, New York, 399 pp., 1964.

15. Larochelle, A., Paleomagnetism of the Monteregian Hills: further new results, J. Geophys. Res., 74, 2570-2575, 1969.

16. Lee, C., H. Lee, H. Liu, C. Liu and S. Yeh, Preliminary study of paleomagnetism of some Mesozoic and Cenozoic redbeds of South China, Acta Geologica Sinica, 43, 173-180, 1963 (translated by E. R. Hope, Directorate of Scientific Information Services, DRB Canada T 8 C, 1966).

17. McElhinny, M. W., Palaeomagnetic directions and pole positions--VIII. Pole numbers 8/1 to 8/186, Geophys. J. R. astr. Soc., 15, 409-430, 1968.

18. _____, Palaeomagnetic directions and pole positions--IX. Pole numbers 9/1 to 9/159, Geophys. J. R. astr. Soc., 16, 207-224, 1968.

19. _____, Palaeomagnetic directions and pole positions--X. Pole numbers 10/1 to 10/200, Geophys. J. R. astr. Soc., 18, 305-327, 1969.

20. _____, Palaeomagnetic directions and pole positions--XI. Pole numbers 11/1 to 11/90, Geophys. J. R. astr. Soc., 20, 417-429, 1970.

21. Opdyke, N. D. and H. Wensink, Paleomagntism of rocks from the White Mountain plutonic-volcanic series in New Hampshire and Vermont, J. Geophys. Res., 71, 3045-3051, 1966.

22. Pecherskiy, D. M., Paleomagnitnyye issledovaniya mezozoyskikh otlozheniy Severo-Vostoka SSSR (Paleomagnetic investigations of the Mesozoic formations of Northeast U.S.S.R.), Akad. Nauk SSSR Izv. Fizika Zemli, no. 6, 69-83, 1970.

23. Peterson, N. D. and A. E. M. Nairn, Palaeomagnetism of Permian redbeds from the south-western United States, Geophys. J. R. astr. Soc., 23, 191-205, 1971.

24. Pospelova, G. A., G. Ya. Larionova and A. V. Anuchin, Paleomagnetic investigations of Jurassic and Lower Cretaceous sedimentary rocks of Siberia, Internat. Geol. Rev., 10, 1108-1118, 1968.

25. Saad, A. H., Paleomagnetism of Franciscan ultramafic rocks from Red Mountain, California, J. Geophys. Res., 74, 6567-6578, 1969.

26. Shive, P. N., Paleomagnetism of the Niobrara formation (abstract), EOS Trans. Amer. Geophys. Union, 52, 822, 1971.

27. Symons, D. T. A., Paleomagnetism of the Triassic Guichon Batholith and rotation in the Interior Plateau, British Columbia, Canadian J. Earth Sciences, 8, 1388-1396, 1971.

28. _____, Paleomagnetism of the Jurassic Island Intrusives of Vancouver Island, British Columbia, Geol. Survey of Canada Paper 70-63, 1-17, 1971.

29. Vine, F. J., Paleomagnetic evidence for the northward movement of the North Pacific basin during the past 100 m.y. (abstract), Trans. Amer. Geophys. Union, 49, 156, 1968.

REFERENCES

REFERENCES

Atwater, Tanya, Implications of plate tectonics for the Cenozoic tectonic evolution of western North America, Bull. Geol. Soc. Amer., 81, 3513-3536, 1970.

Barnes, F. F., Geologic map of lower Matanuska Valley, Alaska, U.S. Geol. Survey Misc. Investigations Map I-359, 1962.

Beck, M. E. and Linda Noson, Anomalous paleolatitudes in Cretaceous granitic rocks, Nature, 235, 11-13, 1972.

Bingham, Douglas K., Paleosecular variation of the geomagnetic field in Alaska, Ph.D. dissertation, Univ. of Alaska, 143 pp., May, 1971.

Brew, D. A., R. A. Loney and L. J. P. Muffler, Tectonic history of southeastern Alaska, in A Symposium on Tectonic History and Mineral Deposits of the Western Cordillera in British Columbia and Neighboring Parts of the United States, Can. Inst. Min. Metall., Spec. Vol. 8, pp. 149-170, 1966.

Briden, James C., Paleoclimatic evidence of a geocentric axial dipole field, in Phinney, Robert A., editor, The History of the Earth's Crust, Princeton, pp. 178-194, 1968.

Bullard, Edward, J. E. Everett and A. G. Smith, The fit of the continents around the Atlantic, in A Symposium on Continental Drift, Royal Soc. London Philos Trans., Ser. A., no. 1088, 41-51, 1965.

Burk, C. A., Geology of the Alaska Peninsula - Island Arc and Continental Margin, Geol. Soc. Amer. Mem. 99, 250 pp., 1965.

Cameron, Christopher P., Paleomagnetism of Shemya and Adak Islands, Aleutian Islands, Alaska, Ph.D. dissertation, Univ. of Alaska, 164 pp., May, 1970.

Cameron, Christopher P. and David B. Stone, Outline geology of the Aleutian Islands with paleomagnetic data from Shemya and Adak Islands, Sci. Rept., Univ. of Alaska, Geophys. Inst. and Geology Dept. UAG R-213, 153 pp., 1970.

Capps, S. R., Geology of the upper Matanuska Valley, Alaska, with a section on the igneous rocks by J. B. Mertie, Jr., U.S. Geol. Survey Bull. 791, 92 pp., 1927.

_____, Geology of the Alaska Railroad region, U.S. Geol. Survey Bull. 907, 201 pp., 1940.

Carey, S. W., The tectonic approach to continental drift, in Carey, S. W., editor, Continental Drift--A Symposium, Hobart, Tasmania Univ. Geology Dept., pp. 177-355, 1958.

Chantry-Price, R. E., A palaeomagnetic investigation of some post-carboniferous rocks from Alaska, M.S. dissertation, Univ. of Newcastle upon Tyne, 130 pp., 1967.

Churkin, Michael, Jr., Paleozoic tectonic history of the Arctic Basin north of Alaska, Science, 165, 549-555, 1969.

_____, Paleozoic and Precambrian rocks of Alaska and their role in its structural evolution, U.S. Geol. Survey Open File Rept. 448, 131 pp., 1970a.

_____, Fold belts of Alaska and Siberia and drift between North America and Asia, in Adkison, W. L. and M. M. Brosge, editors, Proceedings of the Geological Seminar on the North Slope of Alaska, Los Angeles, Pacific Sec., Amer. Assn. Petroleum Geologists, pp. G1-G14, 1970b.

Coats, R. R., Reconnaissance geology of some western Aleutian Islands, Alaska, U.S. Geol. Survey Bull. 1028-E, 83-100, 1956.

Collinson, D. W., K. M. Creer and S. K. Runcorn, editors, Methods in Palaeomagnetism, Elsevier, New York, 609 pp., 1967.

Cox, A. and R. Doell, Review of paleomagnetism, Bull. Geol. Soc. Amer., 71, 645-768, 1960.

Creer, K. M., Application of rock magnetism to investigations of the secular variation during geologic times, in Magnetism and the Cosmos, NATO Advanced Study Inst. on Planetary and Stellar Magnetism, Univ. of Newcastle upon Tyne, 1965, Elsevier, New York, pp. 45-59, 1967.

Detterman, R. L. and J. K. Hartsock, Geology of the Iniskin-Tuxedni Region, Alaska, U.S. Geol. Survey Prof. Paper 512, 78 pp., 1966.

Doell, Richard R. and Allan Cox, The accuracy of the paleomagnetic method as evaluated from historic Hawaiian lava flows, J. Geophys. Res., 68, 1997-2009, 1963.

_____, Palaeomagnetic sampling with a portable coring drill, in Collinson, D. W., K. M. Creer and S. K. Runcorn, editors, Methods in Palaeomagnetism, Elsevier, Amsterdam, pp. 21-25, 1967.

Erickson, B. H., D. K. Rea and F. P. Naugler, Chinook trough: A probable consequence of north-south sea-floor spreading (abstract), Amer. Geophys. Union Trans., 50, 663, 1969.

Fisher, Sir Ronald, F. R. S., Dispersion on a sphere, Proc. Roy. Soc. A, 217, 295-305, 1953.

Foster, John H., A paleomagnetic spinner magnetometer using a fluxgate gradiometer, Earth Planet. Sci. Lett., 1, 463-466, 1966.

Francheteau, Jean, C. G. A. Harrison, J. G. Slater and M. L. Richards, Magnetization of Pacific seamounts: a preliminary polar curve for the northeastern Pacific, J. Geophys. Res., 75, 2035-2061, 1970.

Grantz, Arthur, Generalized geologic map of the Nelchina area, Alaska, showing igneous rocks and larger faults, U.S. Geol. Survey Misc. Investigations Map I-312, 1960a.

_____, Geologic map of Talkeetna Mountains (A-2) quadrangle, Alaska, and the contiguous area to the north and northwest, U.S. Geol. Survey Misc. Investigations Map I-313, 1960b.

_____, Geologic map of Talkeetna Mountains (A-1) quadrangle, and the south third of Talkeetna Mountains (B-1) quadrangle, Alaska, U.S. Geol. Survey Misc. Investigations Map I-314, 1960c.

_____, Geologic map and cross section of the Anchorage (D-2) quadrangle and northeasternmost part of the Anchorage (D-3) quadrangle, Alaska, U.S. Geol. Survey Misc. Investigations Map I-342, 1961a.

_____, Geologic map of the north two-thirds of Anchorage (D-1) quadrangle, Alaska, U.S. Geol. Survey Misc. Investigations Map I-343, 1961b.

_____, Stratigraphic reconnaissance of the Matanuska Formation in the Matanuska Valley, Alaska, U.S. Geol. Survey Bull. 1181-I, 11-133, 1964.

_____, Strike-slip faults in Alaska, Ph.D. dissertation, Stanford Univ., 82 pp., 1966.

Hamilton, Warren, The Uralides and the motion of the Russian and Siberian Platforms, Bull. Geol. Soc. Amer., 81, 2553-2576, 1970.

Hayes, Dennis E. add Walter C. Pitman III, Magnetic lineations in the North Pacific, in Hays, James D., editor, Geological Investigations of the North Pacific, Geol. Soc. Amer. Mem. 126, pp. 291-314, 1970.

Irving, E., Paleomagnetism and its Application to Geological and Geophysical Problems, Wiley and Sons, New York, 399 pp., 1964.

Jackson, E. D., Eli A. Silver, and G. B. Dalrymple, Hawaiian-Emperor Chain and its relation to Cenozoic circumpacific tectonics, Bull. Geol. Soc. Amer., 83, 601-618, 1972.

Keller, A. S. and J. T. Cass, Petroliferous sand of the Chignik Formation at Chignik Lagoon, Alaska, U.S. Geol. Survey Open File Rept. 138, 5 pp., 1956.

Keller, A. S. and H. N. Reiser, Geology of the Mount Katmai area, Alaska, U.S. Geol. Survey Bull. 1058-G, 261-298, 1959.

King, Philip B., Tectonic Map of North America, U.S. Geol. Survey, 1969.

LePichon, Xavier, Sea-floor spreading and continental drift, J. Geophys. Res., 73, 3661-3697, 1968.

McElhinny, M. W., Statistics of a spherical distribution, in Collinson, D. W., K. M. Creer and S. K. Runcorn, editors, Methods in Palaeomagnetism, Elsevier Amsterdam, pp. 313-321, 1967.

_____, Palaeomagnetic directions and pole positions--VIII. Pole numbers 8/1 to 8/186, Geophys. J. R. astr. Soc., 15, 409-430, 1968a.

_____, Palaeomagnetic directions and pole positions--IX. Pole numbers 9/1 to 9/159, Geophys. J. R. astr. Soc., 16, 207-224, 1968b.

_____, Palaeomagnetic directions and pole positions--X. Pole numbers 10/1 to 10/200, Geophys. J. R. astr. Soc., 18, 305-327, 1969.

_____, Palaeomagnetic directions and pole positions--XI. Pole numbers 11/1 to 11/90, Geophys. J. R. astr. Soc., 20, 417-429, 1970.

McKenzie, D. P. and R. L. Parker, The north Pacific: an example of tectonics on a sphere, Nature, 216, 1276-1280, 1967.

Martin, G. C. and F. J. Katz, Geology and coal fields of the lower Matanuska Valley, Alaska, U.S. Geol. Survey Bull. 500, 98 pp., 1912.

Moffit, F. H., Geology of the Slana-Tok district, Alaska, U.S. Geol. Survey Bull. 904, 54 pp., 1938.

Moore, J. Casey, Uplifted trench sediments: southwestern Alaska-Bering Shelf edge, Science, 175, 1103-1105, 1972.

Morgan, W. Jason, Deep mantle convection plumes and plate motions, Amer. Assn. Petroleum Geologists Bull., 56, 203-213, 1972.

Nagata, Takesi, Rock Magnetism, Maruzen, Tokyo, 350 pp., 1961.

Naugler, Frederic P. and David K. Rea, Abyssal hills and sea-floor spreading in the central North Pacific, Bull. Geol. Soc. Amer., 81, 3123-3128, 1970.

Opdyke, N. D. and K. W. Henry, A test of the dipole hypothesis, Earth Planet. Sci. Lett., 6, 139-151, 1969.

Payne, Thomas G., Mesozoic and Cenozoic tectonic elements of Alaska, U.S. Geol. Survey Misc. Investigations Map I-84, 1955.

Pitman, W. C., III, and D. E. Hayes, Sea-floor spreading in the Gulf of Alaska, J. Geophys. Res., 73, 6571-6580, 1968.

Pitman, Walter C. III, and Manik Talwani, Sea-floor spreading in the North Atlantic, Bull. Geol. Soc. Amer., 83, 619-646, 1972.

Plafker, George, Tectonic deformation associated with the 1964 Alaska earthquake, Science, 148, 1675-1687, 1965.

Reed, Bruce L. and Marvin A. Lanphere, Age and chemistry of Mesozoic and Tertiary plutonic rocks in southcentral Alaska, Bull. Geol. Soc. Amer., 80, 23-49, 1969.

Richter, D. H., Geology of the Upper Slana-Mentasta area, Southcentral Alaska, Alaska Div. of Mines and Minerals Geologic Rept. 30, 25 pp., 1967.

Richter, D. H. and N. A. Matson, Jr., Quaternary faulting in the eastern Alaska Range, Bull. Geol. Soc. Amer., 82, 1529-1540, 1971.

Roddick, J. A., Tintina trench, J. Geology, 75, 23-32, 1967.

Runcorn, S. K., On the hypothesis that the mean geomagnetic field for parts of geologic time has been that of a geocentral axial multipole, J. Atmos. Terr. Phys., 14, 167-174, 1959a.

_____, On the theory of the geomagnetic secular variation, Ann. de Geophys., 15, 87-92, 1959b.

St. Amand, Pierre, Geological and geophysical synthesis of the tectonics of portions of British Columbia, the Yukon Territory, and Alaska, Bull. Geol. Soc. Amer., 66, 1343-1370, 1957.

Scholl, D. W., M. S. Marlow, J. S. Creager, M. L. Holmes, S. C. Wolf and A. K. Cooper, A search for the seaward extension of the Kaltag fault beneath the Bering Sea, Geol. Soc. Amer., Abstracts with Programs, 2, 141-142, 1970.

Stoneley, Robert, The structural development of the Gulf of Alaska sedimentary province in southern Alaska, Quart. J. Geol. Soc. London, 123, 25-57, 1967.

_____, A note on the structural evolution of Alaska, J. Geol. Soc., 127, 623-628, 1971.

Strangway, David W., History of the Earth's Magnetic Field, McGraw-Hill, New York, 168 pp., 1970.

Tailleur, I. L. and W. P. Brosge, Tectonic history of northern Alaska, in Adkison, W. L. and M. M. Brosge, editors, Proceedings of the Geological Seminar on the North Slope of Alaska, Los Angeles, Pacific Sec., Amer. Assn. Petroleum Geologists, pp. E1-E120, 1970.

Vine, F. J., Paleomagnetic evidence for the northward movement of the North Pacific basin during the past 100 m.y. (abstract), Trans. Amer. Geophys. Union, 49, 156, 1968.

Vlasov, G. M., editor, Geologiya SSSR, Tom XXXI, Kamchatka, Kuril'skiye i Komandorskiye ostrova, Chast' I, Geologicheskoye opisaniye (Geology of the USSR, Vol. 31, Kamchatka, Kuril and Komandorskiye Islands, Part I Geological description), Izdatel'stvo "Nedra," Moscow, 1964, NASA TT F-11, 529, 1, 428 pp., 1967.

Waring, G. A., Geology of the Anthracite Ridge coal district, Alaska, U.S. Geol. Survey Bull. 861, 57 pp., 1936.

Watson, Geoffrey S. and E. Irving, Statistical methods in rock magnetism, Mon. Not. Roy. astr. Soc. Geophys. Suppl., 7, 289-300, 1957.

Wheeler, J. O., Whitehorse map-area, Yukon Territory 105 D, Geol. Survey of Canada Mem. 312, 156 pp., 1961.